

## INFORMATION TO USERS

This manuscript has been reproduced from the microfilm master. UMI films the text directly from the original or copy submitted. Thus, some thesis and dissertation copies are in typewriter face, while others may be from any type of computer printer.

**The quality of this reproduction is dependent upon the quality of the copy submitted.** Broken or indistinct print, colored or poor quality illustrations and photographs, print bleedthrough, substandard margins, and improper alignment can adversely affect reproduction.

In the unlikely event that the author did not send UMI a complete manuscript and there are missing pages, these will be noted. Also, if unauthorized copyright material had to be removed, a note will indicate the deletion.

Oversize materials (e.g., maps, drawings, charts) are reproduced by sectioning the original, beginning at the upper left-hand corner and continuing from left to right in equal sections with small overlaps.

ProQuest Information and Learning  
300 North Zeeb Road, Ann Arbor, MI 48106-1346 USA  
800-521-0600

**UMI**<sup>®</sup>



**IDENTIFICATION OF GLYCOSYLATED PROTEINS  
IN ALZHEIMER'S DISEASE BRAIN**

**by**

**YU HUANG**

**A dissertation submitted to the Graduate Faculty in Biology  
in partial fulfillment of the requirements for the degree of  
Doctor of Philosophy, The City University of New York**

**2004**

UMI Number: 3115259

Copyright 2004 by  
Huang, Yu

All rights reserved.

UMI<sup>®</sup>

---

UMI Microform 3115259

Copyright 2004 by ProQuest Information and Learning Company.  
All rights reserved. This microform edition is protected against  
unauthorized copying under Title 17, United States Code.

---

ProQuest Information and Learning Company  
300 North Zeeb Road  
P.O. Box 1346  
Ann Arbor, MI 48106-1346

©2004


YU HUANG

All Rights Reserved

This manuscript has been read and accepted for the Graduate Faculty in Biology in Satisfaction of the dissertation requirement for the degree of Doctor of Philosophy.

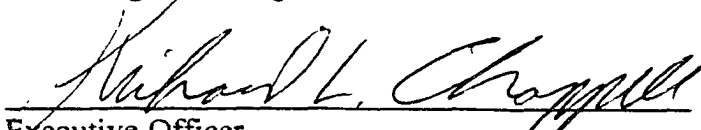
12/18/03

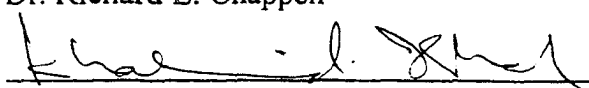
Date

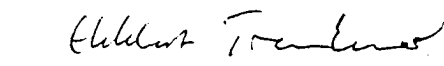
  
Chair of Examining Committee,  
Dr. Cheng-Xin Gong, Institute for Basic Research


1/20/04

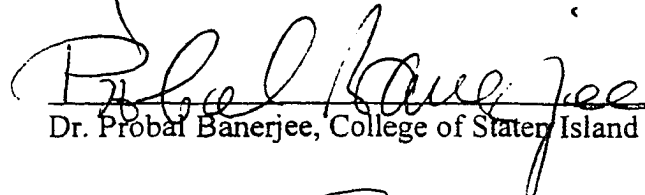
Date

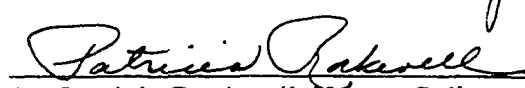
  
Executive Officer,  
Dr. Richard L. Chappell

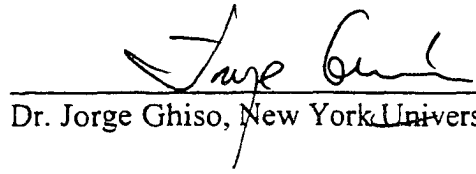
  
Dr. Khalid Iqbal, Institute for Basic Research

  
Dr. Ekkhart Trenkner, Institute for Basic Research

  
Dr. Richard Carp, Institute for Basic Research

  
Dr. Probal Banerjee, College of Staten Island

  
Dr. Patricia Rockwell, Hunter College

  
Dr. Jorge Ghiso, New York University

Supervising Committee

The City University of New York

## **Abstract**

# **IDENTIFICATION OF GLYCOSYLATED PROTEINS IN ALZHEIMER'S DISEASE BRAIN**

**By**

**Yu Huang**

**Advisors: Professor Cheng-Xin Gong and Professor Khalid Iqbal**

Alzheimer's disease (AD) is a common neurodegenerative disorder with unknown molecular pathogenesis. We recently found that in AD brain, tau is also aberrantly glycosylated besides being abnormally hyperphosphorylated, suggesting that the protein glycosylation system might be affected in AD brain. Here, we developed methodologies for isolation of glycoproteins from human brain homogenates. It included membrane protein extraction, ion-exchange chromatography, and lectin affinity chromatographies. By combining these methodologies with mass spectrometry analysis, we identified 12 predominant glycoproteins from AD brain. Nine of these identified proteins are previously characterized proteins and have been reported to be glycosylated. The rest three proteins are unknown proteins that have not yet been purified or characterized, but their primary structures can be deduced from human genome database. Comparison of lectin-stainings of glycoproteins between AD and control brains revealed that two proteins (43 kDa and 35 kDa, respectively) were increased and another 180 kDa protein

was decreased in AD brain. One of these proteins, the 43 kDa protein, was identified as human acid ceramidase (AC). Western blot analysis suggested that the increased lectin staining was due to an elevated level of AC rather than elevated glycosylation. Immunohistochemical studies revealed that AC was expressed mainly in neurons and some astrocytes. It also co-localized with neurofibrillary tangles. In addition, we discovered that two inflammation-activated proteins, inhibitor  $\gamma$  of nuclear factor  $\kappa$ B ( $I\kappa B\gamma$ ) and glial fibrillary acidic protein (GFAP), were up regulated in AD.

Identification of major brain glycoproteins suggests these glycoproteins might play important roles in central nervous system and provide new information to understand the biophysiological functions of brain glycoproteins. Our finding that several glycoproteins are altered in AD brain supports our hypothesis that the glycosylation system might be affected in AD. The accumulation of AC in AD brain and its co-localization with neurofibrillary tangles implied that AC might be involved in pathophysiology of AD. Our discovery that both  $I\kappa B\gamma$  and GFAP are up regulated provides a possible molecular mechanism of inflammation activation of AD brain. Taken together, these studies provide new avenues to understanding the molecular mechanisms of AD.

## ACKNOWLEDGMENTS

I would like to express my deepest appreciation to my mentors, Dr. Cheng-Xin Gong, Head of Brain Metabolism Laboratory, at the New York State Institute for Basic Research in Developmental Disabilities (IBR), and Dr. Khalid Iqbal, Chairman of Department of Neurochemistry and Head of Chemical Neuropathology laboratory at IBR, for their perpetual guidance, precious advice, tremendous encouragement and generous support throughout my graduate research.

My great gratitude to Dr. Inge Grundke-Iqbal, Head of Neuroimmunology Laboratory at IBR, for her invaluable suggestions and kindness.

I am appreciative to the members of my Ph.D. Research Committee, Dr. Ekkhart Trenkner, Dr. Patricia Rockwell, Dr. Probal Banerjee, and Dr. Richard Carp for their trust and advice.

I am also grateful to Dr. Fei Liu for her help in the use of several techniques and her critical discussions; to Dr Yu-Wen Hwang for his help with my data processing and analysis; to Dr. Ezzat El-Akkad for his help with my experiments of preparative electrophoresis and column chromatographies; to Dr. Hitoshi Tanimukai for his help in immunohistochemical studies; to Dr. Hong-Hui Chen for his assistance in enlightening me with various computer-related problems; and to all other of my fine colleagues at IBR, Dr. Alejandra Alonso, Dr. Abdur Rahman, Mr. Mike Fenko, Dr. Niloufar Haque, Dr. Sabiha Khatoon, Ms. Tanweer Zaidi and Ms. Yunn Chyn Tung, for their support, constructive comments, cooperative attitude, and unforgettable friendship.

To Dr. Konrad Sandhoff of University of Bonn, Germany for his kind gifts of human acid ceramidase antibodies.

To the sub-program in Neurosciences, Ph.D. program in Biology, the City University of New York, Dr. Ekkehart Trenkner, Dr. Cheng-Xin Gong and Dr. Khalid Iqbal for their financial support during my Ph.D. study.

Last but not least, my special appreciation to my parents and my wonderful daughter, Elaine H. Cui, for their love, which encouraged me to overcome all the difficulties I have ever met.

## CONTENTS

<b>1.</b>	<b>INTRODUCTION AND BACKGROUND .....</b>	<b>1</b>
1.1.	<b>Brain Aging .....</b>	1
1.2.	<b>Incidence of AD .....</b>	1
1.3.	<b>Clinical Diagnosis of AD .....</b>	2
1.4.	<b>Neuropathological/Histopathological Diagnosis of AD .....</b>	3
1.5.	<b>Etiology of AD .....</b>	6
1.6.	<b>Pathogenesis of AD .....</b>	7
1.6.1.	<b>Amyloid Hypothesis .....</b>	8
1.6.2.	<b>Oxidative Stress Hypothesis .....</b>	9
1.6.3.	<b>Cholesterol Hypothesis .....</b>	11
1.6.4.	<b>Calcium Signaling Deficit Hypothesis .....</b>	11
1.6.5.	<b>Central Cholinergic Deficit Hypothesis .....</b>	12
1.6.6.	<b>Brain Energy Metabolism Deficiency Hypothesis .....</b>	13
1.6.7.	<b>Tau Hypothesis – Neurofibrillary Degeneration .....</b>	13
1.7.	<b>AD and Other Tauopathies .....</b>	15
1.8.	<b>Post-translational Modification of Proteins involved in AD .....</b>	17
1.8.1	<b>Abnormal Hyperphosphorylation of Proteins in AD .....</b>	17
1.8.2	<b>Protein Glycosylation .....</b>	18
1.8.3	<b>Protein Glycosylation involved in AD .....</b>	19
<b>2.</b>	<b>SPECIFIC AIMS .....</b>	<b>22</b>

<b>3. MATERIALS AND METHODS .....</b>	<b>23</b>
<b>3.1. Brain Tissue .....</b>	<b>23</b>
<b>3.2. Chemicals and Reagents .....</b>	<b>24</b>
<b>3.3. Tissue Homogenates .....</b>	<b>25</b>
<b>3.4. Lectin Blot Analysis .....</b>	<b>27</b>
<b>3.5. Western Blot Analysis .....</b>	<b>28</b>
<b>3.6. In Vitro Deglycosylation .....</b>	<b>28</b>
<b>3.7. Subcellular Fractionation .....</b>	<b>29</b>
<b>3.8. Membrane Protein Extraction .....</b>	<b>31</b>
<b>3.9. Lectin Affinity Chromatography .....</b>	<b>31</b>
<b>3.10. DEAE-Ion Exchange Chromatography .....</b>	<b>35</b>
<b>3.11. High Performance Liquid Chromatography (HPLC) .....</b>	<b>35</b>
<b>3.12. Immunoprecipitation .....</b>	<b>36</b>
<b>3.13. Preparative SDS-PAGE .....</b>	<b>38</b>
<b>3.14. Ammonium Sulfate Precipitation .....</b>	<b>38</b>
<b>3.15. Identification of Proteins .....</b>	<b>38</b>
<b>3.16. Immunohistochemistry .....</b>	<b>39</b>
<b>4. RESULTS .....</b>	<b>40</b>
<b>4.1. Development of Methodology for Comparative Analysis of       Glycoproteins Between Control and Alzheimer's Disease Brains .....</b>	<b>41</b>
<b>4.2. Identification of Major Glycoproteins in AD Brain Grey Matter .....</b>	<b>56</b>
<b>4.3. Three Major Glycoproteins Are Altered in AD Brain .....</b>	<b>66</b>

4.4. One of the Inhibitors of Nuclear Factor $\kappa$ B (NF $\kappa$ B), I $\kappa$ B $\gamma$ , Is Up Regulated in AD Brain .....	83
5. DISCUSSION .....	93
6. CONCLUSION .....	102
7. REFERENCES .....	103

**LIST OF FIGURES**

<b>Fig. 1. Amyloid cascade hypothesis</b>	<b>10</b>
<b>Fig. 2. Tau hypothesis</b>	<b>16</b>
<b>Fig. 3. Subcellular fractionation scheme</b>	<b>30</b>
<b>Fig. 4. Membrane protein preparation</b>	<b>31</b>
<b>Fig. 5. ConA affinity chromatography scheme</b>	<b>33</b>
<b>Fig. 6. SNA and GNA chromatography scheme</b>	<b>34</b>
<b>Fig. 7. HPLC sample preparation</b>	<b>37</b>
<b>Fig. 8. Coomassie blue staining and lectin blots of SDS-PAGE of homogenates from Control and AD cerebral cortex</b>	<b>42</b>
<b>Fig. 9. Coomassie blue and lectin blots of cytosolic proteins from control and AD cerebral cortex</b>	<b>43</b>
<b>Fig. 10. Coomassie blue and lectin blots of hippocampal membrane proteins</b>	<b>43</b>
<b>Fig. 11. Coomassie blue and lectin blots of synaptosomal membrane proteins from control and AD cerebral cortex</b>	<b>44</b>
<b>Fig. 12. Coomassie blue and lectin blots of homogenates from control and AD brain white matter</b>	<b>44</b>
<b>Fig. 13. Coomassie blue staining and lectin blots of various subcellular fractionations of control and AD cerebral cortex</b>	<b>45</b>
<b>Fig. 14. ConA affinity chromatography of a mixture of Carboxypeptidase Y (positive control) and BSA</b>	<b>47</b>

<b>Fig. 15. Analysis of ConA affinity chromatography of membrane extract from AD cerebral cortex</b>	<b>49</b>
<b>Fig. 16. Analysis of DEAE-ion exchange chromatography of ConA-binding proteins</b>	<b>50</b>
<b>Fig. 17. Lectin blots of proteins eluted from DEAE-ion exchange column (0 ~ 1 M NaCl)</b>	<b>53</b>
<b>Fig. 18. Analysis of SNA and PNA affinity chromatographies of fetuin as positive control of SNA, and asialofetuin as positive control of PNA</b>	<b>53</b>
<b>Fig. 19. Analysis of SNA, PNA, DSA and GNA affinity chromatographies of eluted proteins from DEAE-ion exchange chromatography</b>	<b>54</b>
<b>Fig. 20. Analysis of ConA affinity chromatography of membrane extract from an AD brain</b>	<b>58</b>
<b>Fig. 21. DEAE-ion exchange chromatography of ConA-binding glycoproteins from an AD brain</b>	<b>61-62</b>
<b>Fig. 22. Analysis of tandem SNA and GNA affinity chromatography of Eluate I from DEAE-ion exchange chromatography</b>	<b>63</b>
<b>Fig. 23. Coomassie blue-stained bands of glycoproteins eluted from SNA and GNA columns and cut out for identification by mass spec</b>	<b>64</b>
<b>Fig. 23A. Identification of GNA-8 by mass spectrometry.</b>	<b>65</b>
<b>Fig. 24. Tau pathology in homogenates from AD and control brains</b>	<b>67</b>
<b>Fig. 25. Analysis of ConA affinity chromatography of control and AD brain membrane extracts</b>	<b>69</b>
<b>Fig. 26. Quantitation and comparison of ConA-binding glycoproteins between control and AD brains</b>	<b>70-71</b>

<b>Fig. 27. The different protein patterns were shown on GNA blots under reducing or non-reducing conditions</b>	<b>74</b>
<b>Fig. 28. Identification of glycoproteins that are altered in AD</b>	<b>75</b>
<b>Fig. 29. Confirmation of the 43 kDa glycoprotein as human AC by Western blots</b>	<b>76</b>
<b>Fig. 30. Normalized glycosylation level of AC <math>\beta</math>-subunit</b>	<b>76</b>
<b>Fig. 31. In vitro deglycosylation of AC <math>\beta</math>-subunit from control and AD brains</b>	<b>77</b>
<b>Fig. 32. Gene sequences of AC from rat, mouse and human</b>	<b>78</b>
<b>Fig. 33. Immunohistochemistry of AC in human brain temporal cortex</b>	<b>81</b>
<b>Fig. 34. Double immunohistochemical labeling of AC and NFTs in AD cerebral cortex</b>	<b>82</b>
<b>Fig. 35. Coomssie blue staining and MAA blot of control and AD brain homogenates</b>	<b>85</b>
<b>Fig. 36. Subcellular distribution of the 45 kDa protein</b>	<b>86</b>
<b>Fig. 37. Subcellular localization of 45 kDa protein which is altered in AD</b>	<b>86</b>
<b>Fig. 38. Silver staining and MAA blot of aliquots from HPLC</b>	<b>87</b>
<b>Fig. 39. Coomassie blue stained 45 kDa protein band was cut for N-terminal amino acid sequencing</b>	<b>88</b>
<b>Fig. 40. Western blots of homogenates from grey matter of control and AD brains</b>	<b>89</b>

<b>Fig. 41. Western blots homogenates from white matter of control and AD brains</b>	<b>89</b>
<b>Fig. 42. Western blots of Pellet 1 (nuclear fraction) of subcellular fractionation from control and AD brain homogenates</b>	<b>89</b>
<b>Fig. 43. Immunoprecipitation of I<math>\kappa</math>B<math>\gamma</math> from nuclear fraction of AD brain</b>	<b>90</b>
<b>Fig. 44. Removal of sialic acid by HCl treatment</b>	<b>91</b>
<b>Fig. 45. Further purification of 45 kDa band by ammonium sulfate precipitation and preparative SDS-gel electrophoresis</b>	<b>92</b>

**LIST OF TABLES**

<b>Table 1. Control and AD Brain Tissues Used for Tissue Homogenates</b>	<b>23</b>
<b>Table 2. Control and AD Brain Tissues Used for Membrane Extracts</b>	<b>24</b>
<b>Table 3. Lectins used in this study</b>	<b>26</b>
<b>Table 4. Eluting Conditions of SNA, PNA, DSA and GNA Affinity Chromatography</b>	<b>34</b>
<b>Table 5. A Representative Yield of Membrane Extract Preparation from Temporal Cortex (9.24 g)</b>	<b>46</b>
<b>Table 6. Yield of ConA Affinity and DEAE-ion Exchange Chromatographies of Membrane Proteins from Cerebral Cortex</b>	<b>48</b>
<b>Table 7. Yields from SNA, PNA, DSA and GNA Affinity Chromatographies</b>	<b>55</b>
<b>Table 8. Preparation of brain membrane extract from frontal and temporal cortex (90.5g) of an AD brain</b>	<b>56</b>
<b>Table 9. Mass Spectrometric Analysis of Major AD Brain Glycoproteins</b>	<b>64</b>
<b>Table 10. Preparations of membrane extract from six control and six AD brains</b>	<b>66</b>

# **1. INTRODUCTION AND BACKGROUND**

## **1.1. Brain Aging**

With improvement in modern medicine, early diagnostic laboratory tests, preventive medicine and treatment of diseases at early stages, the human life span continues to extend throughout the modern world. Hence, brain aging becomes one of the greatest scientific challenges of the 21<sup>st</sup> century. However, the mechanism underlying brain aging is largely unknown. With increase in longevity of life, people face increasing incidence of age-associated decreases in cognition that ranges from normal old age memory deficit to mild cognitive impairment to dementia. Age has a powerful effect on enhanced susceptibility to neurodegenerative diseases, such as Alzheimer's disease (AD), one of the most devastating brain disorders of elderly people.

## **1.2. Incidence of AD**

AD was first described by Alois Alzheimer in 1907. It is the most common cause of dementia among people age 65 and older. An estimated 10% of American over the age of 65 and 50% of those over age 85 has AD [Alzheimer's disease forum ([www.alzforum.org](http://www.alzforum.org)), 2003]. It presents a major health problem because of its enormous impact on individuals, families, the health care system, and society as a whole. In the United States alone, it is estimated that 4.5 million people currently suffer from AD. The prevalence doubles every five years beyond age 65 (Bick and Katzman, 2000). The

problem becomes even more acute in the light of recent reports, which predict that the lifespan of people will continue to extend. AD puts a heavy economic burden on society. As the third most expensive disease to treat in the U.S., the national cost of caring for patients with AD is estimated to be close to \$100 billion annually [Alzheimer's disease forum ([www.alzforum.org](http://www.alzforum.org)), 2003]. The escalating growth of the elderly population assures that the profound economic and social impact of AD will increase.

### **1.3. Clinical Diagnosis of AD**

AD is a progressive brain degeneration that occurs gradually and results in memory loss, behavior and personality changes, and a decline in thinking abilities. These abnormalities are related to the breakdown of the connections between neurons and neuronal death. AD progresses slowly, it takes two to twenty years, from early, mild forgetfulness to a severe loss of mental function. The insidious onset of AD is characterized by a subtle decline of memory functions in a state of clear consciousness. Memory loss represents the earliest sign of AD. In addition to memory loss, patients in the early stages of AD often show impairments in at least one of other areas of cognition, for instance, praxis, language, calculation, perception, and judgment. With advanced disease, the deficits become more profound, whereas patients may exhibit gross behavioral disturbances such as aggression, agitation, and social inappropriateness or even frank psychosis (with delusions and hallucinations). In late stages, virtually all patients are profoundly demented, incontinent, bedridden and unable to feed themselves.

Most commonly, people with AD die from pneumonia or lack of nutrition (NIA and NIH, Progress report on Alzheimer's disease. 1999; 2000).

Currently, clinicians use several tools to diagnose "possible AD" or "probable AD" in a patient who has difficulties with memory or other mental functions. These tools include a patient history, physical exam, laboratory tests, brain scans, and a series of psychometric tests that measure memory, language skills, and other abilities related to brain functioning. However, clinical diagnosis only has 80-90% accuracy. A conclusive diagnosis, neuropathological/histopathological diagnosis, can only be made by examining the brain after death in an autopsy to determine the presence of characteristic plaques and tangles in certain brain regions (NIA and NIH, Progress report on Alzheimer's disease. 1999; 2000).

#### **1.4. Neuropathological/Histopathological Diagnosis of AD**

Histopathologically, AD is characterized by presence of two major brain lesions, i.e., extracellular deposition of  $\beta$ -amyloid ( $A\beta$ ) as neuritic (senile) plaques and intracellular neurofibrillary tangles (NFTs). Amyloid plaques are dense, largely insoluble deposits of protein and cellular materials. NFTs are composed of insoluble twisted fibers that build up inside affected neurons. Significant advances on their compositions, the mechanisms by which they form, and their possible roles in the development of AD were reported only in the last two decades.

In AD, plaques develop first in areas of the brain used for memory and other cognitive functions (Swaab, et al., 2002). They consist of largely insoluble deposits of

A $\beta$ , a protein fragment cleaved from a larger protein called  $\beta$ -amyloid precursor protein (APP). Senile plaques are surrounded by dystrophic and degenerating neurites and by microglia and astrocytes (Mantyh, et al., 1997). APP is a transmembrane protein that may play an important role in the growth and survival of neurons. It can be processed by two pathways (for review, see Gooch and Stennett, 1996). It is normally cleaved between residues 687 and 688 of the protein by a protease named  $\alpha$ -secretase. This cleavage site is within the A $\beta$  region, hence this pathway does not produce A $\beta$  and is not amyloidogenic. In the second pathway, APP is cleaved by two separate proteases named  $\beta$ -secretase and  $\gamma$ -secretase at residue 671 and around residue 713, respectively. The cleavages by this pathway produce A $\beta$  and therefore are amyloidogenic. It is believed that the amyloidogenic pathway of APP processing is activated in AD. A $\beta$  aggregates into long filaments outside the cell and forms the plaque core. A $\beta$  is neurotoxic, and has been reported to cause inflammation in the brain, generate free radicals, diminish local blood flow, and increase intracellular Ca<sup>2+</sup> (Coon, et al., 1999). Microglia and astrocytes can release bioactive molecules such as inflammatory cytokines, reactive oxygen species and nitric oxide or perturb glutamate transport (Mantyh, et al., 1997). Along with membrane attack complex composed of complements, A $\beta$  and glial cells might mediate deleterious effects on nearby neurons, leading to cell death (Mantyh, et al., 1997; Hardy, et al., 2000).

NFTs, the second hallmark of AD pathology, are composed of paired helical filaments (PHFs) that are ultrastructurally unlike any of the normal neurofibrils. The major component of the PHFs is the abnormally hyperphosphorylated form of microtubule-associated protein tau (Grundke-Iqbal, et al., 1986a; Lee, et al., 1991). Tau is

normally a cytosolic protein, the function of which is to stimulate and stabilize microtubule formation from tubulin subunits. The integrity of the microtubule system is essential for the transport of materials between cell body and synaptic terminals of neurons. Under normal conditions, tau contains 2-3 mole of phosphate per mole of tau. However, in AD brain, tau is 3-4 fold more phosphorylated (Ksiezak-Reding, et al., 1990; Kopke, et al., 1993). In the human brain, there are six isoforms of tau with apparent molecular weights of 48-67 kDa generated by alternative splicing of mRNA from a single gene (Goedert, et al., 1989; Buee, et al., 2000). All of these isoforms have been found in highly phosphorylated forms in PHFs (Grundke-Iqbal, et al., 1986a, 1986b; Goedert, et al., 1992). To date, more than 30 phosphorylation sites have been identified in PHF-tau, while only some of these sites are partially phosphorylated in normal situations (for review and summary, see Lovestone and Reynald, 1997; Liu, et al., 2002c). The abnormal hyperphosphorylation of tau may result from an imbalance of the activities of tau protein kinase(s) and phosphatase(s). Previous studies suggested that a defect of phosphatase activities in AD brain might be the cause of this imbalance (Gong, et al., 1993; 1995). In AD brain, the neuronal microtubule system is progressively disrupted and replaced by the appearance of bundles of PHFs as the NFTs. This collapse of the axonal transport may result in compromised neurotransmission between nerve cells and later may lead to neuronal death (Iqbal, et al., 2000).

## 1.5. Etiology of AD

The etiology of AD has not been well understood until now. Although the risk of developing AD increases with age, AD and dementia symptoms are not generally believed as a part of normal aging. AD and other dementing disorders are caused by diseases that affect the brain. In the absence of disease, the human brain often can function well at least into the tenth decade of life. It is believed that AD results from many interrelated factors, including genetic, metabolic, and environmental. The disease develops as a result of a complex cascade of events that take place over time inside the brain. The disease can be triggered by any number of changes in this cascade, and these events interact differently in different people. Generally speaking, there are genetic and non-genetic factors that cause AD.

Two types of AD exist: familial AD (FAD), which follows a certain inheritance pattern, and sporadic AD, where no obvious inheritance pattern is seen. Because of differences in the age at onset, AD is also described as early-onset (occurring in people younger than 65) or late-onset (occurring in those 65 and older). Early-onset AD is rare (about 10% of cases) and generally affects people aged 30 to 60. Some forms of early-onset AD are inherited. Early-onset AD also often progresses faster than the more common, late-onset form (NIA and NIH, Progress report on Alzheimer's disease. 1999; 2000).

All FAD known so far has an early-onset, and is caused by mutations in three genes located on three different chromosomes. These genes are presenilin-1 (PS-1), presenilin-2 (PS-2) or  $\beta$ -amyloid precursor protein (APP), located on chromosomes 14, 1, and 21,

respectively (Goate, et al., 1991; Sherrington, et al., 1995). FAD follows an autosomal dominant inheritary patterns. Some evidence shows that the mutations in APP and presenilins make it more likely that  $\beta$ -peptide will be snipped out of the APP precursor, thus causing more  $\beta$ -amyloid to be made.

Genetics play a role in the development of late-onset AD as well. An increased risk for late-onset AD has been found with inheritance of one or two copies of the apolipoprotein E epsilon4 (APOE  $\epsilon$ 4) allele on chromosome 19 (Roses, et al., 1994; Hardy, 1996). The mere inheritance of one or two APOE  $\epsilon$ 4 alleles does not predict AD with certainty; that is, a person carrying one or two APOE  $\epsilon$ 4 alleles may not get the disease and a person who develops AD may not have any APOE  $\epsilon$ 4 alleles. The mechanisms in which the APOE  $\epsilon$ 4 protein increases the likelihood of developing AD are not understood, but one possibility is that it facilitates  $\beta$ -amyloid build-up and tau phosphorylation, and thus contributes to the onset of AD (Strittmatter, et al., 1995; Cummings, et al., 1998).

The etiology of sporadic AD is not known. Sporadic AD is generally believed multi-etiological, including metabolic dysregulation, oxidative stress, brain inflammation and brain infarction (Iqbal, et al., 2000). Exploration of these factors will help to reveal the disease mechanisms.

## **1.6. Pathogenesis of AD**

Although AD was first described 100 years ago, the pathogenesis of the disease has not been well understood. There are several hypotheses trying to interpret the molecular

mechanism of AD. Among them, amyloid hypothesis and tau hypothesis are two dominant AD hypotheses. Other hypotheses include Oxidative Stress Hypothesis, Cholesterol Hypothesis, Calcium Signaling Deficit Hypothesis, Central Cholinergic Deficit Hypothesis, and Brain Deficient Energy Metabolism Hypothesis. Because AD is a multi-factorial disorder, its molecular pathogenesis may involve several mechanisms.

### *1.6.1. Amyloid Hypothesis*

Amyloid  $\beta$ -peptide, the sticky peptide prominent in the  $\beta$ -plaques, is believed to play a very important role in AD pathogenesis. It is a 39-43 residue peptide with a molecular weight of  $\sim 4$  kDa. The major  $A\beta$  species found in vivo has 40 amino acids and hence named  $A\beta_{40}$ . Another isoform of  $A\beta$ ,  $A\beta_{42}$ , which has two additional hydrophobic residues, Ile and Ala, is more hydrophobic and has higher aggregation potential. Hence, it is more amyloidogenic and toxic. Interestingly mutation in any of APP, PS1, or PS2 genes facilitates the production and accumulation of  $A\beta_{42}$ . Fig. 1 summarises an amyloid cascade hypothesis that demonstrates a sequence of pathogenic events that lead to AD (Hardy and Selkoe, 2002; De Felice and Ferreira, 2002). However, there are several concerns with this hypothesis. Although the amyloid hypothesis offers a broad framework to explain AD pathogenesis, it is currently lacking in detail, and certain observations do not fit easily with the simplest version of the hypothesis. First, the most frequently voiced objection is that the number of amyloid deposits in the brain does not correlate well with the degree of cognitive impairment that patients experienced in life. Second, another concern arises from the fact that all AD-causing mutations in APP, PS1,

or PS2 increase A $\beta$  deposition, yet the degree to which a particular mutation affects A $\beta$  production in cell culture shows no simple correlation with the age at which it first produces symptoms. Third, in considerable part, the amyloid hypothesis remains controversial because a specific neurotoxic species of A $\beta$  and the nature of its effects on neuronal function have not been defined in vivo. Fourth, transgenic mice undergoing progressive A $\beta$  deposition often do not show significant neuronal loss and neurofibrillary degeneration as seen in AD. Finally, recent analyses suggest that the formation of amyloid plaques often represent a process separate from dementia and AD (Hardy and Selkoe, 2002; Weiner and Selkoe, 2002). Even though these weaknesses of amyloid hypothesis certainly point to important gaps in our understanding of AD, none of them provides a compelling reason to abandon this hypothesis.

### ***1.6.2. Oxidative Stress Hypothesis***

Oxidative stress, which occurs as a result of over-production of free radicals, may play a role in neuronal damage and death in AD. There is increasing evidence that free radical damage to brain lipids, carbohydrates, proteins, and DNA is involved in neuronal death in neurodegenerative disorders (for review, see Retz, et al., 1998; Bhel, 1999; Ho, et al., 2001; Floyd and Hensley, 2002; Koutsilieri, et al., 2002). In autopsied brains, there is an increase in lipid peroxidation, a decline in polyunsaturated fatty acids (PUFA) and an increase in 4-hydroxynonenal (HNE), a neurotoxic aldehyde product of PUFA oxidation (Markesbery and Lovell, 1998). Increased protein oxidation and a marked decline in oxidative-sensitive enzymes, glutamine synthetase and creatinine kinase, are

found in the brain in AD (Markesbery and Carney, 1999). Increased DNA oxidation, especially 8-hydroxy-2'-deoxyguanosine (8-OHdG) is present in the brain in AD (Gabbita, et al., 1998). Immunohistochemical studies show the presence of oxidative stress products in neurofibrillary tangles and senile plaques in AD (Markesbery and Carney, 1999). Markers of lipid peroxidation (HNE, isoprostanes) and DNA oxidation (8-OHdG) are increased in cerebrospinal fluid of AD patients (Lovell and Markesbery, 2001). Overall these studies indicated that oxidative stress is important in the pathogenetic cascade of neurodegeneration in AD. Presenilins and APP mutations also increase the strength of oxidative stress in AD brains (Mattson, 2002).

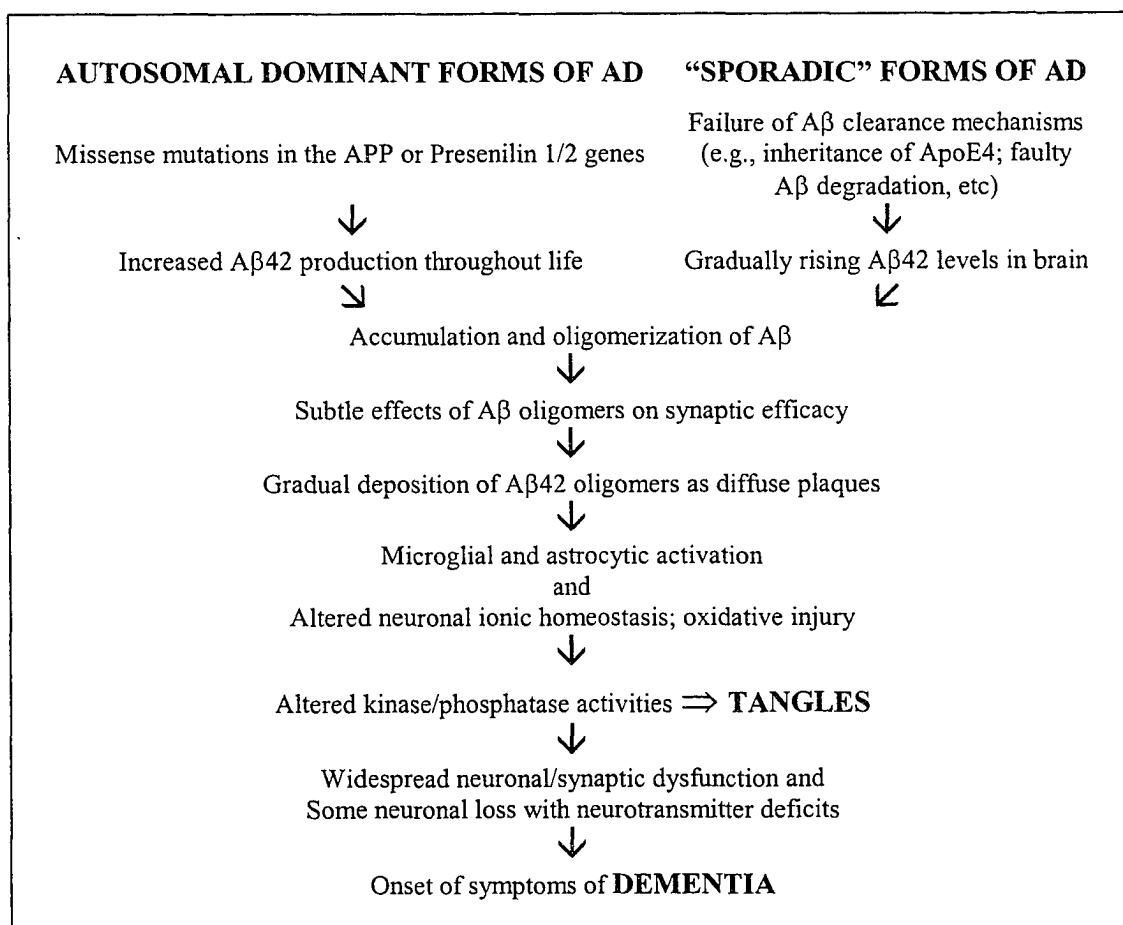


**Fig. 1. Amyloid Cascade Hypothesis**

### ***1.6.3. Cholesterol Hypothesis***

A hallmark of all forms of AD is an abnormal accumulation of the A $\beta$  in specific brain regions. Both the generation and clearance of A $\beta$  are regulated by cholesterol (Yanagisawa and Matsuzaki, 2002). Elevated cholesterol levels increase A $\beta$  in cellular and most animal models of AD, and drugs that inhibit cholesterol synthesis lower A $\beta$  in these models (Refolo, et al., 2000; 2001). Recent studies show that not only the total amount, but also the distribution of cholesterol within neurons, impacts A $\beta$  biogenesis (Puglielli, et al., 2001). The identification of a variant of the APOE gene as a major genetic risk factor for AD is also consistent with a role for cholesterol in the pathogenesis of AD. Clinical trials have recently been initiated to test whether lowering plasma and/or neuronal cholesterol levels is a viable strategy for treating and preventing AD (Puglielli et al., 2003).

### ***1.6.4. Calcium Signaling Deficit Hypothesis***

Calcium signaling mediates many life processes including fertilization, gene expression, cell division, growth and differentiation, muscle contraction, neurotransmission and memory formation. Calcium-mediated activities in human life are highest in young adulthood but diminish during aging, indicating that calcium signaling potency (or intracellular calcium levels) must be decreased in aging and AD. A potential explanation for this phenomenon could be that the calcium-mediated processes are also energy-dependent processes, because they all utilize the free energy reserve of the body

for “useful” work, and it is known that calcium gradient formation and calcium movement across cell membranes are driven by energy-dependent systems. This intimate relationship between energy and calcium signaling implies that the potency of calcium signaling would be affected by changes of energy levels, which would necessarily decline in aging. These may underlie the deficit of calcium signaling in the presymptomatic stage of AD. This hypothesis proposed that A $\beta$  and tau accumulation, which are two hallmarks in AD brain, is the result of inactivation, rather than overactivation, of some calcium-dependent enzymes (Chen, 1998a, 1998b, 1998c, Chen et al., 1999). This is because most enzyme activities should be diminished, rather than overactivated, during aging. These findings suggested that intracellular calcium deficit might be a common cause for the plaque and tangle accumulation underlying sporadic AD.

#### ***1.6.5. Central Cholinergic Deficit Hypothesis***

The central cholinergic hypothesis is the oldest AD hypothesis, which states that the basal forebrain neurons are severely affected in AD resulting in a cerebral cholinergic deficit that underlies the memory loss and other cognitive symptoms (for review, see Geula and Mesulam, 1994). This hypothesis was based on studies of the brains of individuals with advanced dementia over three decades ago and served as the rationale for development of drugs of acetylcholinesterase inhibitors currently approved for AD treatment (Bartus, 2000). However, this hypothesis is now challenged by a new study that demonstrated cortical and hippocampal activities of choline acetyltransferase, an enzyme responsible for synthesis of acetylcholine, is increased rather than decreased in early mild

cognitive impairment and early stage of AD (DeKosky, et al., 2002). This study suggested that the earliest cognitive deficits in AD involve brain changes other than simply cholinergic system loss.

#### ***1.6.6. Brain Energy Metabolism Deficiency Hypothesis***

Age-related changes in the composition of membranes and in glucose/energy metabolism along with a sympathetic tone in the brain are assumed to be cellular/molecular risk factors for AD (Mattson, et al., 1999). In its pathogenesis, the desensitization of the neuronal insulin receptors similar to non-insulin dependent diabetes mellitus may be of pivotal significance. This abnormality along with a reduction in insulin concentration is assumed to induce a cascade-like process of disturbances including decreases in cellular glucose, acetylcholine, cholesterol, and ATP, associated with changes in the metabolism of amino acids and fatty acids. There is evidence that the reductions in the availability of both glucose/energy and insulin contribute to the formation of hyperphosphorylated tau protein, which is regarded as the most important neurofibrillary degeneration in AD (Hoyer, 2000).

#### ***1.6.7. Tau Hypothesis - Neurofibrillary Degeneration***

Formation of NFTs in the brain is a characteristic lesion of AD and is also seen in several other neurodegenerative diseases (for review, see Lee, et al., 2001). NFTs are composed of PHFs, the major component of which is the microtubule-associated protein

tau found in an abnormally hyperphosphorylated state (Grundke-Iqbal et al., 1986a; 1986b; Iqbal et al., 1989). Although the biochemical requirements for PHF formation remains to be defined, significant evidence suggests that abnormal hyperphosphorylation of tau is responsible for the loss of its biological activity, gain of its toxicity and its transformation from normal soluble tau into insoluble PHF-tau (Alonso et al., 1994, 1996, 1997, 2001a, 2001b). Hence, the dysregulation of tau cascade is the center of another major hypothesis of AD pathogenesis (Iqbal, et al., 2000). Fig. 2 summarizes the tau hypothesis.

Tau promotes the binding of GTP to tubulin and its assembly into microtubules and maintains the structure of microtubules (Weingarten et al., 1975; Khatoon et al., 1995). Microtubules are necessary for the axonal transport. A significant consequence of tau hyperphosphorylation in AD is the reduction in its ability to bind to microtubules and to promote microtubule assembly. A pool of cytosolic unpolymerized abnormally hyperphosphorylated tau isolated from AD brain (AD P-tau) failed to promote the polymerization of microtubules (Alonso et al., 1994). It has also been reported that in AD brain the pool of tau that is able to bind to microtubules is significantly reduced and the degree of impairment in microtubule binding correlates with the extent of NFT (Bramblett et al., 1992). While PHF-tau is unable to bind to microtubules, dephosphorylation restores its ability to bind to microtubules and promotes microtubule assembly (Bramblett et al., 1993; Iqbal et al., 1994; Wang et al., 1995). The levels of total tau in AD cerebral cortex are 4-8 folds higher than those in the corresponding tissue from age-matched control cases. The increase in tau level is in the form of

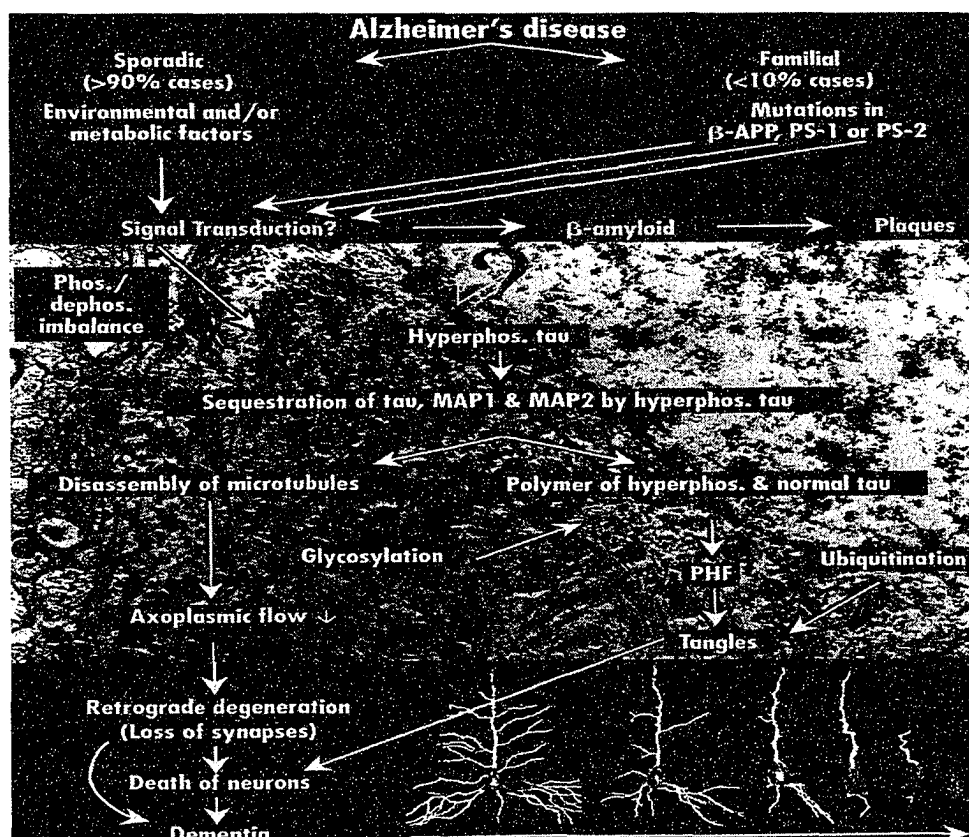
hyperphosphorylated tau, whereas the level of normal tau in AD brain is similar to that in control brains (Khatoon et al., 1992; 1994).

Neurons also contain high molecular weight-microtubule associated proteins (HMW-MAPs), such as MAP1 and MAP2, which also promote assembly and maintain the structure of microtubules. Recent studies have shown that AD P-tau can associate to normal tau, MAP1 and MAP2, and sequester them from stimulating microtubule assembly (Alonso et al., 1996; 1997). Thus, it can be postulated that hyperphosphorylation of tau destabilizes the microtubule network, disrupts axonal transport, generates NFT and ultimately axonal degeneration associated with neuronal death. As consequences of these events, corticocortical connections would be disrupted leading to impairments of synaptic transmission followed by the emergence of cognitive impairments in AD.

### **1.7. AD and Other Tauopathies**

In addition to AD, a group of heterogeneous dementias and movement disorders, which are characterized neuropathologically by prominent intracellular accumulations of abnormal filaments formed by tau, appears to share common mechanisms of disease. They are collectively known as neurodegenerative tauopathies that include Down's syndrome, frontotemporal dementia with parkinsonism linked to chromosome 17 (FTDP-17), Pick's disease and several others (for review, see Lee et al., 2001). Despite their diverse phenotypic manifestations, brain dysfunction and degeneration in tauopathies is linked to the progressive accumulation of filamentous tau inclusions, and this, together with the absence of other disease-specific neuropathological abnormalities, provided

circumstantial evidence implicating abnormal tau in disease onset and progression. However, this point of view remained unproven until 1998, when multiple tau gene mutations were discovered in FTDP-17 (Foster et al., 1997, Hutton et al., 1998, Poorkaj et al., 1998, Spillantini et al., 1998c), thereby providing direct evidence that tau abnormalities alone are sufficient to cause neurodegenerative disease. This seminal finding opened new avenues for investigating the role of tau abnormalities in multi-mechanisms of brain dysfunction and degeneration.



I. Grundke-Iqbal, K. Iqbal, 1999,  
 What is the most promising target for the treatment of Alzheimer's disease: Inhibition of  $\beta$ -amyloidosis or abnormal hyperphosphorylation of tau? *The News*. (1) 4-5.

**Fig. 2. Tau Hypothesis**

## **1.8. Post-translational Modifications of Proteins involved in AD**

Many proteins are subjected to co-translational or post-translational modifications before folding into an appropriate conformation and becoming biologically active. These modifications include phosphorylation, glycosylation, methylation, acylation, acetylation, and proteolytic processing. Several proteins involved in the pathogenesis of AD are modified proteins. For examples, tau, APP, and presenilins are normally phosphoproteins, and the phosphorylation regulates their activity/processing (Gooch and Stennett, 1996). APP and presenilins are also modified by glycosylation that plays an important role in the processing/trafficking of the proteins (Georgopoulou, et al., 2001). Proteolytic processing is believed necessary for presenilin to have its activity of  $\gamma$ -secretase (Roberts, 2002; Tandon and Fraser, 2002), whereas the various proteolytic sites of APP determine whether the cleaved products are amyloidgenic (For review, see Van Gassen and Annaert, 2003).

### ***1.8.1. Abnormal Hyperphosphorylation of Proteins in AD***

Abnormal co- and post-translational modifications of some key proteins have been implicated in the molecular mechanism of AD. Abnormal hyperphosphorylation of tau is one of the most notable biochemical changes in AD brain (Grundke-Iqbal, et al., 1986b) and appears to be critical to the neurofibrillary degeneration of AD (Iqbal, et al., 2000). In addition to tau, some other proteins such as neurofilaments,  $\beta$ -tubulin, and  $\beta$ -catenin are also hyperphosphorylated (Wang et al., 2001; Vijayan et al., 2001; Gong et al., 2003).

This has probably resulted from a phosphorylation/dephosphorylation imbalance due to a decrease in protein phosphatase activities in AD brain (Gong et al., 1993; 1995).

### ***1.8.2. Protein Glycosylation***

Protein glycosylation is one of the most common modifications of membrane-bound and secreted eukaryotic proteins. The vast majority of cell surface and secreted proteins are glycoproteins. Through glycosylation, oligosaccharides are covalently attached to the side chains of polypeptides co-translationally and/or post-translationally in rough endoplasmic reticulum and Golgi apparatus. According to the nature of glycosidic bonds, two major types of linkages are defined: O-linkage and N-linkage. In the former case, sugars are transferred one by one to hydroxyl groups of serine or threonine residues of polypeptides from an active form of sugar donor, uridine diphosphate(UDP)-sugar, by the catalysis with a large number of enzymes named glycosyltransferases. The specificity of these enzymes depends on the nature of the glycoconjugate acceptor, i.e., the glycoprotein, the non-reducing terminal sugar and the oligosaccharide sequence. The result of this specificity is the formation of certain structures, the exclusion of others and the existence of ordered pathways in the formation of defined oligosaccharide structures. In the case of N-linked glycosylation, the sugar chain is transferred from dolichol diphosphate-oligosaccharides to the amide group of asparagine side chain of acceptor proteins by the catalysis of various protein-oligosaccharide transferases. The oligosaccharides attached on the protein are further processed by removing and adding a variety of sugars when the glycoprotein moves through endoplasmic reticulum to Golgi

apparatus (Verbert and Cacan, 1999). This process is called the maturation of the glycoprotein.

In general, carbohydrates attached to proteins through glycosylation are critical to a variety of functions of the protein, such as structural and antigenic determinants, cell adhesion, membrane transport, growth factor binding, targeting and receptors. Because of the hydrophilicity of the sugars, covalently attached carbohydrates maintain the solubility of glycoproteins and ensure the correct folding of the extracellular domains. A defective glycosylation of glycoproteins has been implicated in the pathogenesis of a number of inherited or acquired human diseases such as congenital anemia, rheumatoid arthritis, and liver cancer (Verma and Davidson, 1994; Koscielak, 1995; Breen, et al., 1998).

### ***1.8.3. Protein Glycosylation involved in AD***

The molecular pathogenesis of AD appears to involve a dysregulation of protein glycosylation. Several proteins associated with AD are modified by glycosylation, including APP, presenilins, and tau. It has been demonstrated that the glycosylation may modulate the intracellular sorting of APP and therefore may play a role in generation of A $\beta$  peptides (Yazaki, et al., 1996). The O-glycosylated clathrin assembly protein AP180, which plays a critical role in synaptic vesicle recycling, is reduced in AD brain (Yao, et al., 1998). The O-GlcNAcylation of the detergent insoluble cytoskeleton proteins was reported to be increased in AD (Griffith and Schmitz, 1995), though the total O-GlcNAcylation level of brain homogenate seems decreased in AD (unpublished data).

The expression of sialyltransferase that transfers sialic acid onto oligosaccharides of the glycoproteins is down regulated in AD brain (Maguire and Breen, 1995).

Our lab recently discovered that tau is aberrantly glycosylated in AD brain (Wang, et al., 1996; Liu et al., 2002a). Our finding was in agreement with a previous observation that found the presence of glucose and mannose in PHFs (Goux, et al., 1995). Deglycosylation of PHF tangles by endoglycosidase F/N-glycosidase F untwists PHFs into bundles of straight filaments ( $2.5 \pm 0.5$ nm in diameter), suggesting that glycosylation might be involved in the maintenance of PHF structure. Therefore, it appears that while the abnormal hyperphosphorylation makes tau dysfunctional and polymerized, the glycosylation probably helps maintain and stabilize the NFTs. In addition, the aberrant tau glycosylation promotes subsequent phosphorylation and inhibits subsequent dephosphorylation of tau in vitro (Liu et al., 2002a, 2002b, 2002c), suggesting that it may play a role in the abnormal hyperphosphorylation and hence neurofibrillary degeneration of AD. However, all the previously identified glycoproteins with classical N- and O-linked glycosylation are either secreted proteins or membrane-bound proteins. The discovery that tau isolated from AD brain is also modified by these types of glycosylation is the first report showing a cytoplasmic protein modified by classical glycosylation. It is currently not known how tau becomes glycosylated. One possibility would be that glycosyltransferases leak from endoplasmic reticulum and Golgi apparatus into cytoplasmic compartment of the affected neurons in AD brain. The abnormalities of these subcellular organelles of neurons have been reported in AD (Gray, et al., 1987). Hence, it is possible that the protein glycosylation system might be disrupted in AD brain, which may cause abnormal glycosylation of other proteins besides tau.

In 1984, a novel type of protein glycosylation by O-linked N-acetylglucosamine (O-GlcNAc) was discovered by Hart and his colleagues (Torres and Hart, 1984; Hart, 1997). This O-GlcNAcylation occurs in nucleoplasmic and cytoplasmic compartments rather than endoplasmic reticulum and Golgi (Snow and Hart, 1998). It is highly dynamic, with rapid cycling in response to cellular signals or cellular stages (Haltiwanger, et al., 1990; Dong and Hart, 1994; Griffith and Schmitz, 1995). All proteins modified with O-GlcNAcylation identified so far are also phosphoproteins (Hart, et al., 1996). Interestingly, O-GlcNAcylation has been found in many cytoskeletal proteins such as neurofilaments (Dong, et al., 1993), synapsins (Luthi, et al., 1991), cytokeratins (Chou, et al., 1992), high molecular weight microtubule associated proteins MAP1, MAP2 and MAP4 (Ding and Vandre, 1996), and tau (Arnold, et al., 1996). A mis-regulation of protein O-GlcNAcylation has been proposed in neurodegenerative diseases (Zachara and Hart, 2002).

## 2. SPECIFIC AIMS

AD is a multi-factorial degenerative disorder and its pathogenic mechanism has not been understood. One of the most characteristic biochemical changes in AD brain is the abnormal hyperphosphorylation of tau, which consequently aggregates into NFTs of PHFs. Our group recently discovered that in addition to the abnormal hyperphosphorylation, tau in AD is abnormally glycosylated, suggesting that the protein glycosylation system may be affected in AD brain. Based on these findings, we hypothesized that there are other neuronal glycoproteins that are also altered in AD brain and these glycoproteins might be involved in the molecular pathogenesis of AD. The goal of this project is to identify these altered glycoproteins in addition to tau in AD brain.

To test our hypothesis, we propose to:

1. Identify major glycoproteins in AD brain;
2. Search for glycoproteins that are altered in AD brain;
3. Investigate the subcellular distribution of the altered glycoproteins in AD brain;
4. Isolate and identify these altered glycoproteins.

### 3. MATERIALS AND METHODS

#### 3.1. Brain Tissue

The brain tissues of 12 AD patients with a mean age of  $73.6 \pm 8.9$  yrs and 12 controls with a mean age of  $75.5 \pm 8.8$  yrs were chosen for the present study. All the AD brains had been histopathologically confirmed and contained the lesions of plaques and tangles that are specific for AD. Detailed information is listed in the Table 1 and Table 2. The human brain tissues were obtained from Harvard Brain Tissue Resource Center, Mclean Hospital, Belmont, MA; National Alzheimer's Disease Brain Bank, University of California, San Diego, CA; and Netherlands Brain Bank, The Netherlands.

**Table 1. Control and AD Brain Tissues Used for Tissue Homogenates**

Cases	Brain Region	Age (yr)	Sex	Post-mortem Delay (hr)
Control 1	Frontal Cortex	83	M	8
Control 2	Frontal Cortex	59	F	4.5
Control 3	Frontal Cortex	73	M	7
Control 4	Temporal Cortex	83	F	8
Control 5	Temporal Cortex	82	M	5.5
Control 6	Temporal Cortex	84	M	4.5
Mean $\pm$ SD	-	$75.5 \pm 8.8$	-	$6.25 \pm 1.6$
AD 1	Frontal Cortex	70	F	4.5
AD 2	Frontal Cortex	63	F	3.5
AD 3	Frontal Cortex	79	M	7
AD 4	Temporal Cortex	87	F	3
AD 5	Temporal Cortex	69	M	4
AD 6	Temporal Cortex	77	F	5
Mean $\pm$ SD	-	$73.6 \pm 8.9$	-	$5.1 \pm 2.0$

**Table 2. Control and AD Brain Tissues Used for Membrane Extracts**

Cases	Brain Region	Age	Sex	Post-mortem Delay (hr)
Control 1 (#2153)	Frontal Cortex	82	M	6
Control 2 (#2100)	Frontal Cortex	65	F	4
Control 3 (#2249)	Frontal Cortex	76	M	5.5
Control 4 (#2173)	Temporal Cortex	78	M	3
Control 5 (#1000)	Temporal Cortex	62	M	6.1
Control 6 (#1833)	Temporal Cortex	79	F	5.5
Mean $\pm$ SD	-	73.6 $\pm$ 8.2	-	5.0 $\pm$ 1.2
AD 1 (#2409)	Frontal Cortex	55	F	9
AD 2 (#2319)	Frontal Cortex	79	M	8
AD 3 (#3524)	Frontal Cortex	83	M	4.5
AD 4 (#3358)	Temporal Cortex	79	M	3.4
AD 5 (#4039)	Temporal Cortex	74	M	2.2
AD 6 (#4040)	Temporal Cortex	69	M	1
Mean $\pm$ SD	-	73.2 $\pm$ 10.1	-	4.7 $\pm$ 3.2

### 3.2. Chemicals and Reagents

Tau antibodies 92e and R134d were raised in our lab. PHF-1 was a gift from Dr. P. Davies of Albert Einstein College of Medicine, Bronx, NY, USA. I $\kappa$ B $\gamma$  polyclonal antibody and anti-mouse/rabbit-HRP were from Santa Cruz Biotechnology Labs, Santa Cruz, CA, USA. Polyclonal antibody anti-human acid ceramidase was a gift from Dr. K. Sandhoff, University of Bonn, Germany.

Methyl- $\alpha$ -D-Mannopyranoside,  $\beta$ -Lactose, D(+)-Galactose, N-Acetyl-D-Glucosamine and Coomassie Brilliant Blue G were from Sigma-Aldrich, St. Louis, MO, USA.

ConA, GNA, SNA, PNA and DSA agarose were from Vector Laboratories, Inc., Burlingame, CA, USA.

DEAE-sephacel agarose was from Amersham Biosciences Corp., Piscataway, NJ, USA.

Silver staining kit, protein G beads and BSA standard were from Pierce Biotechnology Inc., Rockford, IL, USA.

PNGase F was from New England Biolabs Inc., Beverly, MA, USA.

Caboxypeptidase Y, fetuin and asialofetuin were from Roche Molecular Biochemicals, Indianapolis, IN, USA.

Lectins used in this study were listed in Table 3.

### **3.3. Tissue Homogenate**

Gray matter was dissected from brain regions rich in plaques and tangles of AD cases and from the same regions of age-matched control brains (Table 1 and 2). Homogenates (10%) were made from these tissues at 4°C using a Teflon glass homogenizer in a buffer containing 50 mM Tris, pH 7.6, 150 mM NaCl, 1 mM CaCl<sub>2</sub>, 1 mM MnCl<sub>2</sub>, 1 mM MgCl<sub>2</sub>, 0.5 mM PMSF, 2 µg/ml Leupeptin, 2 µg/ml Aprotinine, and 1 µg/ml Pepstatin A. Homogenates were aliquoted and stored at – 80°C.

**Table 3. Lectins used in this study**

Lectin (abbreviation)	Specificity*	Conjugation	Final conc. ( $\mu\text{g/ml}$ )	Source
Abrus precatorius agglutinin (APA)	$\beta$ -Gal	Biotin	2	Sigma-Aldrich <sup>^</sup>
Bauhinia purpurea (BPA)	Gal $\beta$ 1- 3GalNAc	Biotin	2	Sigma-Aldrich <sup>^</sup>
Caragana arborescens (CAA)	GalNAc	Biotin	2	Sigma-Aldrich <sup>^</sup>
Concanavalin A (ConA)	$\alpha$ -Man	HRP	4	EY Lab <sup>#</sup>
Datura stramonium agglutinin (DSA)	Gal $\beta$ 1- 4GlcNAc	HRP	20	EY Lab <sup>#</sup>
Galanthus nivalis agglutinin (GNA)	$\alpha$ -Man (terminal)	HRP	4	EY Lab <sup>#</sup>
Lens culinaris (LCA)	$\alpha$ -Man (with fuc.)	Biotin	2	Sigma-Aldrich <sup>^</sup>
Maackia amurensis agglutinin (MAA)	SA $\alpha$ 2-3Gal	HRP	10	EY Lab <sup>#</sup>
Peanut agglutinin (PNA)	Gal $\beta$ 1- 3GalNAc	HRP	20	EY Lab <sup>#</sup>
Ricinus communis (RCA)	GalNAc, $\beta$ Gal	HRP	5	Sigma-Aldrich <sup>^</sup>
Salbicus mogra agglutinin (SNA)	SA $\alpha$ 2-6Gal	HRP	40	EY Lab <sup>#</sup>
Tetragonolobus purpureas (TGP)	$\alpha$ -L-Fuc	HRP	40	Sigma-Aldrich <sup>^</sup>
Ulex europaeus (UEA I)	$\alpha$ -L-Fuc	HRP	40	Sigma-Aldrich <sup>^</sup>
Wheat germ agglutinin (WGA)	GlcNAc	HRP	5	EY Lab <sup>#</sup>
Wistaria floribunda (WFA)	GalNAc	Biotin	2	Sigma-Aldrich <sup>^</sup>

\*: The terminal sugars of the oligosaccharides of glycoproteins that is specifically recognized by the lectin are listed in this column.

<sup>^</sup>: Sigma-Aldrich, St. Louis, MO.

<sup>#</sup>: EY Laboratories, Inc., San Mateo, CA.

Abbreviations: Fuc, fucose; Gal, D-galactose; GalNAc, N-acetyl-D-galactosamine; Glc, D-glucose; GlcNAc, N-acetyl-D-glucosamine; Man, mannose; SA, Sialic acid; HRP, Horseradish Peroxidase.

### 3.4. Lectin Blot Analysis

AD and control homogenate samples were resolved by 10% or 15% SDS-polyacrylamide gel electrophoresis (PAGE) as described originally by Laemmli (Laemmli, 1970), followed by transferring proteins electrophoretically to Immobilon (PVDF) membranes (Millipore, Bedford, MA, USA). After transferring, the membranes were blocked by 3% BSA-TBS (bovine serum albumin-50 mM Tris buffer, pH 7.6, 150 mM NaCl) for at least 30 min, then washed with TBS (50 mM Tris, pH 7.6, 150 mM NaCl in H<sub>2</sub>O) for 10 min twice and Buffer I (1 mM MgCl<sub>2</sub>, 1 mM MnCl<sub>2</sub>, 1 mM CaCl<sub>2</sub>, in TBS) for 10 min once. The blots were incubated with various lectin solutions diluted in Buffer I for 1 hr, then washed with TBS for 10 min three times. Lectins themselves are proteins or glycoproteins. They are commonly used to detect and identify glycoconjugates, since they each specifically bind to different sugar moieties (Cummings, 1994). These lectins were pre-conjugated with digoxigenin, horseradish peroxidase (HRP), or biotin (Table 3). For HRP-conjugated lectins, such as ConA, RCA, TGP, WGA, and UEA, the blots were developed right away in developing solution (40 mg DAB, 25  $\mu$ l 30% H<sub>2</sub>O<sub>2</sub> in 80 ml TBS). For biotin or digoxin-labelled lectins, the blots were incubated with avidin-HRP (final concentration 2  $\mu$ g/ml in TBS, Pierce) and anti-DIG-AP (10  $\mu$ l in 10 ml TBS, Dig Glycan Differentiation Kit, Roche), respectively, for another 1 hr. After washing with TBS for 10 min three times, the blots were developed. For AP (Alkaline Phosphatase) labeled lectins, the developing solution was the mixture of 4-nitro blue tetrazolium chloride (NBT), 5-bromo-4-chloro-3-indoyl phosphate (BCIP), and 0.1 M NaHCO<sub>3</sub> (1:1:98).

### 3.5. Western Blot Analysis

AD and control homogenate samples were resolved by 10% or 15% SDS-polyacrylamide gel electrophoresis (PAGE) as described originally by Laemmli (Laemmli, 1970), followed by transferring proteins electrophoretically to Immobilon-P (PVDF) membranes (Millipore, Bedford, MA, USA). After transferring, the membranes were blocked by 5% milk-TBS, and incubated with the appropriate primary antibodies, followed by incubation with HRP (horseradish peroxidase) labeled secondary antibodies. After the membranes were washed adequately with TBS, the membranes were incubated with ECL reagents (1:1) or developing solution (40 mg DAB, 25  $\mu$ l 30% H<sub>2</sub>O<sub>2</sub> in 80 ml TBS). The visualized protein bands were quantitated with TINA 2.0 software.

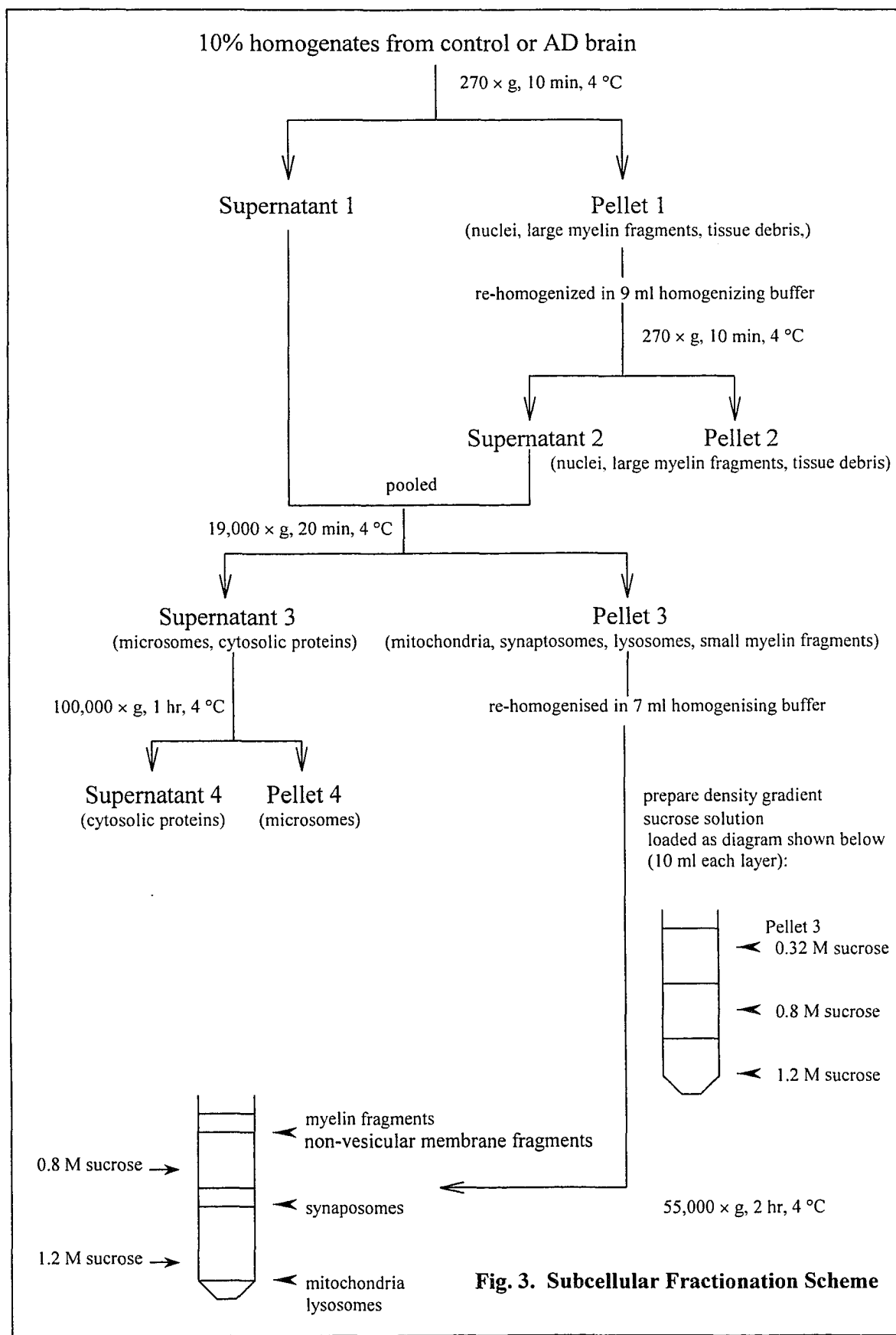
### 3.6. In Vitro Deglycosylation

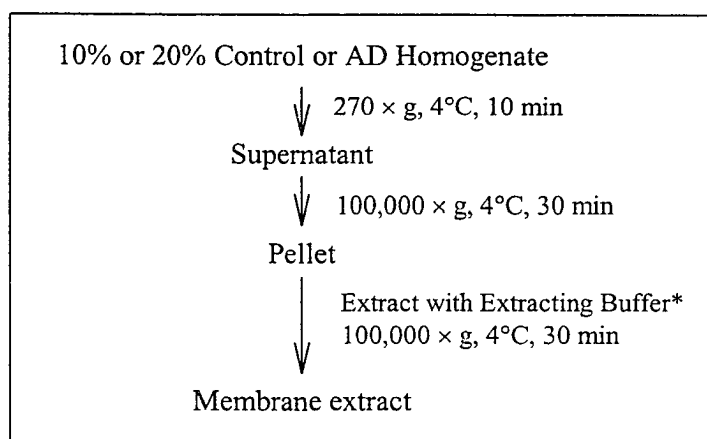
ConA-positive glycoprotein mixtures were first dried in speed vacuum concentrator, dissolved in 20% SDS and deionized water to the final concentration of 1% SDS, and then heated in a 95°C water bath for 10 min. The protein mixtures were further diluted with a deglycosylation buffer containing 50 mM NaPO<sub>4</sub>, pH 7.4, 50 mM EDTA, 0.1% NaN<sub>3</sub>, and 0.5% NP-40 to the final concentration of 0.1% SDS. The solution was heated in a 95°C water bath for 10 min and then sonicated in a bath sonicator for 20 min. The sample was then divided into two equal parts. Into one part, 6U/ml PNGase F, 0.5 mM PMSF, 2  $\mu$ g/ml Leupeptin, 2  $\mu$ g/ml Aprotinine, and 1  $\mu$ g/ml Pepstatin A were added. Into the other half, deionized water equal to the total volume of the added enzymes was added. The solutions were then incubated at 37°C overnight, followed by adding reducing (1% BME) or non-reducing (no BME) sample buffer, boiling and bath

sonication for 10 min each, and resolved on 10% or 15% SDS-PAGE for lectin or Western Blots.

### 3.7. Subcellular Fractionation

Subcellular fractionation of brain homogenates was prepared according to the method of Whittaker, et al. (1964) with modifications. Firstly, 10% homogenates were made from brain tissue by using the homogenising buffer as described above plus 0.32 M sucrose and were centrifuged at  $270 \times g$  at  $4^{\circ}\text{C}$  for 10 min. The resulting supernatant and pellet were named as supernatant 1 and pellet 1. Then, pellet 1 containing nuclei, debris, and unbroken cells was re-homogenized in homogenizing buffer and centrifuged again for 10 min. The supernatant 1 and supernatant 2 were pooled together and centrifuged at  $19,000 \times g$  at  $4^{\circ}\text{C}$  for 20 min. The resulting supernatant 3 containing microsomes and cytosolic proteins was centrifuged at  $100,000 \times g$  for 1 hr at  $4^{\circ}\text{C}$  to separate cytosolic proteins into supernatant 4 and microsomes into pellet 4. The pellet 3 was re-homogenised in homogenising buffer and loaded onto the top of 0.32 M, 0.8 M, and 1.2 M sucrose gradients (10 ml each) and centrifuged at  $55,000 \times g$  for 2 hr at  $4^{\circ}\text{C}$  to separate subcellular fractions by velocity sedimentation. The top layer was concentrated with other membrane structures, while mitochondria and lysosomes were focused in the bottom layer. The layer located between the two sucrose gradient layers and in the middle of the tube contained synaposomes (Fig. 3). Each layer was collected separately. Before storing at  $-80^{\circ}\text{C}$ , the subcellular fractions were re-homogenised with homogenising buffer and aliquoted after measuring protein concentration by using Bradford method (Bradford, 1976).





\* Extracting Buffer: 0.5 % Triton X-100, 0.05 % SDS, 1 mM CaCl<sub>2</sub>, 1 mM MgCl<sub>2</sub>, 1 mM MnCl<sub>2</sub> in TBS.

**Fig. 4. Membrane Protein Preparation**

### 3.8. Membrane Protein Extraction

AD brain temporal cortex was dissected and made into 10% or 20% homogenate in homogenising buffer described above. Then the homogenate was centrifuged at 270 × g for 10 min at 4°C. The resulting supernatant was centrifuged at 100,000 × g for 30 min at 4°C. The resulting pellet contained most membrane structures of the neural cells. Then the pellet was extracted in buffer containing 0.5% Triton X-100, 0.05% SDS, 1 mM CaCl<sub>2</sub>, 1 mM MgCl<sub>2</sub>, 1 mM MnCl<sub>2</sub> in TBS by using homogenizer followed by centrifugation at 100,000 × g for 30 min at 4°C to get the supernatant. This supernatant called membrane extract contained membrane proteins. The glycoproteins in the membrane extract were further enriched by chromatographies described below. The procedure of membrane protein extraction is outlined in Fig. 4.

### 3.9. Lectin Affinity Chromatography

1). *ConA* affinity chromatography:

ConA agarose beads (from Vector) were first washed extensively with the membrane extracting buffer. Then the membrane extract was mixed with ConA agarose beads at a ratio of 20 mg protein/1 ml beads at room temperature for 2 hrs before packing into a small column (1 × 10 cm). The flow-through during packing was saved and the column was washed with 40 × bed volumes of extracting buffer. The first bed volume of wash was saved as well. The column was then eluted with 10 × bed volumes of pre-warmed (to 60°C) 500 mM Methyl- $\alpha$ -D-Mannopyranoside in the buffer. The eluted fractions were designed as Elution I. Then the column was incubated with 2 × bed volumes of 500 mM Methyl- $\alpha$ -D-Mannopyranoside, 10 mM EDTA, 0.5% Triton, 0.05% SDS in TBS, at room temperature, overnight. The elution was collected at the next day and designed as Elution II (Fig. 5). In elution buffer, Methyl- $\alpha$ -D-Mannopyranoside competed with mannose moieties of glycoproteins to bind with ConA and the high temperature can help to make the mannose moieties more accessible. Even though most of ConA-binding glycoproteins can be eluted out by the conditions of Elution I, some tightly ConA-binding glycoproteins still stayed on the beads. If we incubated ConA beads overnight with 500 mM Methyl- $\alpha$ -D-Mannopyranoside solution plus 10 mM EDTA and minus  $\text{Ca}^{2+}$ ,  $\text{Mg}^{2+}$  and  $\text{Mn}^{2+}$  as compared with Elution I, the tightly ConA-binding glycoproteins eluted out because the metal ions that are essential for ConA binding were chelated by EDTA (Fig. 5).

In big preparations, the binding of glycoproteins (225 mg) to ConA agarose was carried out in the column with a flow rate of 12 ml/hour.

2). *SNA, GNA, PNA and DSA affinity chromatographies:*

We linked in tandem SNA and GNA columns together, SNA column first then GNA column (0.5 × 6 cm, 1.5 ml of bed volume), so the flow-through from SNA column could pass GNA column directly, and we could get better separation of glycoproteins. Large amount of buffer was used to equilibrate the SNA and GNA columns because the protective sugar for stabilizing lectins needed to be washed off. According to binding capacity of both lectins, about 1 mg sample was loaded onto 0.3 ml settled lectin beads, both SNA and GNA. The binding flow rate was controlled to be 1 ml/ hour whereas the eluting flow rate was 6.8 ml/hour. Fractions were collected as 1 ml each. Chromatography profile was drawn by OD<sub>280</sub> protein detector and as equal amount of solution from each fraction was resolved on 10% SDS-PAGE followed by Coomassie blue (20 µl) or lectin staining (5 µl) (Fig. 6).

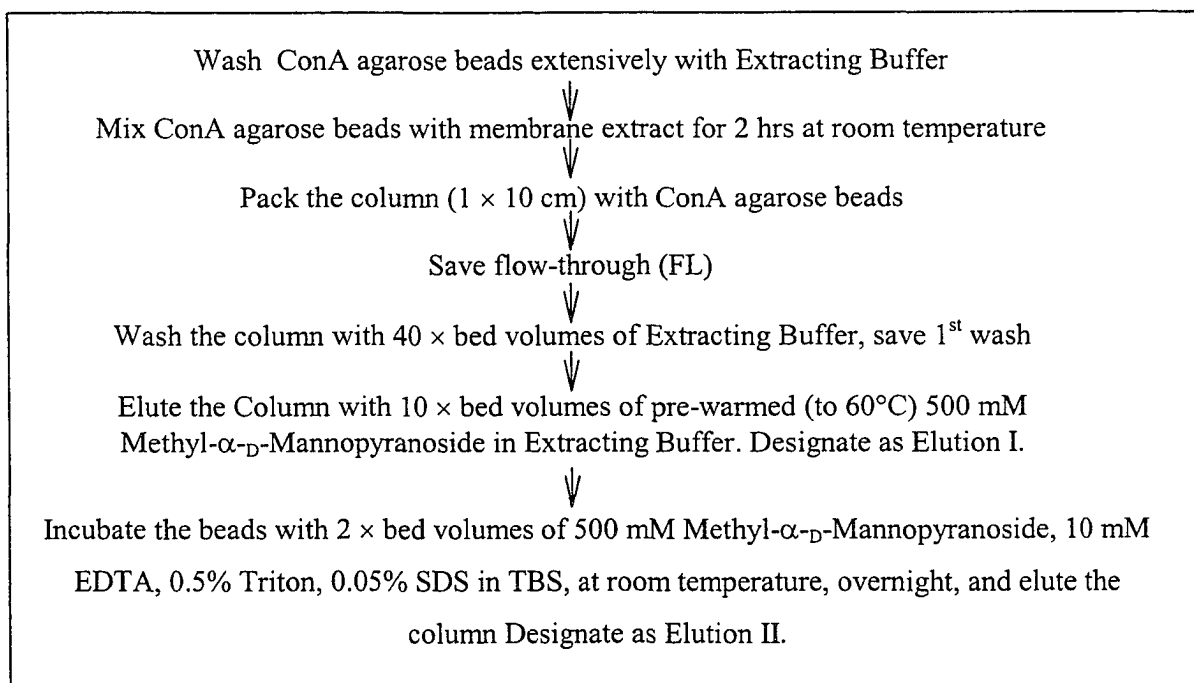


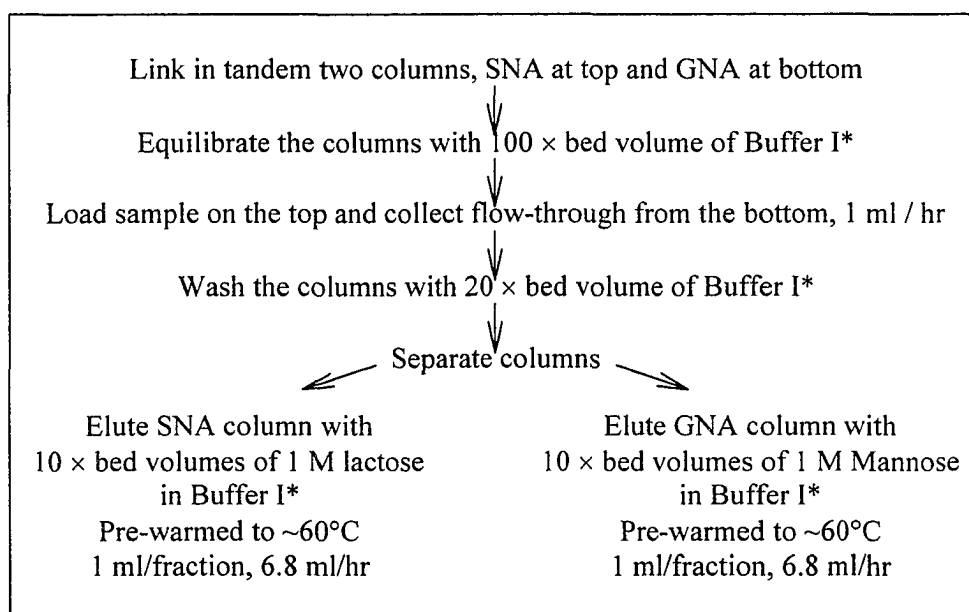
**Fig. 5. ConA Affinity Chromatography Scheme**

**Table 4. Eluting Conditions of SNA, PNA, DSA and GNA Affinity Chromatography**

	E <sub>1</sub>	E <sub>2</sub>	E <sub>3</sub>	E <sub>4</sub>
SNA	0.5 M Lactose in Buffer I*	0.5 M Lactose in 0.2 M Acetic Acid	1 M Lactose in Buffer I*	1 M Lactose 1 M NaCl 10 mM EDTA 50 mM Tris, pH 7.6 60°C
	RT**	RT**	60°C	
PNA	0.2 M Galactose in Buffer I*	0.2 M Galactose in Buffer I*, pH 3.0	0.5 M Galactose in Buffer I*	1 M Galactose 1 M NaCl 10 mM EDTA 50 mM Tris, pH 7.6 60°C
	RT**	RT**	60°C	
DSA	0.3 M GlcNAc in Buffer I*		0.5 M GlcNAc in Buffer I*	1 M GlcNAc 1 M NaCl 10 mM EDTA 50 mM Tris, pH 7.6 60°C
	RT**		60°C	
GNA	0.5 M Mannose in Buffer I*		1 M Mannose in Buffer I*	1 M Mannose 1 M NaCl 10 mM EDTA 50 mM Tris, pH 7.6 60°C
	RT**		60°C	

\* Buffer I: 1 mM CaCl<sub>2</sub>, 1 mM MgCl<sub>2</sub>, 1 mM MnCl<sub>2</sub> in TBS.

\*\* RT: Room Temperature.



\* Buffer I: 1 mM CaCl<sub>2</sub>, 1 mM MgCl<sub>2</sub>, 1 mM MnCl<sub>2</sub> in TBS.

**Fig. 6. SNA and GNA Chromatography Scheme**

Since various lectins have different characters and competitive sugars, eluting conditions of SNA, GNA, PNA and DSA affinity chromatographies were different (see Table 4). From E<sub>1</sub> to E<sub>4</sub>, the conditions were from weak to strong to elute the glycoproteins.

### **3.10. DEAE-Ion Exchange Chromatography**

DEAE sephacel ion exchange column (1.0 × 10 cm) with bed volume of 6 ml was equilibrated with 10 × bed volumes of 50 mM Tris-HCl, pH 7.6 and loaded with dialysed ConA-binding glycoproteins at a ratio of 1 mg protein/3 ml bed volume. After loading samples at a flow rate of 0.1 ml/min, the column was washed with 2 × bed volumes of 50 mM Tris-HCl, pH 7.6 and followed by elution with 10 × bed volumes of 0 ~ 1 M NaCl gradient in 50 mM Tris-HCl, pH 7.6.

### **3.11. High Performance Liquid Chromatography (HPLC)**

The 100,000 × g pellets of homogenates from brain gray matter were re-homogenized at 4°C in buffer (0.1% Triton X-100, 0.1% Tween-20, 300 mM NaCl, 50 mM Tris, PH 7.6, 150 mM NaCl, 1 mM CaCl<sub>2</sub>, 1 mM MnCl<sub>2</sub>, 1 mM MgCl<sub>2</sub>, 0.5 mM PMSF, 2 µg/ml Leupeptin, 2 µg/ml Aprotinine, and 1 µg/ml Pepstatin A), and probe sonicated for 3 min at 4°C. After being chilled on ice for 1 hour, the extracts were centrifuged at 100,000 × g for 30 min, and the resulting supernatants were dialyzed at 4°C over-night followed by polyethylene glycol concentration for 3 hours. The concentrated sample was filtered through 0.22 µm filter, and the filtrates were subjected to HPLC (Fig. 7).

An anion ion exchange column, resource Q (1 ml, Amersham Biosciences), was connected to ÄKTA purifier (Amersham Biosciences). The pH was adjusted to 7.0. Flow rate was controlled at 4 ml/min. Filtered sample (0.5 ml, ~1.2 mg) was injected into equilibrated column. After saving flow-through and wash, fractions (0.5 ml) were collected with 0 ~ 1 M NaCl gradient (fractions 1 ~ 11). Silver staining and MAA blot were employed to check which fractions were rich in the 45 kDa protein.

### 3.12. Immunoprecipitation

Protein G beads (Pierce) were washed three times with immunoprecipitation buffer (IP buffer: 20 mM Na<sub>3</sub>PO<sub>4</sub>, pH 7.5, 500 mM NaCl, 1% NP-40, 0.5% Sodium Deoxycholate, 0.1% SDS, 0.02% NaN<sub>3</sub>). Anti-IκBγ polyclonal antibody 20 μl (about 4 μg IgG) were mixed with 50 μl protein G beads in 150 μl IP buffer and incubated at room temperature for 2 hours. The beads were then washed with IP buffer 5 times, 200 μl each. Protein mixture (100 μg) in 200 μl IP buffer was incubated with beads at 4°C overnight, then washed with IP buffer 5 times, 200 μl each. Immunoprecipitation products were eluted with 50 μl Laemmli buffer and boiled for 5 min, followed by 10% SDS-PAGE.

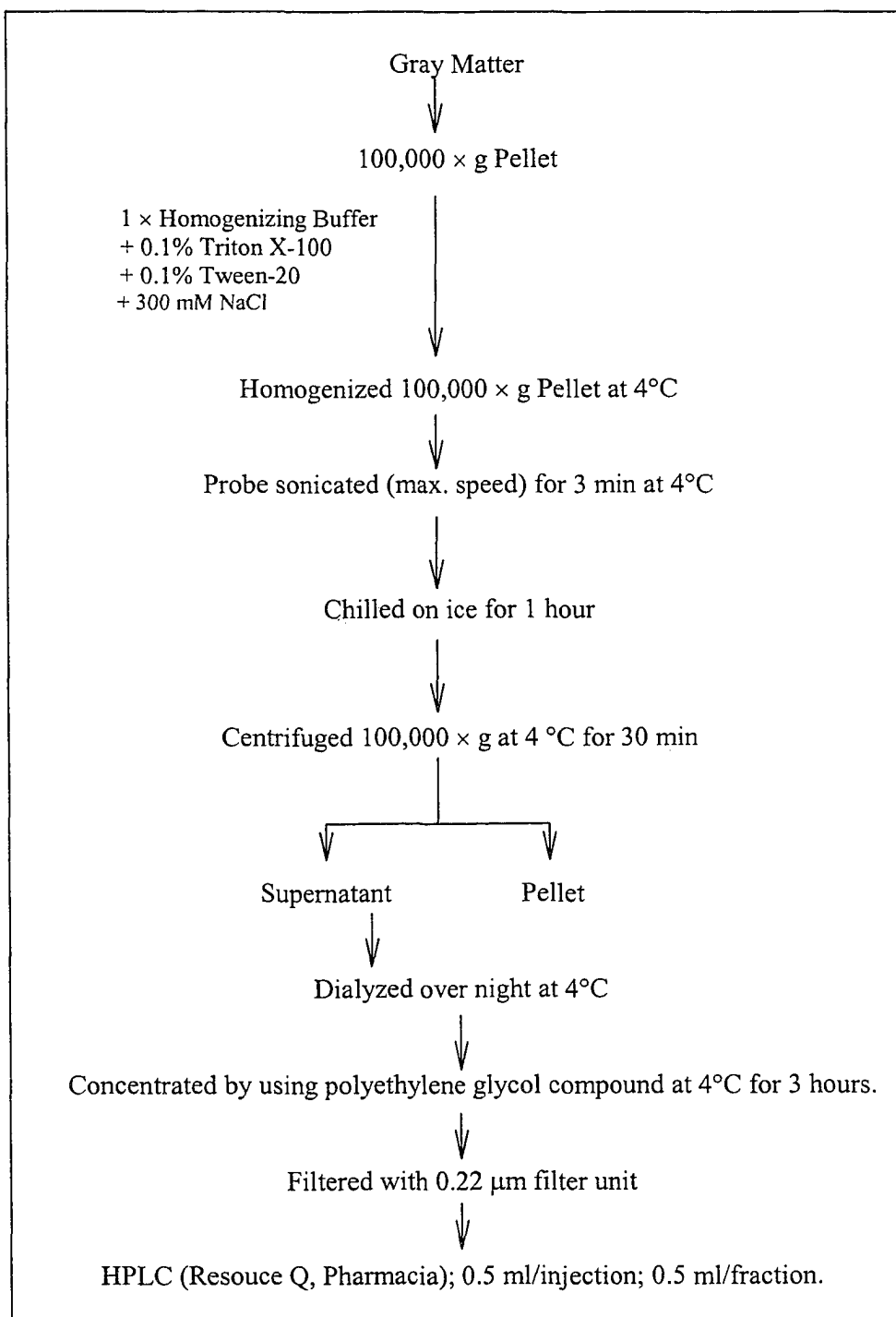


**Fig. 7. HPLC Sample Preparation**

### **3.13. Preparative SDS-PAGE**

Preparative electrophoresis was carried out using Model 491 Prep Cell (Bio-rad Laboratories). It purifies target proteins according to their molecular masses. Protein sample (1 mg) was heated for 5 min in Laemmli buffer before loading on top of the stacking gel of the Prep Cell. Fractions (2 ml each) were collected at a flow rate of 60 ml/hr. Electrophoresis was carried out at a constant voltage of 100 volts. The fractions were concentrated by using Amicon concentrators.

### **3.14. Ammonium Sulfate Precipitation**

Ammonium sulfate saturations of 25%, 40%, 50%, and 60% were used to precipitate the sample prepared for HPLC. Precipitated pellet extract with 25% (p1), 40% (p2), 50% (p3), 60% (p4) ammonium sulfate, 60% ammonium sulfate supernatant (S).

### **3.15. Identification of Proteins**

In order to identify the proteins, we used cold acetone to precipitate purified proteins followed by 10% SDS-PAGE and staining with Coomassie blue. After destaining thoroughly, the gel was washed in deionized water for 3 hours with several changes, and the protein bands were labelled and dissected. Dried in air overnight, the protein bands were analysed by Mass Spectrometry at Beckman Centre, Stanford University, CA, and by N-terminal amino acid sequencing at Molecular Resource Facility, New Jersey Medical School, NJ. ProFound is the search program for mass spec data ([http://129.85.19.192/profound\\_bin/WebProFound.exe?Form=1](http://129.85.19.192/profound_bin/WebProFound.exe?Form=1)) and NCBI BLAST is for N-terminal amino acid sequencing data (<http://www.ncbi.nlm.nih.gov/BLAST/>).

### 3.16. Immunohistochemistry

The control and AD human brain tissue sections (40  $\mu\text{m}$  thick) were treated with 0.3%  $\text{H}_2\text{O}_2$  plus 5% BSA in TBS for 30 min and blocked with 3% normal goat serum (NGS) in BSA/TBS for 10 min. Polyclonal antibody against human acid ceramidase (anti-hAC) was used at 1:500 dilution. After overnight incubation at 4°C with anti-hAC, brain sections were washed with TBS and incubated with anti-rabbit-IgG diluted 1:200 in 1% NGS/BSA/TBS for 1 hour at room temperature. After washing, the Vectastain Elite ABC kit and DAB developing solution were used to visualize the immunohistochemical staining.

For double-immunolabeling of human AC and NFTs, the frozen human brain sections were incubated with both of polyclonal anti-hAC and monoclonal antibody PHF-1 to tau phosphorylated at Ser 396/404 (Otvos, et al., 1994). The anti-hAC immunoreactivity was developed with DAB staining as described above, and the PHF-1 immunoreactivity was developed with a red fluorescence secondary antibody Cy3 anti-mouse IgG (Jackson ImmunoResearch Laboratories, Inc., West Grove, PA). The double immunolabeling was observed under a confocal microscope.

## 4. RESULTS

To test our hypothesis that there are other brain glycoproteins that are altered in AD and these glycoproteins might be involved in the molecular pathogenesis of AD, we:

1. Identified major glycoproteins in AD brain;
2. Searched for glycoproteins that are altered in AD brain;
3. Investigated the subcellular distribution of the altered glycoproteins in AD brain;
4. Isolated and identified these altered glycoproteins.

#### **4.1. Development of Methodology for Comparative Analysis of Glycoproteins Between Control and Alzheimer's Disease Brains**

In order to investigate whether there are any altered glycoproteins in AD brain, we made various crude preparations such as gray matter homogenates, cytosolic fractions, hippocampal membrane fractions, synaptosomal membrane fractions, and white matter homogenates from six AD and six control brains. After electrophoresis in 10% SDS-PAGE and transfer of proteins to Immobilon-P (PVDF) membranes, the glycoproteins on the membrane were detected by lectin blotting technique. Lectins themselves are glycoproteins and they each specifically bind to different sugar moieties (see Table 3). Hence, they are commonly used to detect and identify glycoconjugates (Cummings, 1994).

By comparing the staining of glycoproteins between control and AD cases, we found that in AD homogenate samples, a ~43 kDa protein band had an increased staining by lectin GNA (Fig. 8C, D) that recognizes terminal mannose residues only. The pattern of this band also was different in AD as compared with controls on GNA blot and ConA blot, the latter detects mannose residue (Fig. 8B). The differences of this band were not seen in Coomassie blue-stained gel (Fig. 8A). Because no difference in either pattern or staining intensity of protein band at the molecular weight of 43 kDa was observed in the cytosolic proteins (Fig. 9B, C), the altered protein observed in homogenate samples are probably membrane-associated. We then studied membrane proteins of human brain hippocampus and found similar intensity and pattern alterations of a 43 kDa protein band on ConA and GNA blots as seen in homogenate samples (Fig. 10B, C). We also studied

synaptosomal membrane proteins and homogenates of white matter tissue with the same methods, but did not find any significant changes of the 43 kDa band (Figs. 11&12). In addition to ConA and GNA as shown in Figs. 8 ~ 12, we also examined all these samples with other lectins listed in Table 3. At molecular weight of 43 kDa area, no significant alteration of staining with any of these lectins was observed (data not shown).

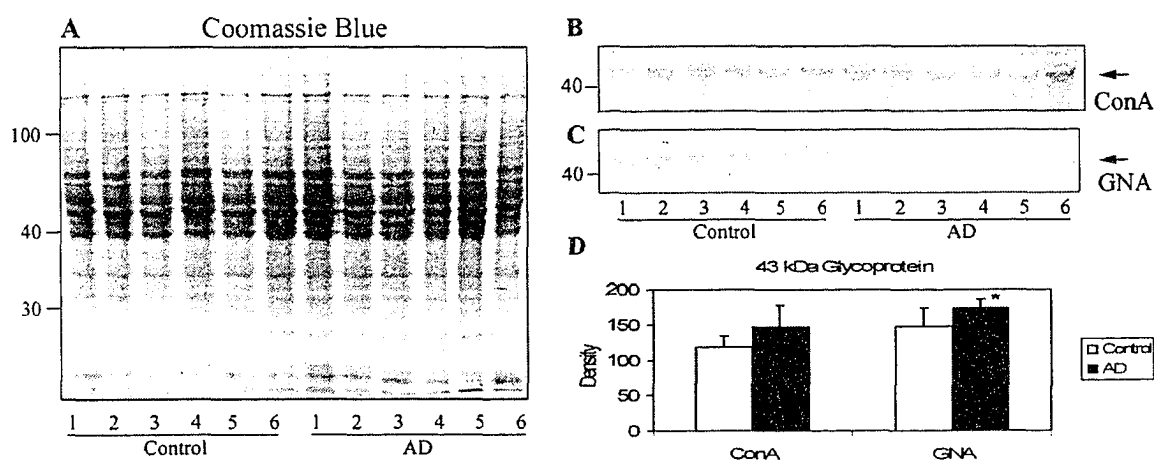


**Fig. 8. Coomassie blue staining and lectin blots of SDS-PAGE of homogenates from Control and AD cerebral cortex.** Brain homogenates (5  $\mu$ g/lane for A and 10  $\mu$ g/lane for B-C) were resolved by 10% SDS-PAGE and stained with Coomassie blue (A), ConA (B), or GNA (C). Note that the 43 kDa protein bands (arrow) that had a different pattern between AD and controls. The staining density of the 43 kDa band was quantitated by densitometry and the data were presented as mean  $\pm$  SD of the density (D). \*:  $p < 0.05$ .

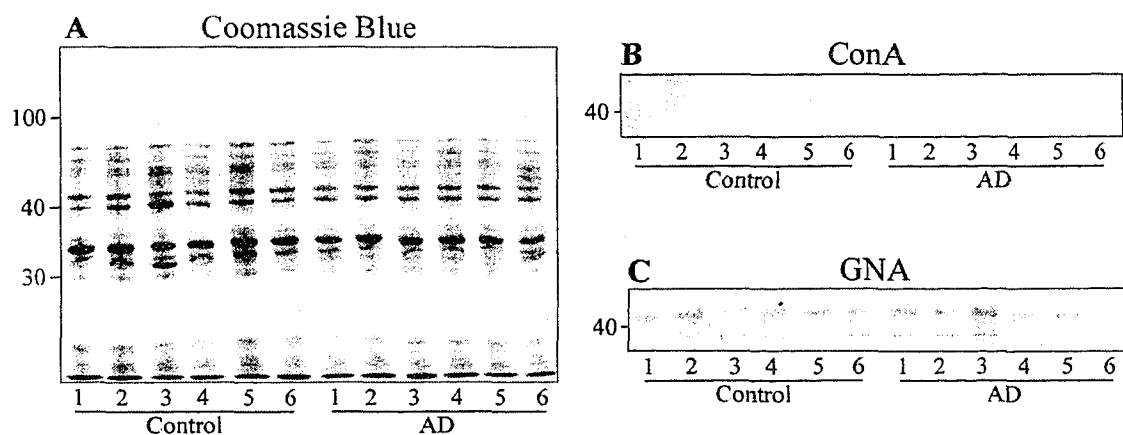


**Fig. 9. Coomassie blue and lectin blots of cytosolic proteins from control and AD cerebral cortex.** Cytosolic protein samples (5  $\mu\text{g}/\text{lane}$  for A and 10  $\mu\text{g}/\text{lane}$  for B-C) were resolved in 10% SDS-PAGE and stained with Coomassie blue (A), ConA (B) or GNA (C).

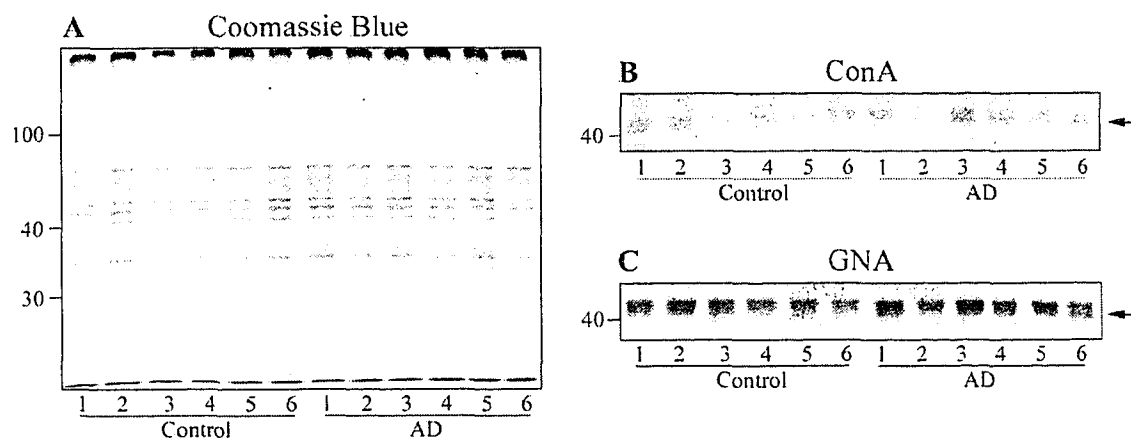


**Fig. 10. Coomassie blue and lectin blots of hippocampal membrane proteins.** Hippocampal membrane protein samples (5  $\mu\text{g}/\text{lane}$  for A and 10  $\mu\text{g}/\text{lane}$  for B-C) were resolved by 10% SDS-PAGE and stained with Coomassie blue (A), ConA (B), or GNA (D).

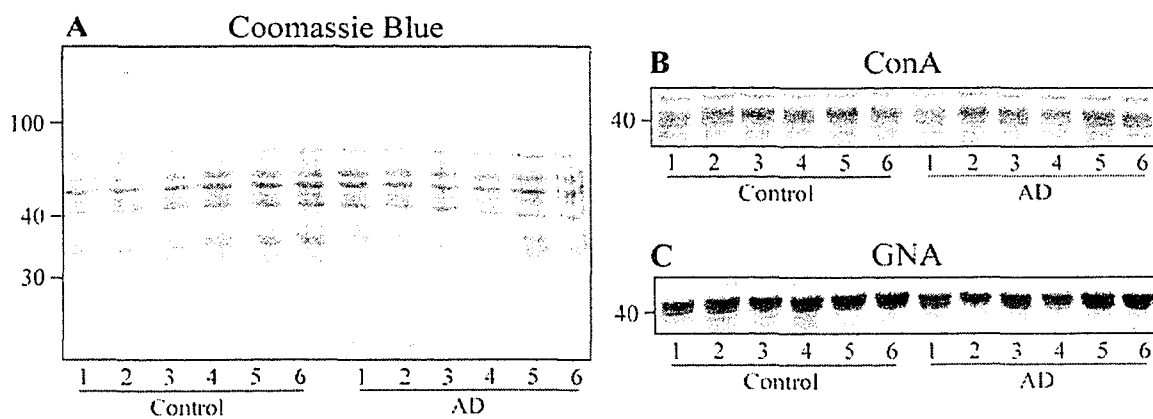


**Fig. 11. Coomassie blue and lectin blots of synaptosomal membrane proteins from control and AD cerebral cortex.** Synaptosomal membrane protein samples (5  $\mu\text{g}/\text{lane}$  for A and 10  $\mu\text{g}/\text{lane}$  for B-C) were resolved in 10% SDS-PAGE and stained with Coomassie blue (A), ConA (B), or GNA (C).

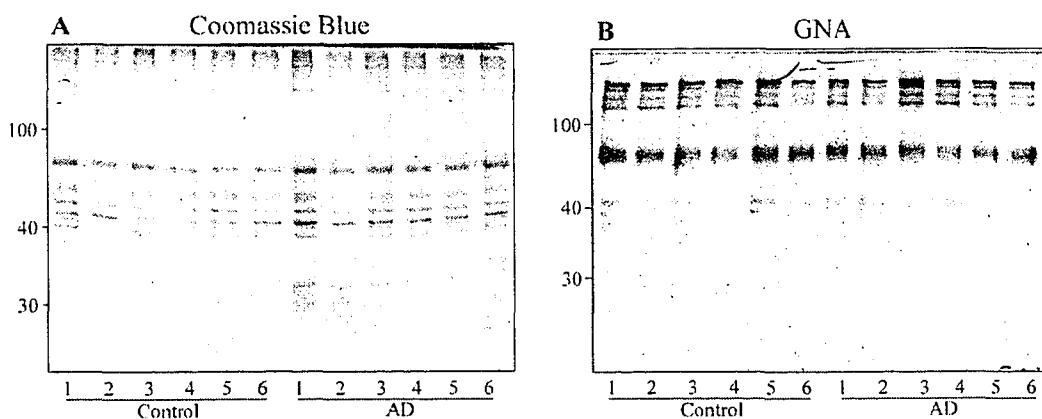


**Fig. 12. Coomassie blue and lectin blots of homogenates from control and AD brain white matter.** White matter homogenate samples (5  $\mu\text{g}/\text{lane}$  for A and 10  $\mu\text{g}/\text{lane}$  for B) were resolved in 10% SDS-PAGE and stained with Coomassie blue (A) and GNA (B).

In order to further investigate the subcellular localization of the 43 kDa protein in human brains, we prepared subcellular fractions (see Fig. 3) to learn its subcellular localization. We studied the subcellular distribution of the altered glycoproteins by lectin blots. We found that the 43 kDa GNA-positive glycoprotein was enriched in fractions of microsomes and lysosomes (Fig. 13). Microsomes are formed from endoplasmic reticulum and Golgi apparatus. It suggested that this 43 kDa protein was glycosylated in the endoplasmic reticulum and Golgi apparatus, because there are a series of enzymes which catalyse protein glycosylation in the lumen of these two organelles. The presence of the 43 kDa protein in lysosomal enriched fractions suggested that it might be associated with an intracellular degradation system.

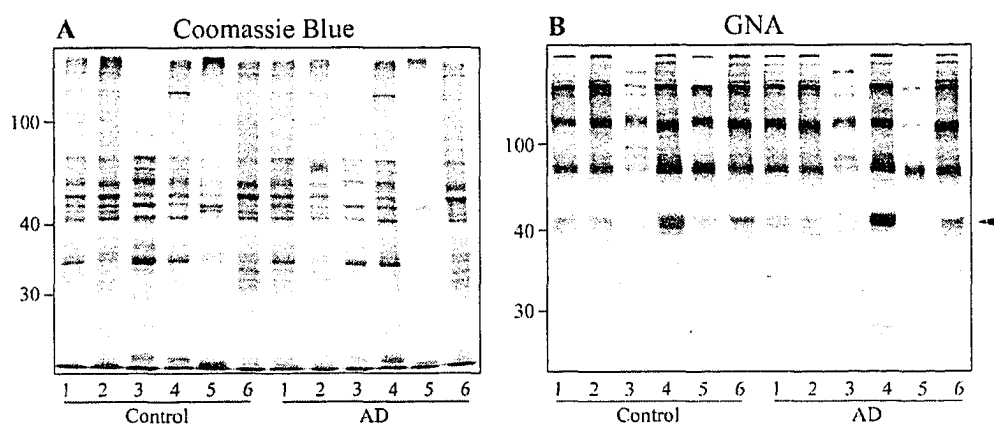


**Fig. 13. Coomassie blue staining and lectin blots of various subcellular fractionations of control and AD cerebral cortex.** Fractionated samples (5  $\mu\text{g}/\text{lane}$  for A and 10  $\mu\text{g}/\text{lane}$  for B) were analysed by 10% SDS-PAGE and stained with Coomassie blue (A) or GNA (B). Lane 1 is 20% homogenate; lane 2 is nuclei and tissue debris fraction (Pellet 1); lane 3 is cytosolic protein fraction (Sup 4); lane 4 is microsome fraction (Pellet 4); lane 5 is synaptosome fraction (mid-layer of sucrose gradient separation); lane 6 is lysosome fraction (bottom-layer of sucrose gradient separation). Note that the 43 kDa glycoprotein (arrow) is enriched in the microsome (lane 4) and lysosome (lane 6) fractions.

Because the 43 kDa glycoprotein was found enriched in the microsomal and lysosomal membrane fractions, we prepared membrane fractions from cerebral cortex and then enriched glycoproteins by chromatographies. This allowed us to partially isolate our target glycoproteins, facilitate the comparison and do further analyses. By using the protocol summarized in Fig. 4, typically a yield of ~50 mg membrane proteins was obtained from 10 g gray matter (Table 5).

**Table 5. A Representative Yield of Membrane Extract Preparation from Temporal Cortex (9.24 g)**

Step	Volume (ml)	Protein		Yield (%)
		Conc. (mg/ml)	Amount (mg)	
10% Homogenate	99.0	10.9	1,079.1	100
1 <sup>st</sup> 100,000 × g Pellet	10.0	92.9	929.0	86
Membrane Extract	10.0	4.8	48.0	4.4

In order to enrich the glycoproteins from membrane extract, we employed ConA affinity chromatography. ConA affinity chromatography is widely used to obtain glycoprotein pool from protein mixtures, because mannose is the most common component of the sugar chain of glycoproteins in nature (Cummings, 1994).

We first tested our ConA-agarose column by applying a mixture of 50 µg carboxypeptidase Y and 3 mg of BSA. Carboxypeptidase Y is a known ConA-binding glycoprotein and commonly used as a positive control of ConA chromatography. As demonstrated in Fig. 14, almost all of the loaded carboxypeptidase Y bound to the ConA column eluted with Methyl- $\alpha$ -D-Mannopyranoside solution. Calculation of the yield indicated that 98% of the loaded carboxypeptidase Y was recovered in the eluate.

When membrane extract of human brain cerebral cortex was subjected to ConA chromatography, we found that no detectable glycoproteins were in the unbound (flow-through and wash) fractions, indicating that almost all ConA-positive glycoproteins were bound to the column (Fig.15 and Table 6). Most of the ConA-binding glycoproteins (~95%) were eluted with 500 mM Methyl- $\alpha$ -D-Mannopyranoside (Elution I). We pooled the peak fractions of glycoproteins together and termed it Pool-1 and the rest of the fractions as Pool-2 of Elution I (Fig. 15A). ConA blot indicated that Pool-1, Pool-2 of Elution I and Elution II had very similar protein pattern (Fig. 15C). A small amount of tightly bound glycoproteins (~5%) was eluted with the hapten sugar plus EDTA (Elution II). The yields are presented in Table 6.

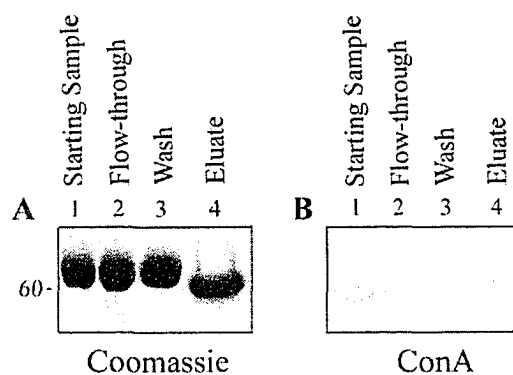


**Fig. 14. ConA affinity chromatography of a mixture of Carboxypeptidase Y (positive control) and BSA.** Carboxypeptidase Y (50  $\mu$ g) and BSA (3 mg) were mixed with Extracting Buffer in a total volume of 4 ml and applied in ConA agarose column (1 ml). A, Coomassie blue staining of aliquots from each step of chromatography (3  $\mu$ g of total proteins per lane). B, ConA blot of aliquots from each step of ConA chromatography (Lane 1 ~ 3, 60  $\mu$ g/lane loaded; lane 4, 1  $\mu$ g/lane loaded).

**Table 6. Yield of ConA Affinity and DEAE-ion Exchange Chromatographies of Membrane Proteins from Cerebral Cortex**

Step	Vol. (ml)	Total protein <sup>#</sup>			ConA- positive protein (%)*	GNA- positive protein (%)*	SNA- positive protein (%)*
		Conc. (mg/ml)	Amount (mg)	Yield (%)			
<b>ConA Chromatography</b>							
Starting Sample ( <i>Membrane Extract</i> )	7.8	4.8	37.4	100	100	-	-
Unbound	15	2.4	35.9	96	0	-	-
Elution I (concentrated)	0.22	15.0	3.3	8.7	~ 95	-	-
Elution II (concentrated)	0.16	3.0	0.47	1.25	~ 5	-	-
<b>DEAE-ion Exchange Chromatography</b>							
Starting Sample ( <i>ConA Column Eluate</i> )	0.22	15.0	3.3	100	100	-	-
Unbound	12	0.01	0.12	4	~ 30	~ 50	~ 0
0.5 ~ 0.6 M NaCl peak	7.5	0.42	3.2	96	~ 70	~ 50	~ 100

# Protein concentration was determined by modified Lowry protein assay.

\* The yields of the specific lectin-positive proteins were estimated based on the intensity of the specific lectin staining.

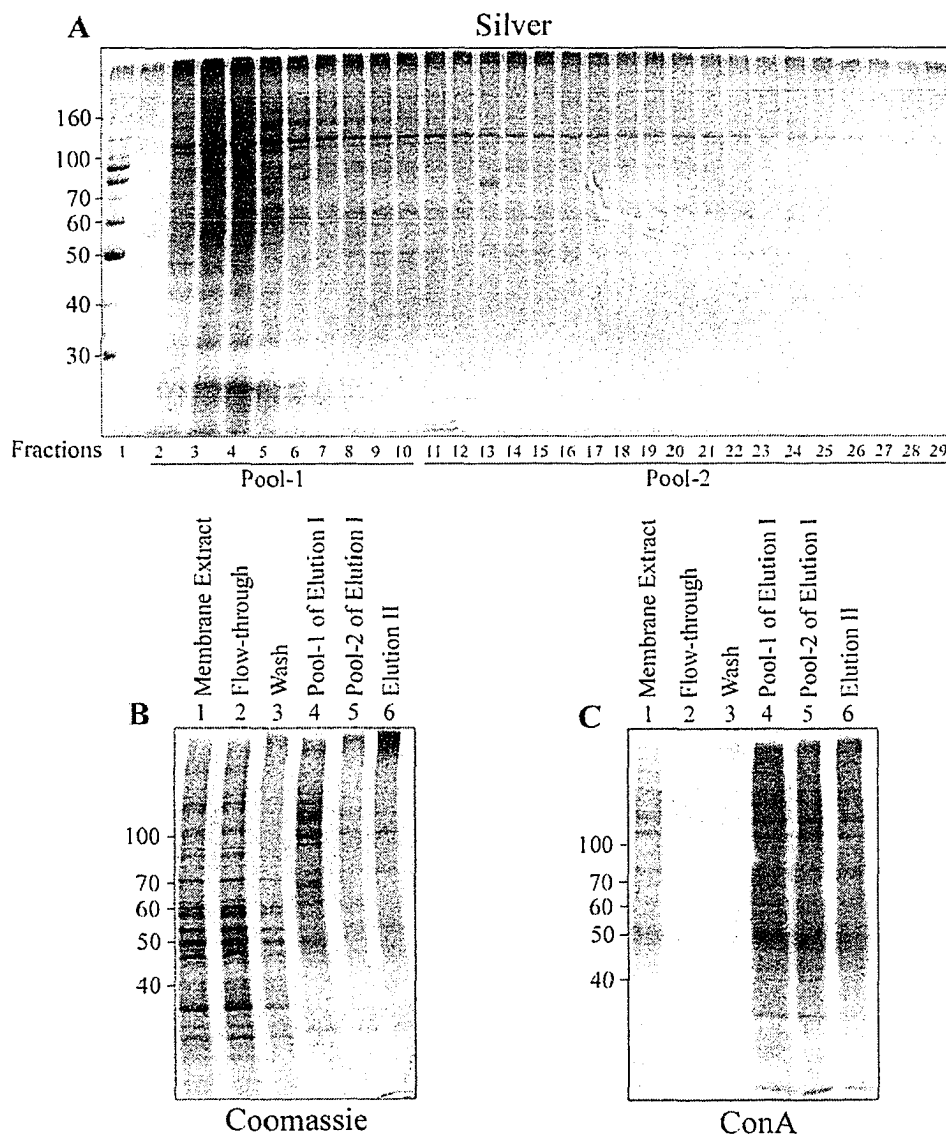


**Fig. 15. Analysis of ConA affinity chromatography of membrane extract from AD cerebral cortex.** A, Silver staining of the fractions 1 ~ 29 (10  $\mu$ l/fraction/lane) of Elution I. Fractions 2 ~ 10 were pooled as Pool-1 and fractions 11 ~ 29 were pooled as Pool-2. B, Coomassie blue staining of aliquots from each step of chromatography (5  $\mu$ g protein per lane). C, ConA blot of aliquots from each step of chromatography (10  $\mu$ g protein per lane). The positions of molecular weight markers in kDa were shown on the left of each panel.

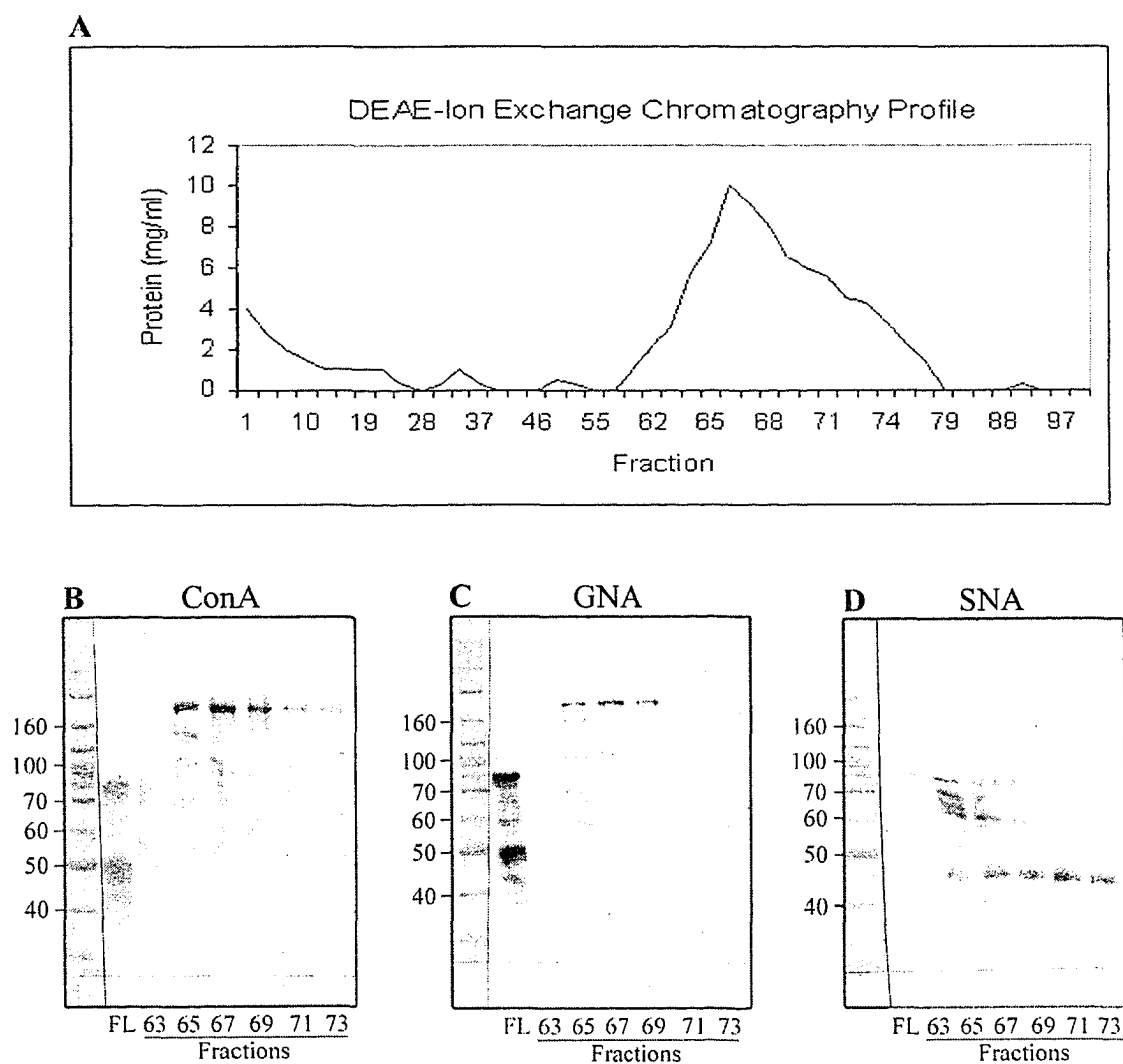


**Fig. 16. Analysis of DEAE-ion exchange chromatography of ConA-binding proteins.** A, Chromatography profile of DEAE-ion exchange chromatography. B, C, and D are ConA, GNA, and SNA blots of unbound proteins (FL) and of fractions ( $0.5 \mu\text{g}/\text{proteins}/\text{lane}$ ) eluted with  $0 \sim 1 \text{ M NaCl}$ . The positions of molecular weight markers in kDa were shown on the left of each panel.

The Pool-1 of Elution I from ConA affinity chromatography, which contains most of the glycoproteins, was further fractionated by DEAE-ion exchange chromatography that separates proteins by charge. Because the eluate from ConA affinity column contained 0.5% Triton and 0.05% SDS, before being loaded onto DEAE column, it was dialysed against 50 mM Tris-HCl, pH 7.6 overnight with four changes of the buffer. The protein concentration was determined by Bradford method (Bradford, 1976).

DEAE-ion exchange chromatography separated the Pool-1 of Elution I of ConA-binding glycoproteins into two major peaks (Fig. 16A). Lectin blot analysis of the column fractions with ConA indicated that approximately 30% of ConA-binding glycoproteins did not bind to DEAE column (Fig. 16B and Table 6). About 50% GNA-positive proteins were in the unbound peak (Fig. 16C and Table 6), whereas none of the SNA-positive proteins were in this peak; they required salt to elute from the column (Fig. 16D). These results indicate that DEAE-ion exchange chromatography can separate glycoproteins containing different sugar moieties.

Glycoproteins separated by DEAE-ion exchange chromatography were further purified by lectin-affinity chromatography. In order to choose the specific lectins for further affinity chromatography, we stained the DEAE-purified samples with several lectins, i.e., WGA, APA, DSA, GNA, SNA, and PNA. We found that this sample bound all these lectins well (Fig. 17). Among them, DSA, GNA, SNA and PNA stained distinct protein bands of this sample and hence were selected to be used for further purification.

Before further purification of the glycoproteins eluted from DEAE-ion exchange column, we used several glycoproteins that are known to bind to these lectins to test the small affinity lectin columns and to standardize the chromatography conditions. A

mixture of 50  $\mu\text{g}$  fetuin and 500  $\mu\text{g}$  BSA was used for standardizing SNA and DSA columns, 50  $\mu\text{g}$  asialofetuin and 500  $\mu\text{g}$  BSA was used for standardizing PNA column, and 50  $\mu\text{g}$  carboxypeptidase Y and 500  $\mu\text{g}$  BSA was used for GNA column. By using the optimised conditions ( $E_1$  and  $E_2$ ) as described in Table 4, we found that these glycoproteins were separated from BSA by these lectin chromatographies. Under these conditions, most of the glycoproteins were bound to the lectin-agarose and eluted in Elution I and II. Fig. 18 demonstrates results of PNA and SNA affinity chromatographies.

We then used these four lectin affinity columns to further isolate glycoproteins eluted from DEAE-ion exchange column. Similarly to the ConA affinity column procedure, we ran SNA, PNA, DSA and GNA columns. Since various lectins have different characters and competitive sugars, eluting conditions of SNA, GNA, PNA and DSA affinity chromatographies were different. From  $E_1$  to  $E_4$ , the conditions were from weak to strong to elute the glycoproteins. Eluting conditions which were used are summarized in Table 4. A amount of samples (FL, W,  $E_1$ ,  $E_3$ , and  $E_4$ ) equivalent to 5  $\mu\text{l}$  agarose beads were analysed by lectin blots (Fig. 19). For SNA column, a relatively small amount of SNA-binding glycoproteins were eluted with  $E_3$ , while a significant amount of SNA-positive glycoproteins still remained on the beads (Fig. 19A). For PNA and DSA columns, most of glycoproteins did not bind (Fig. 19B&C), suggesting these two affinity columns were not suitable for further purification. For GNA column, a big amount of GNA-binding glycoproteins were eluted with  $E_3$  (Fig. 19D). The yields of these columns are summarized in Table 7. SNA and GNA-binding glycoproteins had significant recoveries and clear resolutions in eluted glycoprotein bands, so these two columns were used for further purification of glycoproteins eluted from DEAE-ion exchange column.

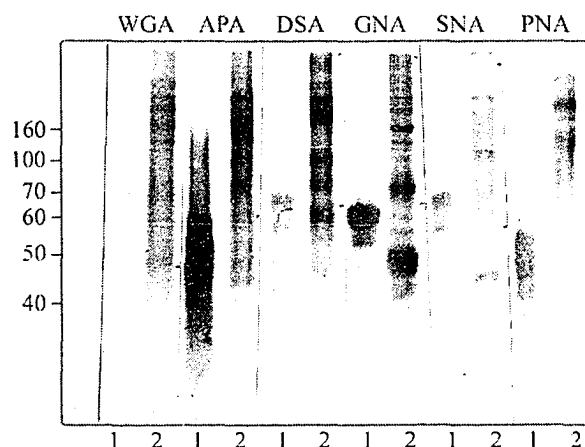


**Fig. 17. Lectin blots of proteins eluted from DEAE-ion exchange column (0 ~ 1 M NaCl).** Lane 1 is positive control (1  $\mu$ g) for each lectin. For WGA, DSA, and SNA blots, the positive control was fetuin. For APA and PNA blots, the positive control was asialofetuin. For GNA blot, the positive control was caboxypeptidase Y. Lane 2 of each blot is the eluate (5  $\mu$ g) from DEAE-ion exchange chromatography. The positions of molecular weight markers in kDa were shown on the left of blot.

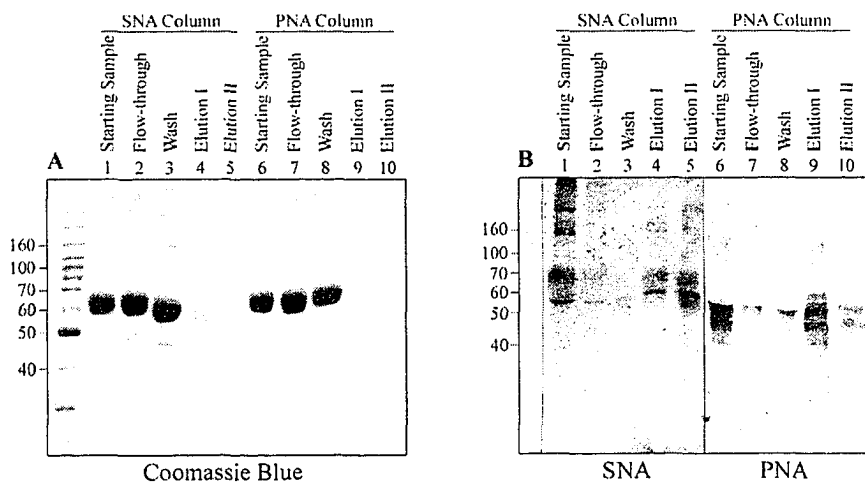


**Fig. 18. Analysis of SNA and PNA affinity chromatographies of fetuin as positive control of SNA, and asialofetuin as positive control of PNA.** A, Coomassie blue staining of equivalent amounts of aliquots from each step of SNA and PNA affinity chromatography. B, SNA and PNA blots of equivalent amount of aliquots from each step of chromatography. The positions of molecular weight markers in kDa were shown on the left of each blot.

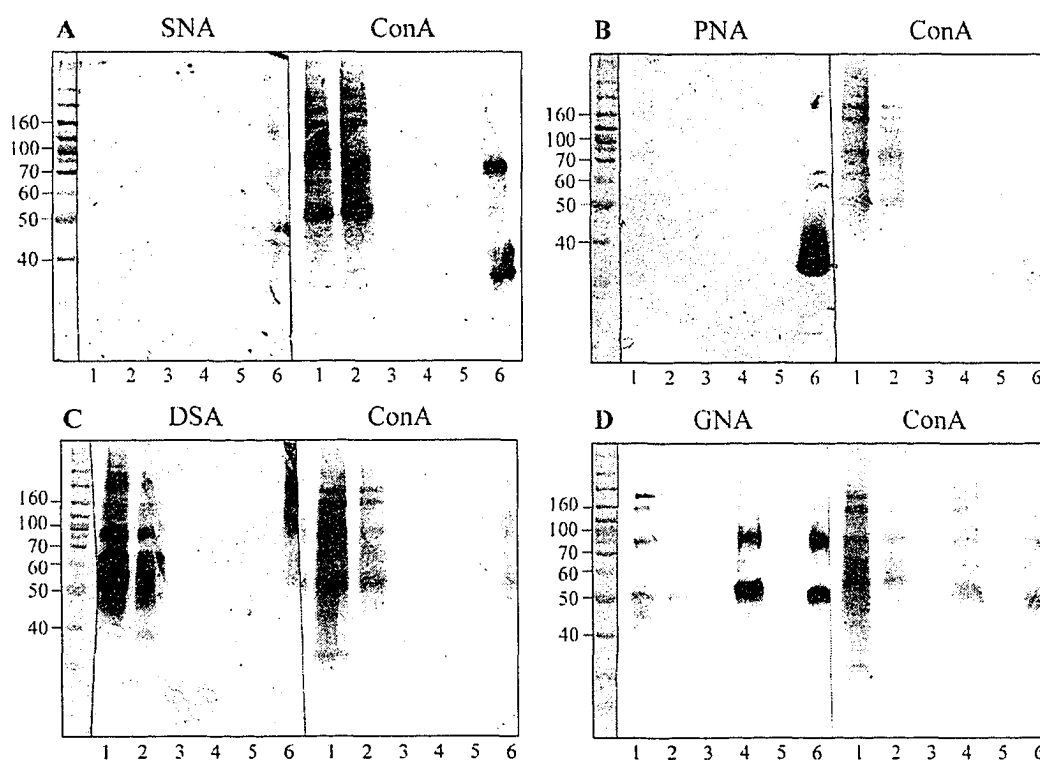


**Fig. 19. Analysis of SNA, PNA, DSA and GNA affinity chromatographies of eluted proteins from DEAE-ion exchange chromatography.** A, B, C, and D are the lectin blots of various fractions of SNA, PNA, DSA and GNA affinity chromatographies, respectively. Left half of each panel is specific lectin staining, and the right half is ConA staining of total glycoproteins. Amount of samples equivalent to 5  $\mu$ l beads were loaded/lane. Lane 1, FL; lane 2, wash; lane 3, E<sub>1</sub>; lane 4, E<sub>3</sub>; lane 5, E<sub>4</sub>; and lane 6, remaining lectin beads after elution. Molecular weight marker was shown on the left in kDa.

**Table 7. Yields from SNA, PNA, DSA and GNA Affinity Chromatographies**

Fractions	Volume ( $\mu$ l)	Protein		
		Conc. (mg / ml)	Amount ( $\mu$ g)	Recovery (%)
SNA				
FL	160	0.35	56	28%
1 <sup>st</sup> W	470	0.11	52	26%
E <sub>1</sub>	420	0.01	4	2%
E <sub>2</sub>	400	0.015	6	3%
E <sub>3</sub>	680	0.022	15	7.5%
E <sub>4</sub>	680	0.008	5	2.5%
PNA				
FL	520	0.24	125	62.5%
1 <sup>st</sup> W	430	0.035	15	7.5%
E <sub>1</sub>	390	0	0	0
E <sub>2</sub>	380	0	0	0
E <sub>3</sub>	670	0	0	0
E <sub>4</sub>	700	0	0	0
DSA				
FL	400	0.3	120	60%
1 <sup>st</sup> W	400	0.11	44	22%
E <sub>1</sub>	490	0	0	0
E <sub>3</sub>	660	0	0	0
E <sub>4</sub>	680	0.00875	6	3%
GNA				
FL	430	0.24	103	52%
1 <sup>st</sup> W	430	0.03	13	6.5%
E <sub>1</sub>	440	0	0	0
E <sub>3</sub>	700	0.024	17	8.5%
E <sub>4</sub>	670	0.0075	5	2.5%

FL, flow-through; 1<sup>st</sup> W, first wash;

E<sub>1</sub>, elution 1; E<sub>2</sub>, elution 2; E<sub>3</sub>, elution 3; E<sub>4</sub>, elution 4.

#### 4.2. Identification of major glycoproteins in AD brain gray matter

As described above, we have developed a methodology for the isolation of glycoproteins and for comparative analysis of glycoproteins between AD and control brains. To identify the major glycoproteins in AD brain, we made a preparation of brain membrane extract from an AD brain frontal and temporal cortex (90.5 g) as described in Materials and Methods. The yield of membrane proteins prepared (Table 8) was proportionally similar to what we obtained in smaller preparations (see Table 5).

**Table 8. Preparation of brain membrane extract from frontal and temporal cortex (90.5g) of an AD brain**

Step	Volume (ml)	Protein		Yield (%)
		Conc. (mg/ml)	Amount (mg)	
10% Homogenate	905.3	7.8	7,061.3	100
1 <sup>st</sup> 100,000 × g Pellet	100.0	55.5	5,545.1	78.5
Membrane Extract	107	2.8	299.6	4.2

The membrane proteins were then subjected to ConA chromatography to separate glycoproteins from non-glycoproteins. Analysis of the ConA chromatography indicated that majority of the membrane proteins were not bound to the ConA column, but all the ConA positive proteins were bound (Fig. 20). The unbound, first eluted peak, and second eluted peak fractions were pooled separately, aliquoted and stored at -70°C for further analysis.

Since the first eluted peak (EI) of ConA chromatography contained most of the glycoproteins, we further fractionated this glycoprotein pool with a DEAE-ion exchange

column after dialysis. The pooled fractions of the first eluted peak were concentrated to about 30 ml with polyethylene glycol at 4°C for 3 hours, and the resulting protein mixture was then pre-warmed to 37°C and dialysed against 1 L of 20 mM  $\text{Na}_2\text{HPO}_4/\text{NaH}_2\text{PO}_4$ , pH 7.4, at room temperature for 2 hours, followed by 4 L of 20 mM Tris-HCl, pH 7.0 at room temperature for 15 hours with two changes.

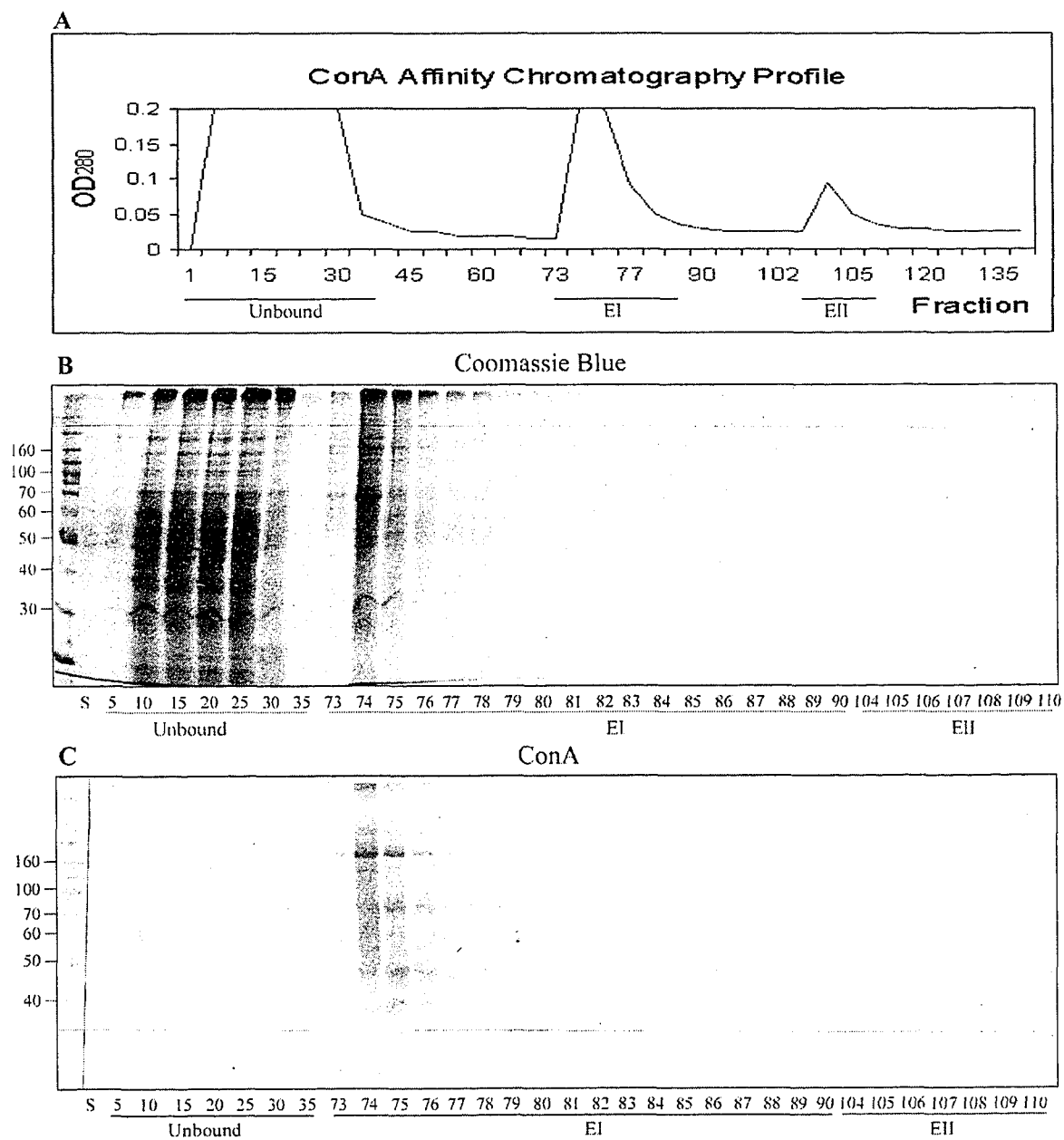


**Fig. 20. Analysis of ConA affinity chromatography of membrane extract from an AD brain.** A, Chromatography profile detected by  $OD_{280}$ . Note that large amount of unbound proteins followed by two eluted peaks, EI and EII. B, Coomassie blue staining of selective fractions (15  $\mu$ l/fraction/lane). C, ConA blot of fractions shown in B (7.5  $\mu$ l/lane). Molecular weight markers in kDa were shown on the left. The numbers under each panel are fraction numbers.

The conditions of DEAE ion exchange chromatography (1.0 × 20 cm, 12 ml of bed volume) were kept the same as described above except changing the column buffer with 50 mM Tris-HCl, pH 7.0 and the flow rate to 0.2 ml/min (1 ml/fraction). The protein concentration of each fraction was determined by Bradford protein assay, and the chromatography profile according to protein amount in each fraction is shown in Fig. 21A. Majority of glycoproteins were eluted by 0.4 ~ 0.7 M NaCl from this column (Fig. 21A). Coomassie blue staining and lectin blot analyses of the fractions indicated that various glycoproteins in the eluted peak had different affinities to SNA and GNA (Fig. 21 B-E). This made it possible that the glycoproteins eluted from DEAE chromatography could be further separated by SNA and GNA affinity columns.

We then used tandem chromatography of SNA and GNA columns to further purify glycoproteins. As shown in Fig. 22, these two lectin columns further isolated specific glycoproteins.

The eluted proteins shown in Fig. 22C and D had been isolated from human brain gray matter through membrane protein extraction, ConA-affinity purification, DEAE-ion exchange chromatography, and a second lectin affinity chromatography with SNA followed by GNA. Theoretically, these proteins are all glycoproteins and represent major brain glycoproteins that can bind with SNA and/or GNA. To identify the nature of these glycoproteins, we collected and concentrated the Fraction 6 of the protein sample eluted from SNA column (see Fig. 22C) and GNA column (see Fig. 22D), respectively, and resolved them in 10% SDS-PAGE. Coomassie blue staining of this gel revealed 4 predominant protein bands of the sample eluted from SNA column and 9 predominant protein bands eluted from GNA column (Fig. 23). We then cut out these individual

protein bands and digested them with trypsin. The resulting peptide mixtures were analyzed by MALDI-TOF mass spectrometry. The mass fingerprints were matched against protein database ProFound. An example of the identification of these glycoproteins, GNA-8, is shown in Fig. 23A.

Out of the 4 protein bands of the sample eluted from the SNA column, 3 bands were successfully identified (Table 9). They were neuronal cell adhesion molecule (band 1),  $\beta$ -globin (band 3), and IgM heavy chain VH1 region precursor (band 4). All of these three proteins were reported to be glycoproteins (Wing, et al., 1992; Castagnola, et al., 1989; Tartakoff and Vassalli, 1979). There was no protein identified with confidence of band 2 based on the mass spectrometry data generated, probably because this band contained more than one predominant proteins.

The nature of all 9 protein bands of the sample eluted from GNA column had been identified by mass spectrometry analysis (Table 9). Among these 9 proteins, two (bands 1 and 4) were unknown proteins that have not yet been identified but can be deduced from human genome. However, according to the prediction of the primary sequences of these proteins, they all contain several Asn-X-Ser/Thr consensus sequences for N-glycosylation (Gupta, et al., 2002, data not shown), which is consistent with our conclusion that they are major glycoproteins in human brain. They all contain one or more predicted transmembrane segments in their protein sequences too (Persson and Argos, 1994, 1996, data not shown), suggesting that they might be membrane proteins. Six out of the nine identified protein bands were contactin precursor (band 2), dipeptidylpeptidase VI (band 3), CD81 partner 3 (band 5), prenylcysteine lyase (band 6), adipocyte plasma membrane-associated protein (band 7), and human acid ceramidase (band 8). Previous studies have

demonstrated that these proteins are glycoproteins (Berglund, et al., 1994; Fan, et al., 1997; Tschantz, et al., 1999; Morita, et al., 2000; Ferlinz, et al., 2001 and Stipp, et al., 2001). Band 9 was identified as MAP4-like protein that contains only one predicted N-glycosylation site, without any transmembrane domain (data not shown).

**See Next Page For Fig. 21.**

**Fig. 21. DEAE-ion exchange chromatography of ConA-binding glycoproteins from an AD brain.** A, Chromatography profile based on Bradford protein assay. The relationship between eluted peaks and NaCl gradient is also shown. The unbound fraction and fractions eluted by 0.4 – 0.7 M NaCl (EI) and 2.0 M NaCl (EII) were pooled separately. B, Coomassie blue staining of starting samples (indicated by S, 30  $\mu$ l/lane), selective unbound (20  $\mu$ l/lane) and EI and EII fractions (10  $\mu$ l/lane). C, D and E, SNA, GNA and ConA blots of selective unbound (5  $\mu$ l/lane) and EI and EII fractions (2.5  $\mu$ l/lane). Note that SNA and GNA mainly stained different ConA-binding glycoproteins and most of SNA and GNA-binding proteins bound to DEAE under our conditions. Molecular weight markers in kDa were shown on the left of each blot.

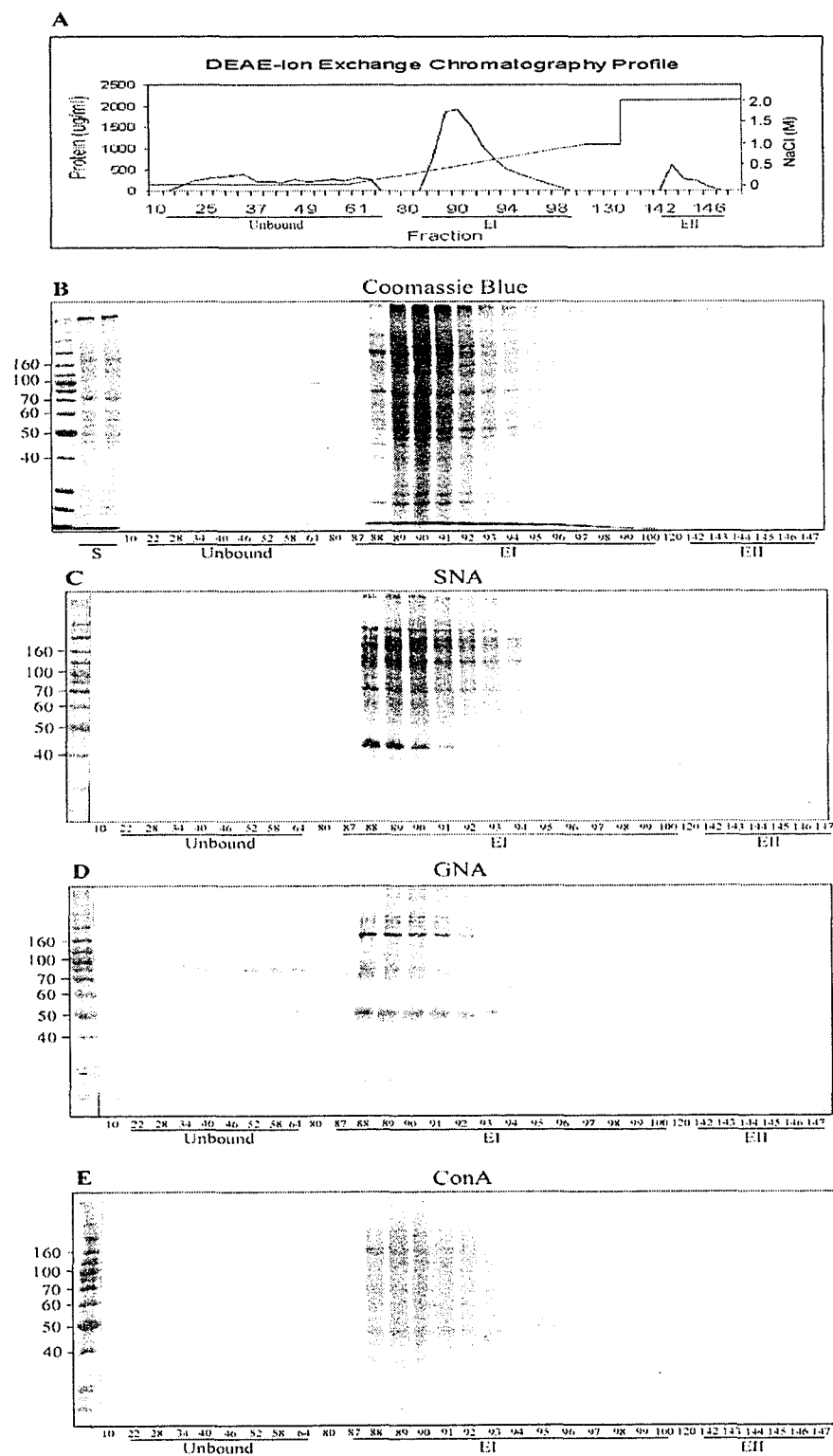
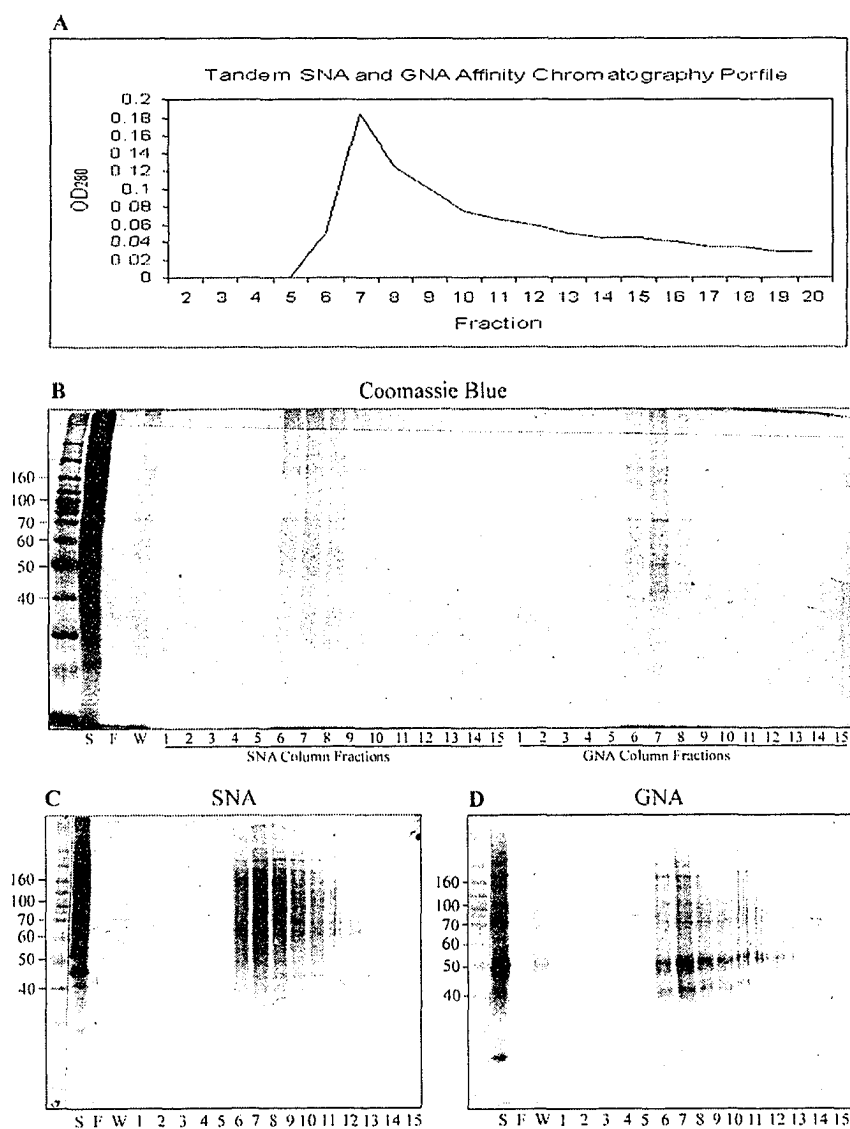


Fig. 21



**Fig. 22. Analysis of tandem SNA and GNA affinity chromatography of Eluate I from DEAE-ion exchange chromatography.** A, Elution profile of SNA column detected by  $OD_{280}$ . Similar elution profile was obtained from GNA column (data not shown). B, Coomassie blue staining (20  $\mu$ l/lane) of starting sample (S), flow-through (F), wash (W) and eluted fractions. The first 15 lanes are SNA column fractions. The second 15 lanes are GNA column fractions. C, SNA blot of (5  $\mu$ l/lane) of starting sample, flow-through, wash and eluted fractions 1 ~ 15. D, GNA blot of (5  $\mu$ l/lane) of starting sample, flow-through, wash and eluted fractions 1 ~ 15. Molecular weight markers in kDa were shown on the left.

**Table 9. Mass Spectrometric Analysis of Major AD Brain Glycoproteins**

Protein Band*	Protein Identified by MS	Z score	Theoretical MW (kDa)	Apparent MW (kDa)	Reported Glycoprotein
SNA 1	Neuronal cell adhesion molecule	0.89	130.61	~130	Yes
SNA 2	ND	NA	NA	~75	NA
SNA 3	Beta-globin	0.12	18.91	~47	Yes
SNA 4	IgM heavy chain VH1 region precursor	0.22	16.29	~30	Yes
GNA 1	Hypothetical protein XP_046809	<0.1	94.40	~230	NA
GNA 2	Contactin precursor	2.15	111.85	~130	Yes
GNA 3	Dipeptidylpeptidase VI (similar to IV)	2.42	91.34	~110	Yes
GNA 4	Hypothetical protein XP_004105	0.15	243.59	~95	NA
GNA 5	CD81 partner 3 (EMI2)	2.39	65.02	~75	Yes
GNA 6	Prenylcysteine lyase	1.05	56.63	~60	Yes
GNA 7	Adipocyte plasma membrane-associated protein	2.36	46.46	~52	Yes
GNA 8	Acid ceramidase	1.68	44.54	~43	Yes
GNA 9	MAP4-like protein	0.60	102.89	~32	NA

\*, see Fig. 23 for the coding of the protein bands; ND, not detectable; NA, not applicable; Database used for protein identification is ProFound ([http://129.85.19.192/profound\\_bin/WebProFound.exe?Form=1](http://129.85.19.192/profound_bin/WebProFound.exe?Form=1)).

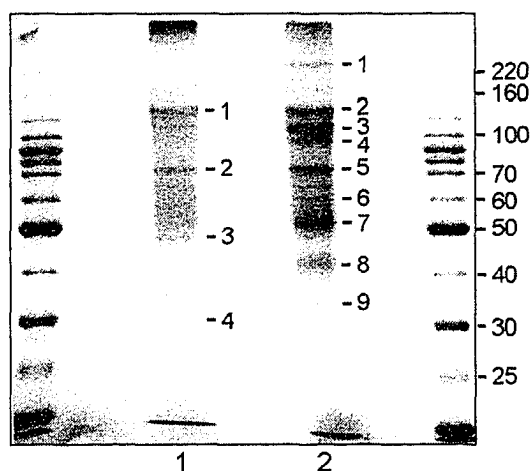
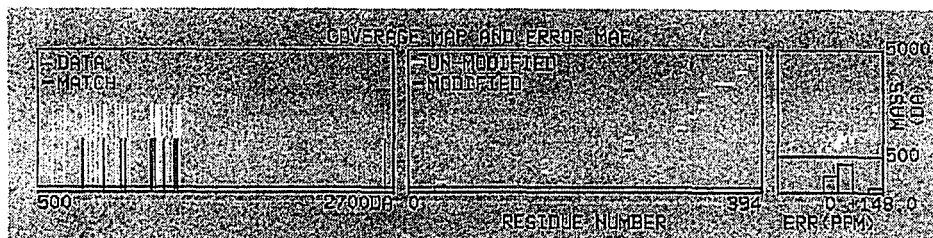


**Fig. 23. Coomassie blue-stained bands of glycoproteins eluted from SNA and GNA columns and cut out for identification by mass spec.** Fraction 6 (200  $\mu$ l) from SNA (Lane 1) or GNA (Lane 2) chromatography was precipitated by cold acetone and resolved on 10% SDS-PAGE. Numbers marked on the right sides of lane 1 and 2 indicate the bands that were cut out and subjected to mass spec analysis. Molecular weight markers in kDa were shown on the left and right of the panel.

Sample ID : Y Huang GNA 8 [ Pass:0]  
 Measured peptides : 28  
 Matched peptides : 11  
 Min. sequence coverage: 26%



Measured Mass (M)	Avg/ Mono	Computed Mass	Error (ppm)	Residues Start	Residues To	Missed Cut	Peptide sequence
788.434	M	788.440	-8	152	158	0	GHLIHR
916.556	M	916.535	23	151	158	1	RGHLIHR
1012.517	M	1012.497	20	378	385	0	GQFETYLK
1045.519	M	1045.498	20	325	332	0	HPFFLDDR
1201.670	M	1201.599	59	325	333	1	HPFFLDRR
1208.626	M	1208.601	21	244	253	0	DAMWIGFLTR
1224.650	M	1224.596	44	244	253	0	DAMWIGFLTR (1)+OH;
1224.650	M	1224.577	60	33	43	0	STVPSGPTFR
1280.658	M	1280.613	35	299	309	0	ESLDVYELDAK
1342.682	M	1342.630	39	313	322	0	WYVQTNLYDR
1365.812	M	1365.775	27	366	377	0	LTVYTLIDVTK
2645.311	A	2644.983	124	343	365	0	TSQENISFETMYDVLSTKPLNPK

#### Unmatched Monoisotopic Masses:

595.368 665.306 811.427 832.409 861.091 891.452 892.491 924.488 992.501 1035.523 1068.531 1241.668 1246.688 1257.657 1308.690 1375.712 1388.803

### ProFound - Search Result Summary

Version 4.10.5  
 The Rockefeller University Edition

Protein Candidates for search BD79ADBC-03A8-EFBF0052 [88967 sequences searched]

Rank	Probability	Est'd Z	Protein Information and Sequence Analyse Tools (T)	%	pl	kDa	Ⓢ
+1	1.0e+000	1.17	T gi 4757786 ref NP_004306.1  (NM_004315) N-acylsphingosine amidohydrolase (acid ceramidase) [Homo sapiens]	17	7.8	44.63	Ⓢ
+2	1.6e-003	0.25	T gi 13431718 sp O9ULV0 MY5B_HUMAN MYOSIN VB (MYOSIN 5B)	8	9.1	146.35	Ⓢ
+3	1.3e-005	-	T gi 126363 sp P25391 LMA1_HUMAN LAMININ ALPHA-1 CHAIN PRECURSOR (LAMININ A CHAIN)	4	5.9	337.14	Ⓢ
4	9.1e-006	-	T gi 6678676 ref NP_031383.1  (NM_007357) low density lipoprotein receptor defect C complementing; brefeldin A-sensitive, peripheral Golgi protein [Homo sapiens]	9	6.2	83.19	Ⓢ
+5	7.9e-006	-	T gi 4773781 ref XP_050079.1  (XM_050079) hypothetical protein FLJ11040 [Homo sapiens]	10	6.7	55.64	Ⓢ
+6	7.5e-006	-	T gi 7243121 dbj BAA92608.1  (AB037791) KIAA1370 protein [Homo sapiens]	9	9.0	125.31	Ⓢ
+7	5.4e-006	-	T gi 4732586 ref XP_002535.4  (XM_002535) hypothetical protein XP_002535 [Homo sapiens]	30	9.9	28.49	Ⓢ
+8	4.8e-006	-	T gi 4885183 ref NP_005210.1  (NM_005219) diaphanous 1; Diaphanous, Drosophila, homolog of, 1; deafness, autosomal dominant 1; hDial [Homo sapiens]	7	5.3	138.96	Ⓢ
+9	4.8e-006	-	T gi 12225240 ref NP_055951.1  (NM_015136) KIAA0246 protein; stabilin 1 [Homo sapiens]	4	6.0	275.33	Ⓢ
+10	4.7e-006	-	T gi 4774901 ref XP_027361.1  (XM_027361) similar to PI-3-kinase-related kinase SMG-1 (H. sapiens) [Homo sapiens]	4	5.9	273.44	Ⓢ

#### NOTE:

1. To search again using unmatched masses, click the symbol Ⓢ.
2. Highly similar protein sequences were given the same rank (IE user: click "\*" to expand/contract).

**Fig. 23A. Identification of GNA-8 by mass spectrometry.** The upper panel is the mass spectrum of GNA-8 digests and the mass of each peptide. The lower panel shows the matches of GNA-8 with ProFound database. The search results indicated that GNA-8 is human acid ceramidase.

### 4.3. Three Major Glycoproteins Are Altered in AD Brain

We applied the above approach to enrich glycoproteins from brain homogenates, to compare brain glycoproteins between AD and controls. For these studies, we used brain tissue from 6 cases of AD and 6 cases of control with similar age and post-mortem delay (Table 2). We first examined the neurofibrillary pathology of these tissue samples by Western blots developed with monoclonal antibody *PHF-1* that is specific to abnormally hyperphosphorylated tau. We found in all 6 AD brain samples but none of the control samples, tau was abnormally hyperphosphorylated and aggregated into high molecular smears (Fig. 24). These data indicated that all the tissue samples obtained from AD brain indeed had neurofibrillary pathology.

**Table 10. Preparations of membrane extract from six control and six AD brains**

	Tissue Weight (g)	10% Homogenate			1 <sup>st</sup> 100,000 × g Pellet			Membrane Extract		
		Vol. (ml)	Conc. (mg/ml)	Protein (mg)	Vol. (ml)	Conc. (mg/ml)	Protein (mg)	Vol. (ml)	Conc. (mg/ml)	Protein (mg)
Control 1	10.4	108	11.4	1,231.2	10	103.9	1,039	9.2	3.2	29.4
Control 2	12.0	125	7.8	975.0	10	83.9	839	9.6	2.5	24.0
Control 3	9.7	103	9.8	1,009.4	10	80.0	800	10.2	2.0	20.4
Control 4	9.9	114	10.5	1,197.0	10	107.1	1,071	9.9	4.3	42.6
Control 5	10.7	115	11.3	1,299.5	10	117.7	1,177	9.8	2.0	19.6
Control 6	9.7	104	10.5	1,092.0	10	90.0	900	9.9	4.9	48.5
<b>Mean ± SD</b>	<b>10.4 ± 0.9</b>	<b>111.5 ± 8.3</b>	<b>10.2 ± 1.3</b>	<b>1,134.0 ± 117.9</b>	<b>10 ± 0</b>	<b>97.1 ± 14.7</b>	<b>971.0 ± 124.7</b>	<b>9.8 ± 0.3</b>	<b>3.2 ± 1.2</b>	<b>30.8 ± 2.1</b>
AD 1	9.8	104	10.9	1,133.6	10	102.0	1,020	10.2	2.6	26.5
AD 2	11.7	124	7.9	979.6	10	79.5	795	9.9	3.4	33.7
AD 3	9.5	101	10.9	1,100.9	10	98.9	989	10	2.8	28.0
AD 4	10.5	113	10.1	1,141.3	10	102.0	1,020	9.9	3.4	33.7
AD 5	9.7	103	11.3	1,163.9	10	104.3	1,043	10.2	2.5	25.5
AD 6	11.0	117	9.9	1,158.3	10	101.0	1,010	8.9	2.9	25.8
<b>Mean ± SD</b>	<b>10.4 ± 0.9</b>	<b>110.3 ± 9.2</b>	<b>10.2 ± 1.2</b>	<b>1112.9 ± 69.0</b>	<b>10 ± 0</b>	<b>98.0 ± 9.2</b>	<b>980.0 ± 92.1</b>	<b>9.9 ± 0.5</b>	<b>2.9 ± 0.4</b>	<b>28.9 ± 3.8</b>
<b>P value</b>	<b>&gt; 0.05</b>	<b>&gt; 0.05</b>	<b>&gt; 0.05</b>	<b>&gt; 0.05</b>	<b>&gt; 0.05</b>	<b>&gt; 0.05</b>	<b>&gt; 0.05</b>	<b>&gt; 0.05</b>	<b>&gt; 0.05</b>	<b>&gt; 0.05</b>

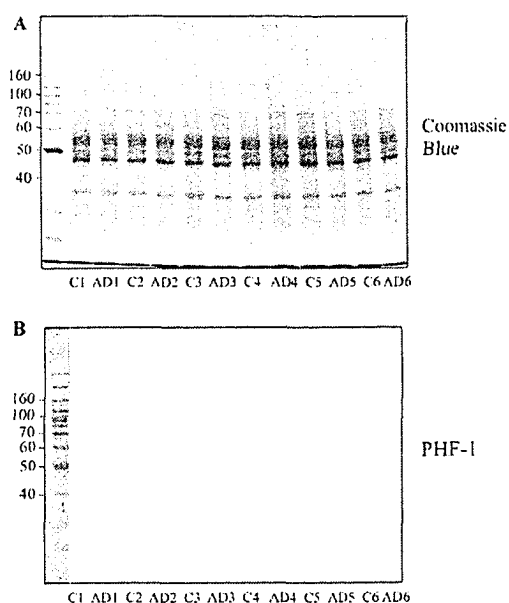


**Fig. 24. Tau pathology in homogenates from AD and control brains.** A, Coomassie blue staining of homogenates (5  $\mu\text{g}/\text{lane}$ ) from six control and six AD brains. B, Western blot of these samples (10  $\mu\text{g}/\text{lane}$ ) probed by monoclonal antibody PHF-1 against abnormally hyperphosphorylated tau at Ser 396/404. Note that the AD samples contained typical tau pathology while the control samples were free of it. Molecular weight markers in kDa were shown on the left of each panel.

We prepared membrane proteins from above-mentioned 12 brain tissue samples as described in Fig. 4. The yields of the preparations are summarized in Table 10. All these 12 membrane preparations were subjected to ConA affinity chromatography to enrich glycoproteins by using the protocol as described above except using smaller columns. Analysis of the ConA chromatography fractions indicated that unlike big preparations demonstrated in Fig. 20 where practically all glycoproteins were bound to the ConA beads, a significant amount of ConA-positive glycoproteins did not bind well in the minicolumn (Fig. 25).

To compare the glycoproteins between AD and control groups, we analysed the pooled peak fractions from E lution I of ConA affinity chromatography by SDS-PAGE and lectin blots. When we loaded the same amount of the glycoprotein samples in each lane, we observed an increased ConA staining of a 43 kDa band and a 35 kDa band detected by ConA in AD group as compared to controls (Fig 26C and D, marked by

arrows). The increase in the 43 kDa protein band was also seen on the Coomassie blue-stained gel (Fig. 26A&B), suggesting the level of this protein is elevated in AD brain. The 35 kDa glycoprotein band clearly seen on the ConA blot was only faintly stained as a smear in the Coomassie blue-stained gel (Fig. 26A, the lowest arrow), suggesting that the 35 kDa proteins is a minor protein but highly glycosylated, especially in AD brain. The increased staining of the 43 kDa and 35 kDa glycoproteins observed in Fig. 26 was not due to any variation or error of sample loading, because there was no difference in either the overall intensity of these samples or the intensity of a 160 kDa band as a reference between the two groups (Fig. 26A&B).

When the same samples were similarly analysed by lectin blot with SNA, we found the staining of a 180 kDa band was significantly decreased in AD brains (Fig. 26 E&F). This protein appeared to be a minor glycoprotein also because it was not clearly seen in the Coomassie blue-stained gel (Fig. 26A).

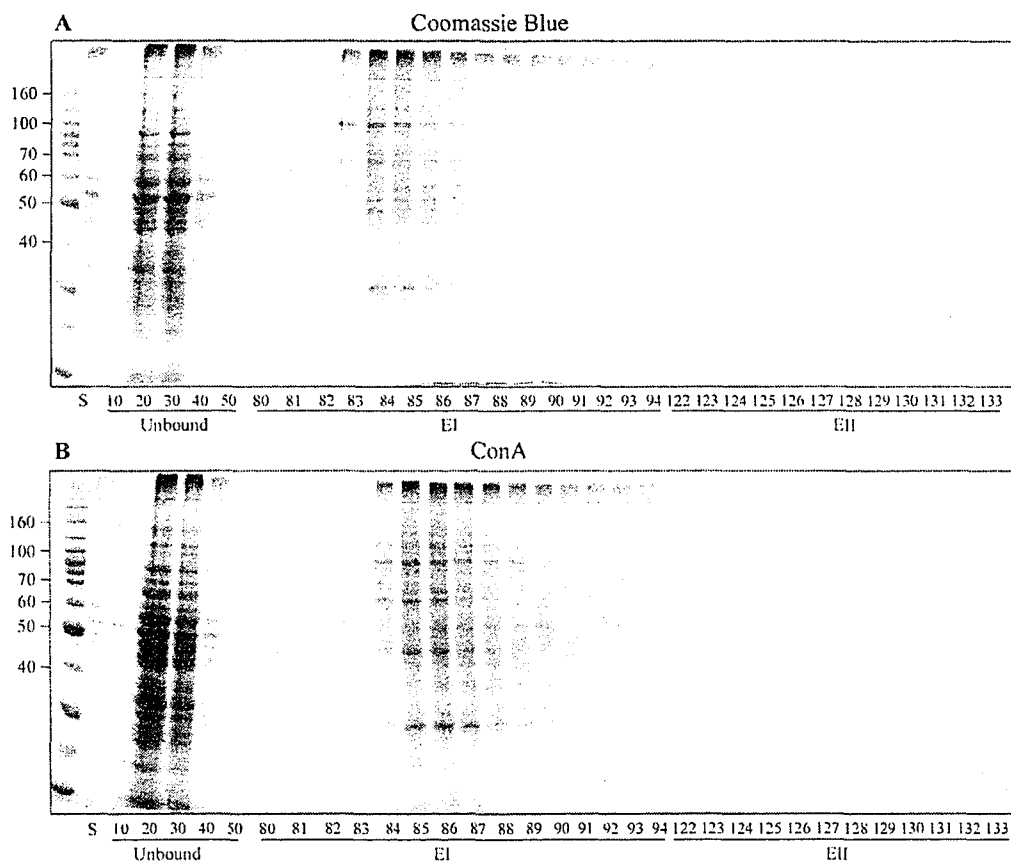


**Fig. 25. A analysis of ConA affinity chromatography of control and AD brain membrane extracts.** A, Coomassie blue staining (50  $\mu$ l/fraction) of selective unbound and EI and EII fractions. B, ConA blot (25  $\mu$ l/fraction) of selective unbound and EI and EII fractions. "S" indicates starting sample (5  $\mu$ g/lane in Coomassie blue stained gel and 10  $\mu$ g/lane in ConA blot). Molecular weight marker was shown on the left in kDa.

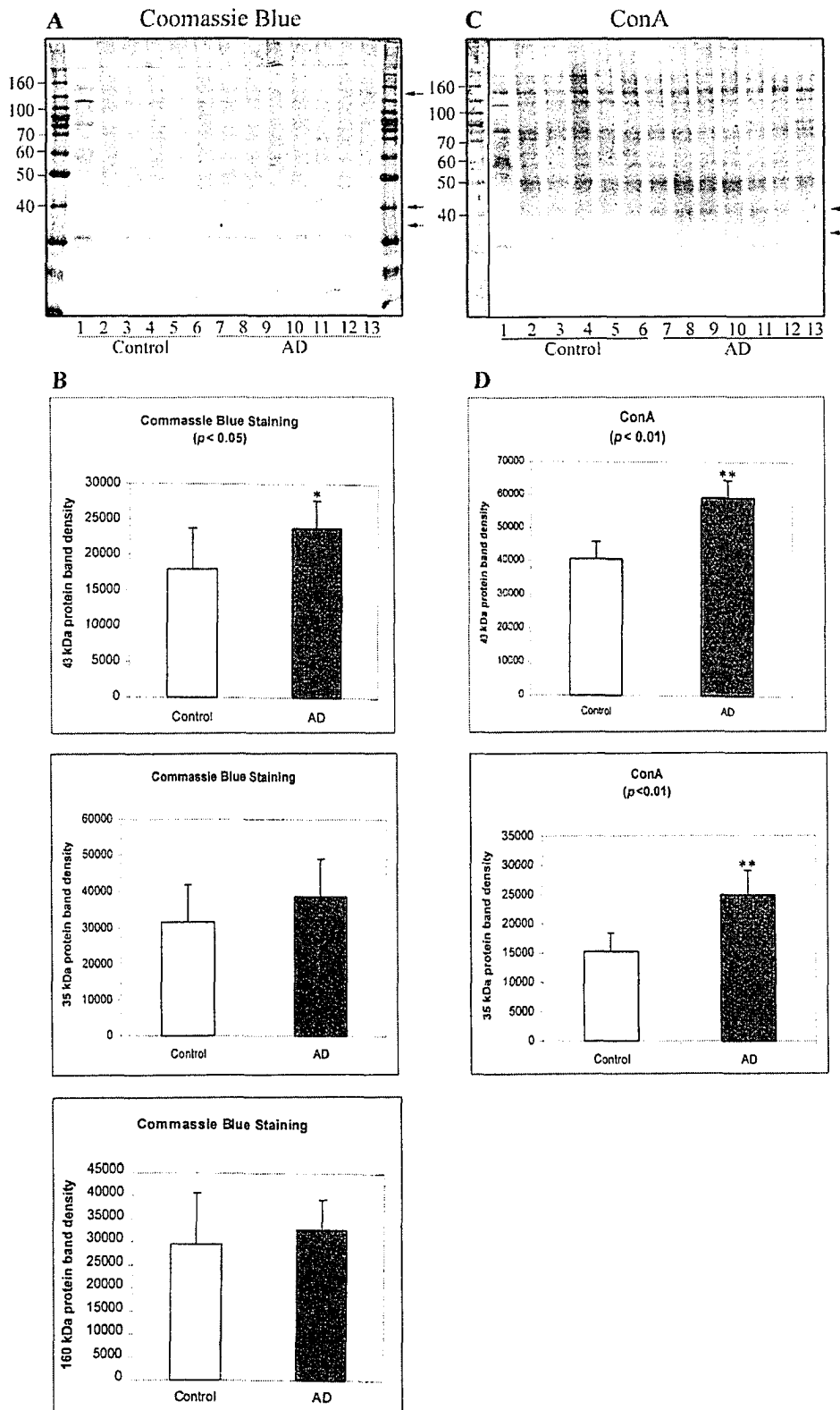


**Fig. 26. (to be continued)**

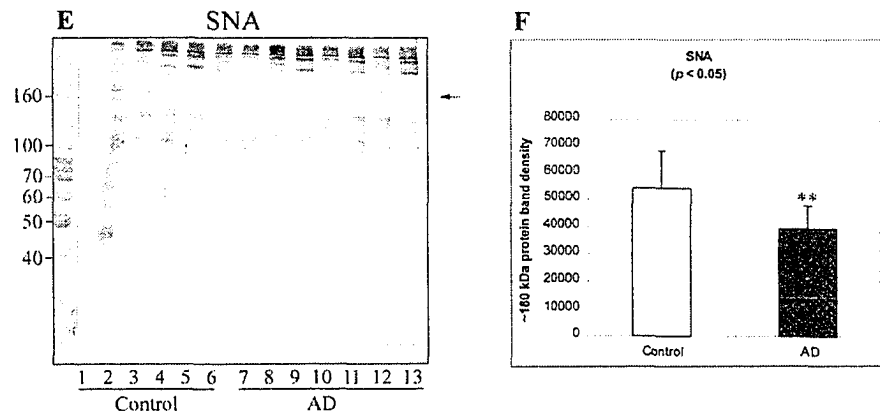


**Fig. 26. Quantitation and comparison of ConA-binding glycoproteins between control and AD brains.** A, Coomassie blue staining of Elution I fractions (EI, 5  $\mu$ g/lane) from ConA affinity chromatography. Lane 1 ~ 6 are control cases and lane 7 ~13 are AD cases. B, Quantitation of 35, 43, and 160 kDa protein bands as marked by arrows in A. C, ConA blot of Elution I (EI, 1  $\mu$ g/lane) from ConA affinity chromatography. D, Quantitation of the 43 kDa and 35 kDa protein bands as marked by arrows in C. E, SNA blot of ConA-binding proteins of Elution I (EI, 1  $\mu$ g/lane) from ConA affinity chromatography. F, Quantitation of 160 kDa protein band in E.

When we analyzed the same samples by GNA blots, we observed that the 35 and 43 kDa glycoprotein bands increased similarly in the AD group (Fig. 27A&B;  $p < 0.01$ ). The GNA blotting was carried out under standard SDS-PAGE conditions, i.e., the electrophoresis was carried out under reducing conditions (1% BME added in sample buffer). When we ran the electrophoresis under non-reducing conditions (no BME added in sample buffer), we found that both the 43 kDa and 35 kDa glycoproteins disappeared on the GNA blot (Fig. 27C). Instead, a 53 kDa protein appeared and the GNA staining of this protein was also increased in AD as compared to controls (Fig. 27C&D;  $p < 0.01$ ). These results suggested that the 53 kDa protein might be a dimer of the 43 kDa or 35 kDa proteins linked to another smaller subunit via disulfide bonds.

To identify the 43 kDa, 35 kDa, and 160 kDa glycoproteins that were found altered in AD brain, we analyzed the ConA-binding proteins together with the isolated

glycoproteins that had been identified by mass spectrometry (see Fig. 23) side by side in a single gel. Analysis of the ConA staining, GNA staining, and Coomassie blue staining suggested that the 43 kDa protein was probably the GNA-8 (acid ceramidase, AC) according to its gel mobility (Fig. 28A). The 35 kDa protein was not enriched in the purified glycoproteins, so that no identification data was available to this protein. With similar approach, we tried to see if the 180 kDa glycoprotein that was found decreased in AD was identified by mass spectrometry. However, this protein did not match with any protein identified (Fig. 28B).

To confirm whether the 43 kDa glycoprotein is indeed AC as suggested by a above analysis, we examined the ConA-binding proteins by using Western blots developed with anti-AC, which is a rabbit polyclonal antibody raised against recombinant human AC. We found that under standard reducing condition, the 43 kDa glycoprotein band was stained by anti-AC (Fig. 29A). Under non-reducing condition, only a 53 kDa band rather than 43 kDa band of the same samples was seen. This phenomenon was the same as we observed on GNA blots (see Fig. 27 A&C). These results strongly suggested that the 43 kDa protein, the lectin staining of which was increased in AD brain, is AC. Consistent with our finding, AC is known to be a heterodimer consisting of a 43 kDa  $\beta$ -subunit and a 13 kDa  $\alpha$ -subunit linked together by a disulfide bond (Bernardo, et al., 1995).

Because the staining of the 43 kDa glycoprotein was found significantly increased in AD brains on both ConA blot (Fig. 26) and GNA blot (Fig. 27), we studied the level of AC in control and AD brains by Western blots. We found that the levels of both of the holoenzyme resolved under non-reducing condition and the  $\beta$ -subunit resolved under reducing condition were significantly increased in AD as compared to controls (Fig.

29B&C). These results further supported our conclusion that the 43 kDa glycoprotein is the  $\beta$ -subunit of AC.

To learn whether the increased ConA and GNA staining of AC was merely due to an increased level of AC in AD brain, or also due to an increased glycosylation of the protein, we analyzed the glycosylation level of AC by normalizing the GNA-staining intensity (Fig. 27A) with the immunoreactivity of this protein (Fig. 29B, lower panel). We did not find any significant difference in the normalized AC glycosylation (Fig. 30). These data suggested that probably the level of AC instead of its glycosylation is increased in AD brain.

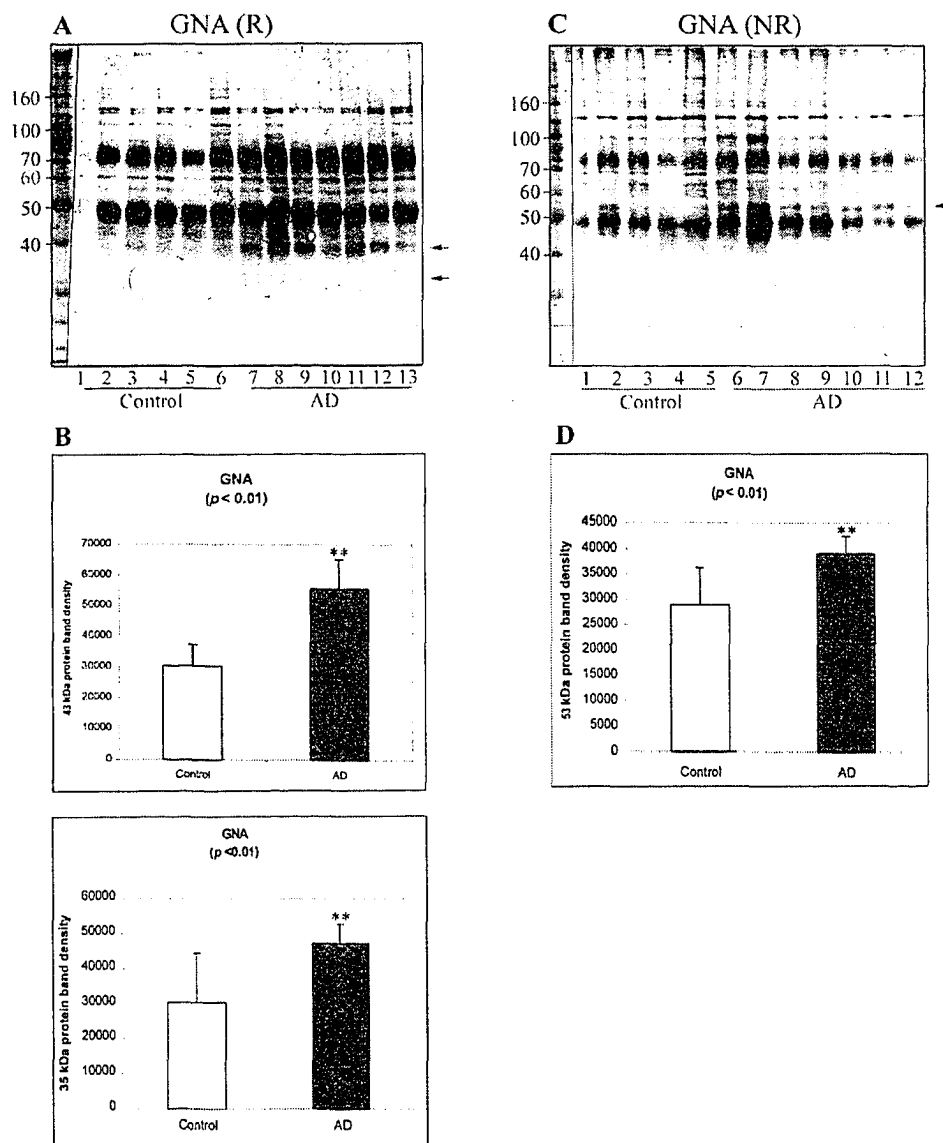


**Fig. 27. The different protein patterns were shown on GNA blots under reducing or non-reducing conditions.** A, GNA blot of ConA-binding glycoproteins of Elution I (EI) from ConA affinity chromatography when SDS-PAGE was carried out under reducing conditions (1% BME freshly added in sample buffer). B, Quantitation analysis of the 43 kDa and 35 kDa protein bands in A. C, GNA blot of the same samples when SDS-PAGE was carried out under non-reducing conditions (no BME added in sample buffer). D, Quantitation analysis of 53 kDa protein band in C.

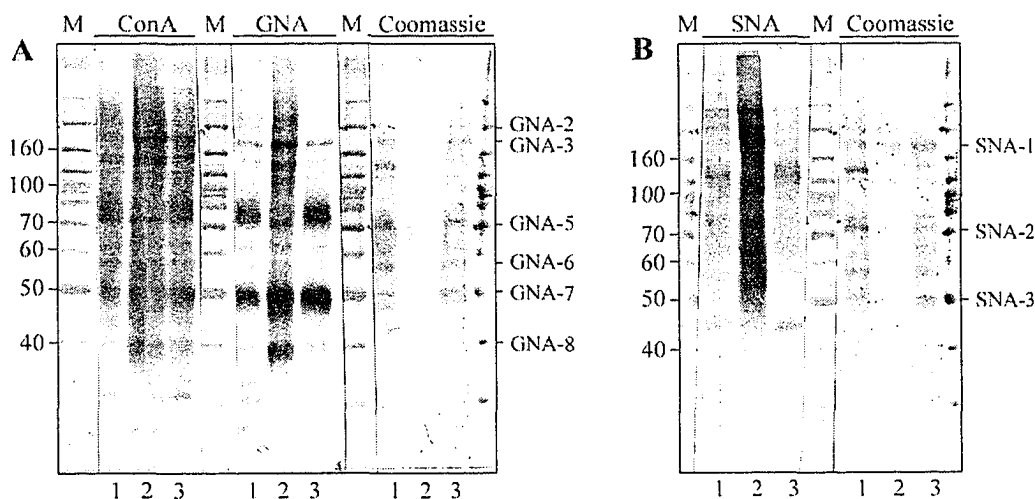


**Fig. 28. Identification of glycoproteins that are altered in AD.** ConA-binding glycoproteins isolated from a control brain (lane 1) and an AD brain (lane 3) were resolved in 10% SDS-PAGE. Lane 2 is the sample shown in Fig. 23, from which bands were analyzed by mass spectrometry (MS). The protein bands that have been identified by MS are marked on the right side of the blots. Matching gel mobility suggested that the 43 kDa band, the ConA and GNA staining of which were increased in AD, may be GNA-8 (human acid ceramidase, AC). The 180 kDa and 35 kDa glycoprotein bands that are also altered on SNA and GNA blots did not match with any protein bands identified by MS.

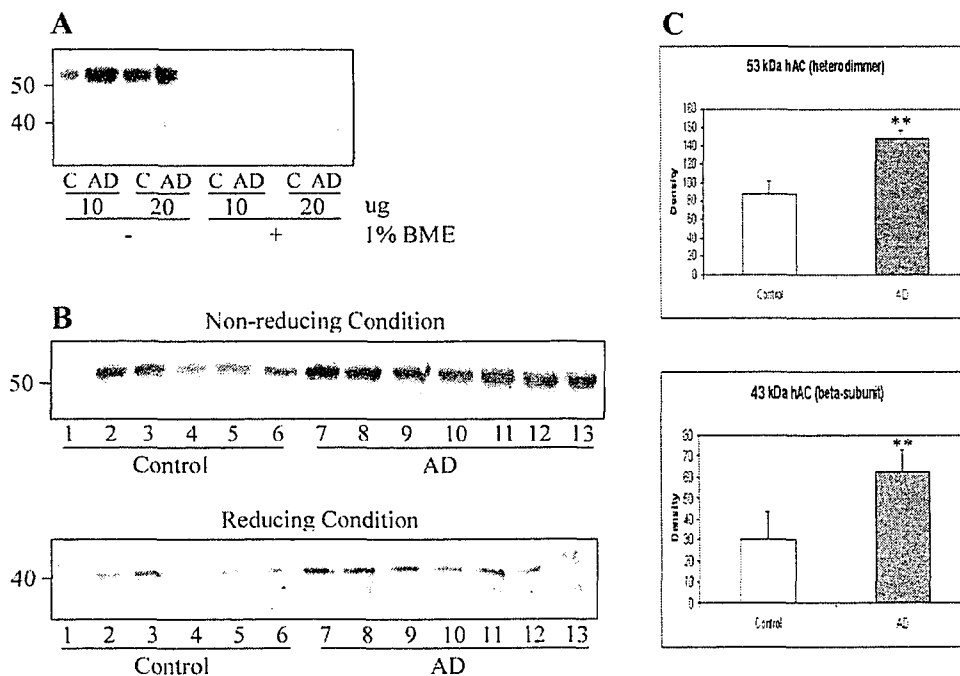


**Fig. 29. Confirmation of the 43 kDa glycoprotein as human AC by Western blots.** A, ConA-binding glycoproteins from a control brain (C) and an AD brain (AD) were resolved in 10% SDS-PAGE under reducing (+ 1% BME) or non-reducing (- BME) conditions. Blot was probed with polyclonal antibody against human AC. Note that the heterodimer AC at ~ 53 kDa under non-reducing condition shifted to the 43 kDa band under reducing condition. Both 53 kDa and 43 kDa bands were seen in lane 4 probably because of the diffusion of 1% BME from the right side to the left. B, ConA-binding glycoproteins (10  $\mu$ g/lane) of control and AD were resolved on 10% SDS-PAGE under non-reducing (upper panel) and reducing (lower panel) conditions, respectively. Blots were probed with polyclonal anti-AC. Note that the expression level of AC is dramatically increased in AD group. C, Quantitation analysis of panel B by densitometry. \*\*,  $p < 0.01$  as compared to controls.

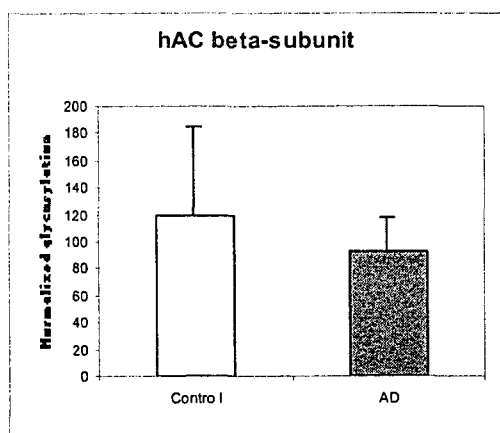


**Fig. 30. Normalized glycosylation level of AC  $\beta$ -subunit.** Band density of AC  $\beta$ -subunits (43 kDa band) on GNA blot was normalized by immunoreactivity on Western blot. There was no significant difference between control and AD groups.

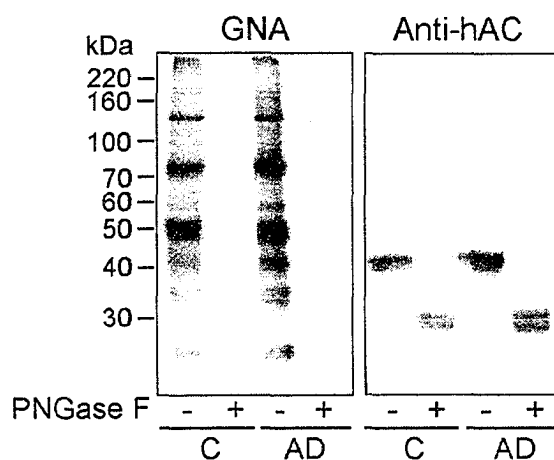


**Fig. 31. In vitro deglycosylation of AC  $\beta$ -subunit from control and AD brains.** ConA-binding glycoproteins from control and AD brains were treated with or without PNGase F, followed by GNA blot or Western blot probed with anti-AC. Note the mobility shift of AC  $\beta$ -subunit and abolishment of GNA staining after PNGase F treatment.

To confirm that the  $\beta$ -subunit of AC is indeed glycosylated, we treated the ConA-binding glycoproteins from control and AD brains with PNGase F, an enzyme that selectively cleaves the bond between the innermost GlcNAc and asparagine residues, and therefore removes N-linked oligosaccharides from proteins (Maley, et al., 1989, Plummer and Tarentino, 1991). After PNGase F treatment, AC  $\beta$ -subunit showed significant mobility shift from 43 kDa to ~30 kDa on Western blot (Fig. 31, right panel), while the GNA staining of most glycoproteins including the 43 kDa  $\beta$ -subunit of AC were abolished (Fig. 31, left panel). These results clearly demonstrated that the  $\beta$ -subunits of AC is indeed glycosylated. Consistent with our finding, the  $\beta$ -subunit of AC has been reported to be glycosylated by N-oligosaccharides (Ferlinz, et al., 2001).

AC is expressed universally in many species, such as rat, mouse and human. Actually, AC was first purified by Gatt from rat brain in 1963 (Gatt, 1963). From then on, the importance of this enzyme was noted and other studies followed. To date, ACs from

rat, mouse and human have been cloned (El Bawab, et al., 2002). Interestingly, rat and mouse ACs share exactly the same amino acid sequence, but different from human AC (Fig. 32). This fact suggested that human AC might perform distinct functions from rat and mouse. However, the functions of AC are still not understood completely, especially in Alzheimer's disease brain.

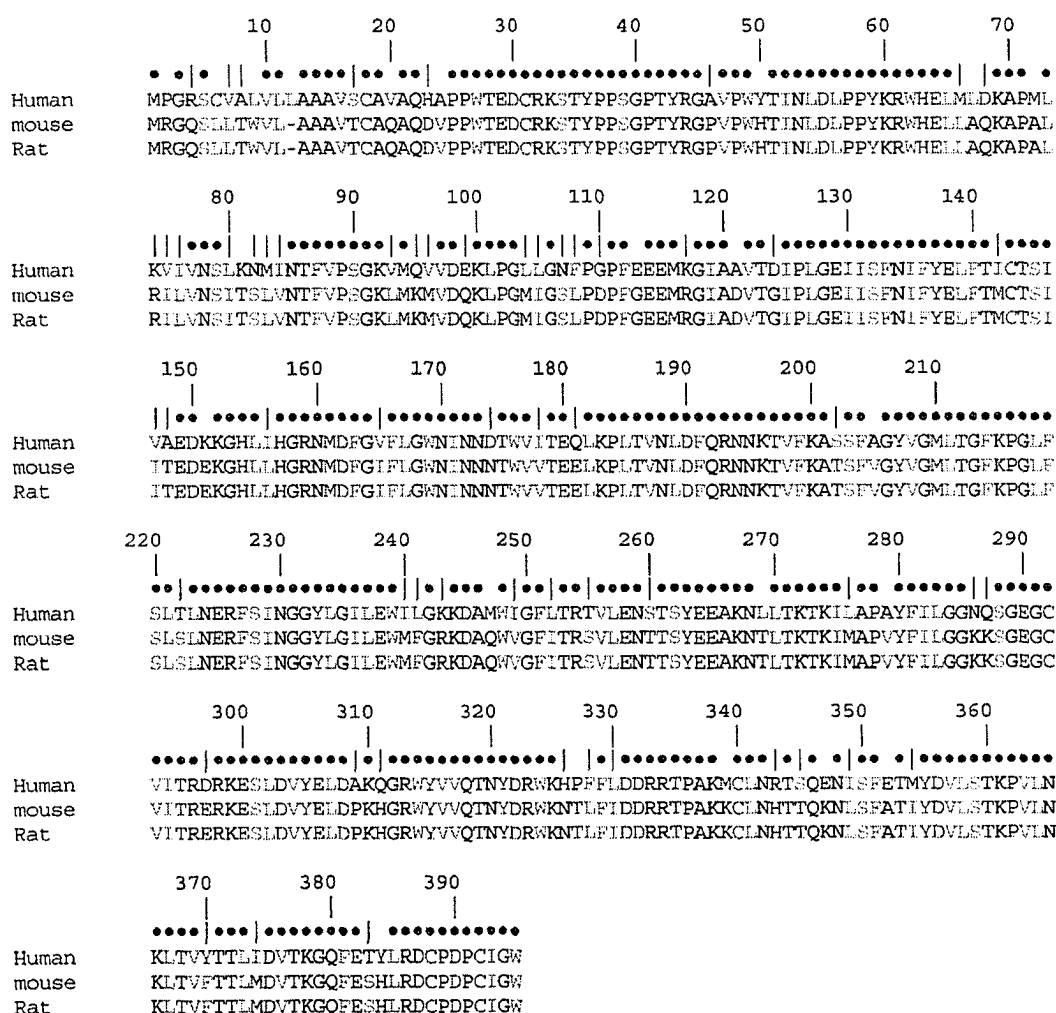


**Fig. 32. Gene sequences of AC from rat, mouse and human.** Different colors represent different types of amino acids. Solid circles indicate identical amino acid residues in all three species. Vertical lines indicate similar amino acids. Blanks show totally different amino acids.

The gene encoding AC has been cloned from several species (El Bawab, et al., 2002), but surprisingly the morphological and cellular distributions of AC in mammalian brain have not yet been studied. We therefore investigated the immunohistochemistry of AC in post-mortem human brain. As demonstrated in Fig. 33, anti-AC stained mostly neurons and some of astrocytes (Fig. 33). The staining appeared specific because a control staining in which the primary antibody was omitted was negative (Fig. 33B). Observed under high magnification, the neuronal staining displayed a typical lysosomal punctuate staining (Fig. 33C). This observation is consistent with previous finding that AC is a lysosomal enzyme (Sugita, et al., 1972). We also stained AD brain tissue sections in parallel with control brain sections, but we did not observe noticeable differences in immunohistochemical staining of AC between AD and control brains (data not shown).

To investigate whether AC co-localizes with NFTs, we performed double immunostaining of AD tissue sections with anti-AC and PHF-1, the later of which is specific to NFTs. We found that most of the PHF-1 positive neurons were also stained by anti-AC, but only some of the AC positive neurons were PHF-1 positive. In neurons positive to both staining, AC appeared to co-localize with NFTs (Fig. 34A-C, arrows). There were a few of PHF-1 positive NFT staining that were not stained by anti-AC (Fig. 34D-F, large arrow head). According to the structures of these NFTs, they may represent the end stage ghost tangles where the neurons had died and all the cellular structures and components had been lost.

In summary, we have found that there were three glycoproteins in the cerebral cortex whose lectin staining was altered in AD brain. The 35 kDa glycoprotein was either elevated in its protein level or its glycosylation level. In contrast, the 180 kDa

glycoprotein that contains a terminal sialic acid was decreased in its protein level or its glycosylation level in AD brain. We have identified the third glycoprotein, the 43 kDa glycoprotein, as human AC  $\beta$ -subunit. The protein level rather than the glycosylation of AC was significantly elevated in AD brain. This enzyme is largely expressed in neurons of human brain and appears to co-localize with most NFTs but not with late stages of NFTs. These results taken together suggested a possible involvement of AC in the pathogenesis of AD.

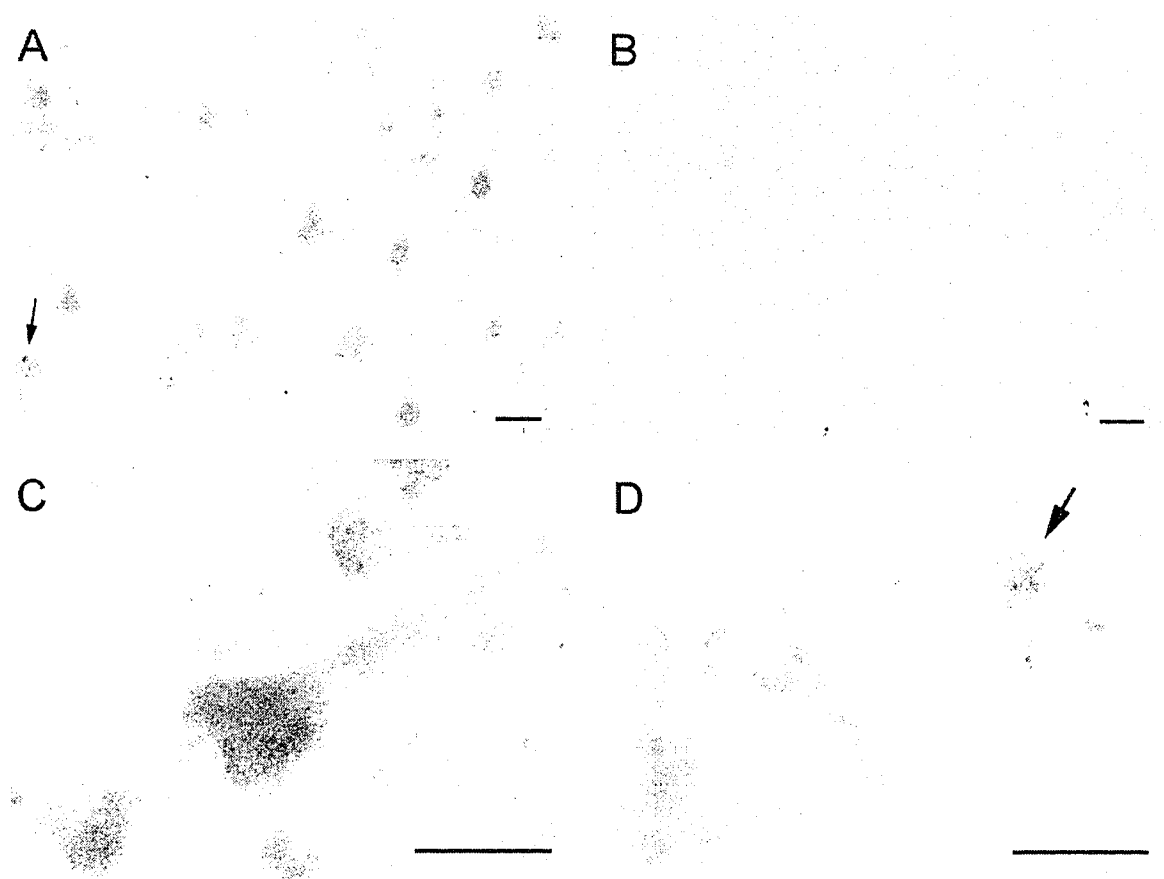


**Fig. 33. Immunohistochemistry of AC in human brain temporal cortex.** Tissue sections were immunostained with anti-AC (A, C, D) or, as a control staining, with the same procedure except the primary antibody was omitted (B). Arrows indicate immunostaining of astrocytes. Magnification bars = 10  $\mu$ m.

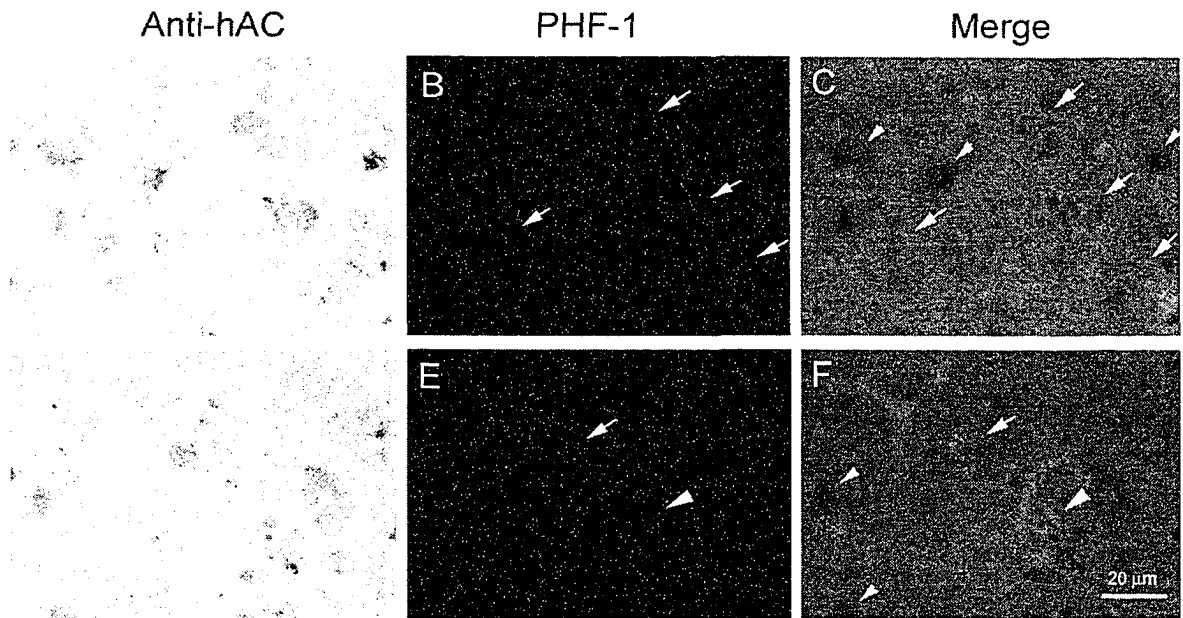


**Fig. 34. Double immunohistochemical labeling of AC and NFTs in AD cerebral cortex.** Tissue sections were double stained with polyclonal anti-AC (A and D, brown) and monoclonal antibody PHF-1 to NFTs (B and E, red fluorescence). The merged images are shown on the right side. Arrows indicate NFTs that are also labeled by anti-AC. Large arrowheads indicate NFTs that are not labeled by anti-AC. Small arrowheads indicate AC positive neurons that are free of NFTs.

#### **4.4. One of the Inhibitors of Nuclear Factor $\kappa$ B (NF $\kappa$ B), I $\kappa$ B $\gamma$ , Is Up Regulated in AD Brain**

When we used lectin blots to compare homogenate proteins between control and AD brain, we found a significant increase in MAA staining of a protein band with apparent molecular weight of 45 kDa in AD brains as compared with controls (Fig. 35). This result suggested that either this 45 kDa protein might be glycosylated with sialic acid to a higher extent in AD than controls, or this protein might be over-expressed in AD brain.

In order to learn the subcellular distribution of the 45 kDa protein, we prepared 100,000  $\times$  g pellet from the homogenates, which mainly contained nuclear and membrane proteins. The supernatant mainly contained cytosolic proteins. Examination of the protein profiles of these two fractions together with the homogenate samples by using lectin blots indicated that the increased staining of the 45 kDa protein with MAA as observed in AD homogenate samples (Fig. 36A, comparing lanes 3, 4 with lanes 1, 2) was also seen in the pellets (Fig. 36A, comparing lanes 11, 12 with lanes 9, 10), but not the supernatants (Fig. 36A, comparing lanes 7, 8 with lanes 5, 6). These results suggested that this 45 kDa protein was nuclear or membrane-associated proteins. On SDS-polyacrylamide gel, tau normally displays as multiple bands in 40-68 kDa ranges due to its multiple isoforms and variable post-translational modifications (Buee, et al., 2000). The AD abnormally hyperphosphorylated tau (AD P-tau) was also recovered from the pellet of 100,000  $\times$  g centrifugation. We, therefore, examined whether the increased 45 kDa protein was hyperphosphorylated tau that was found to be aberrantly glycosylated previously (Wang, et al., 1996). The 100,000  $\times$  g pellets of AD brain homogenates and, as a control, isolated

AD P-tau were resolved in SDS-PAGE and transferred on PVDF membrane. Each of the lanes were cut at the centre into two strips and stained with lectins and anti-tau antibody separately (Fig. 36B). This approach allowed us identify if the 45 kDa band was tau. We found that the pellet samples contained tau at higher molecular range than 45 kDa and no clear tau staining was observed at the 45 kDa band which was lectin positive. On the other hand, the isolated AD P-tau was not stained at 45 kDa with MAA. These data indicated that the 45 kDa protein was not tau.

In order to further investigate the 45 kDa protein which was altered in AD, we did the subcellular fractionation as summarized in Fig. 3. After determining the protein concentration with modified Lowry assay, equal amount of proteins from each fraction were resolved on 10% SDS-PAGE for Coomassie blue staining (5 µg/lane) and MAA blot (10 µg/lane). The 45 kDa protein was enriched in nuclear fractions in both control and AD cases, suggesting that this protein was primarily a nuclear protein (Fig. 37).

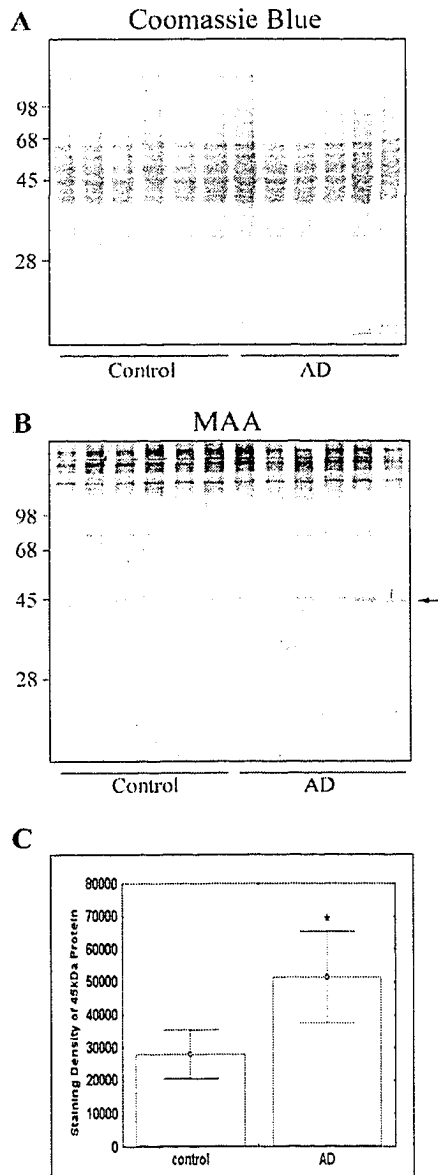


**Fig. 35. Coomassie blue staining and MAA blot of control and AD brain homogenates.** Homogenates (5  $\mu$ g/lane) of cerebral cortex of six AD and six control brains were resolved by 10% SDS-PAGE and then stained with Coomassie blue (A) or probed with lectin MAA (B). The 45 kDa MAA positive band was quantitated by densitometry (C). \*,  $p < 0.05$  as compared with control group.

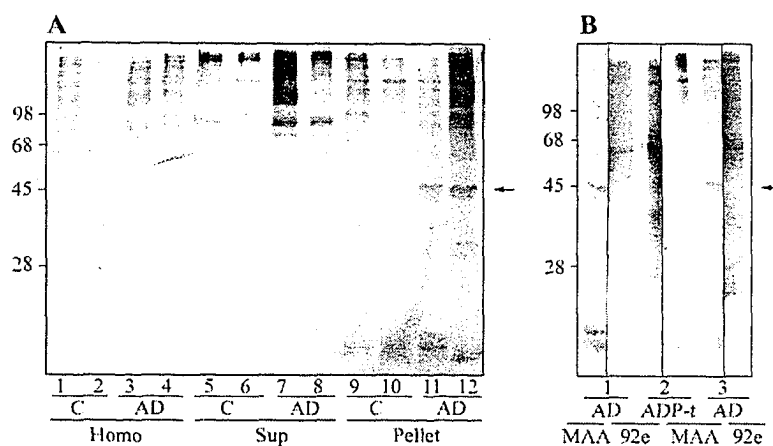


**Fig. 36. Subcellular distribution of the 45 kDa protein.** A, Ten  $\mu\text{g}$  per lane of homogenates (Homo), and their supernatants (Sup) and pellets of  $100,000 \times \text{g}$  centrifugation were subjected to lectin blotting with MAA. Two cases of AD and 2 cases of controls are shown. The arrow indicates the staining of 45 kDa protein which is altered in AD is located in the  $100,000 \times \text{g}$  pellet. B, Western and MAA blots of AD P-tau and  $100,000 \times \text{g}$  pellets of AD brain homogenates. Isolated AD P-tau (3  $\mu\text{g}/\text{lane}$ ) and the pellets (two cases, 10  $\mu\text{g}/\text{lane}$ ) were separated on 10% SDS-PAGE. After transfer of the proteins onto PVDF membrane, each lane of these samples was cut at the centre into two strips. Half of each lane (one strip) was stained with MAA to detect the 45 kDa protein. The other half was stained with anti-tau antibody 92e. The arrow indicates the protein the staining of which was increased in AD brain. Note that this protein is not tau.

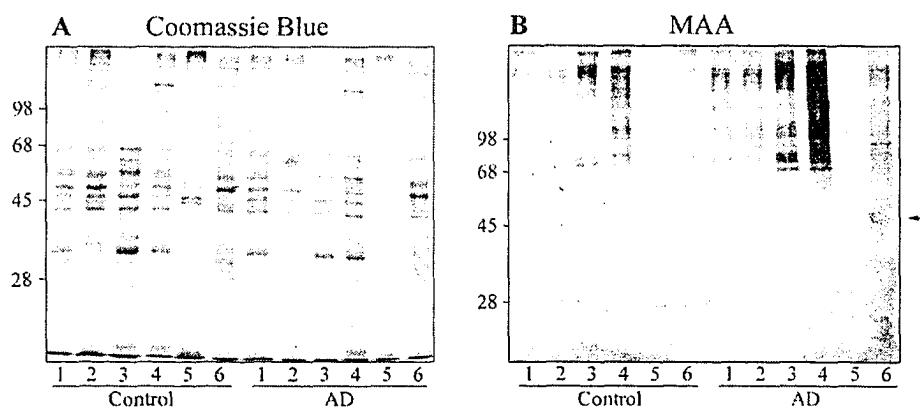


**Fig. 37. Subcellular localization of 45 kDa protein which is altered in AD.** Coomassie blue staining (A) and MAA blot (B) of control and AD subcellular fractions (5  $\mu\text{g}/\text{lane}$  for A and 10  $\mu\text{g}/\text{lane}$  for B). Lane 1, homogenate of cerebral cortex; lane 2, nuclei and tissue debris fraction (Pellet 1); lane 3, cytosolic protein fraction (Sup 4); lane 4, microsomes fraction (Pellet 4); lane 5, synaptosome fraction (mid-layer of sucrose gradient separation); lane 6, lysosome fraction (bottom-layer of sucrose gradient separation). Note that the 45 kDa protein is enriched in the nuclear fractions (arrow).

For the purpose of protein identification, we isolated the 45 kDa protein from 100,000 × g pellet by using HPLC. Analysis of the HPLC fractions by using silver staining and MAA blot indicated that the 45 kDa protein was mainly enriched in the first two fractions in the 0 ~ 1 M NaCl eluted peak (Fig. 38). Hence, we pooled fractions 1 and 2 (200 μl) and resolved on 10% SDS-PAGE after concentration by cold acetone precipitation. Coomassie blue stained gel was matched with MAA blot (Fig. 39). One control and one AD homogenates were used as references. The confirmed 45 kDa protein band was dissected and identified by N-terminal amino acid sequencing. We identified that the 45 kDa protein as IκBγ, one of the inhibitors of nuclear factor κB (NFκB).

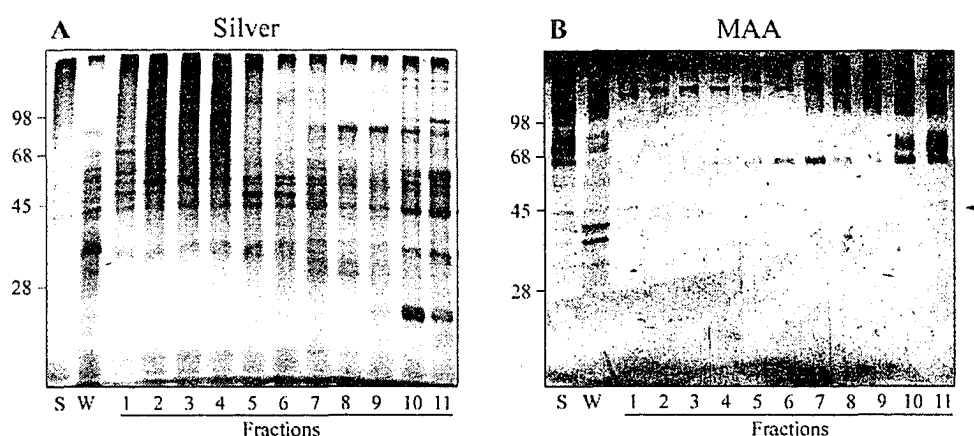


**Fig. 38. Silver staining and MAA blot of aliquots from HPLC.** Silver staining (A) and MAA blot (B) of starting sample (S), wash (W), and Fractions 1 ~ 11 from HPLC of pellet of human brain homogenate. Note that the 45 kDa protein is enriched in fraction 1 and 2.

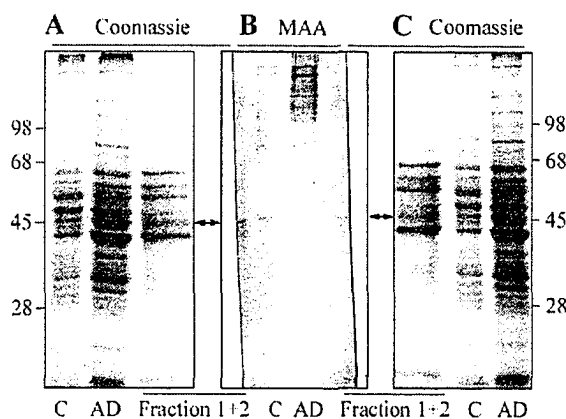


**Fig. 39. Coomassie blue stained 45 kDa protein band was cut for N-terminal amino acid sequencing.** Pooled fractions 1 and 2 (200  $\mu$ l) from HPLC was precipitated by cold acetone and resolved on 10% SDS-PAGE. A and C are duplicates of Coomassie blue stained gel. B is MAA blot. One control and one AD homogenates were used as references. Arrow indicates the 45 kDa protein band that was cut out and analyzed by N-terminal amino acid sequencing.

I $\kappa$ B $\gamma$  is a family of proteins, including I $\kappa$ B $\gamma$ , I $\kappa$ B $\gamma$ -1, I $\kappa$ B $\gamma$ -2 isoforms, which share amino acid sequence with the C-terminal half of NF $\kappa$ B precursor, p105. In contrast to cytoplasmic p70 I $\kappa$ B $\gamma$ , p60 I $\kappa$ B $\gamma$ -1 is found in both the cytoplasm and nucleus, whereas p50 I $\kappa$ B $\gamma$ -2 is predominantly nuclear (Inoue, et al., 1992, Gerondakis, et al., 1993). Because I $\kappa$ B $\gamma$  has not been reported as a glycoprotein, we used Western blot developed with anti-I $\kappa$ B $\gamma$  to confirm whether the 45 kDa protein that was increased in AD was indeed I $\kappa$ B $\gamma$ . This antibody recognizes both the I $\kappa$ B $\gamma$  and p105 (Santa Cruz Biotechnology Labs, Santa Cruz, CA). When we examined the homogenate samples from gray matter, we did not observe clear band at 45 kDa level on Western blots (data not shown). However, we observed a dramatic increase in the immunostaining of p105 (Fig. 40). Similar analysis of the white matter homogenates did not reveal any difference between AD and controls (Fig. 41).

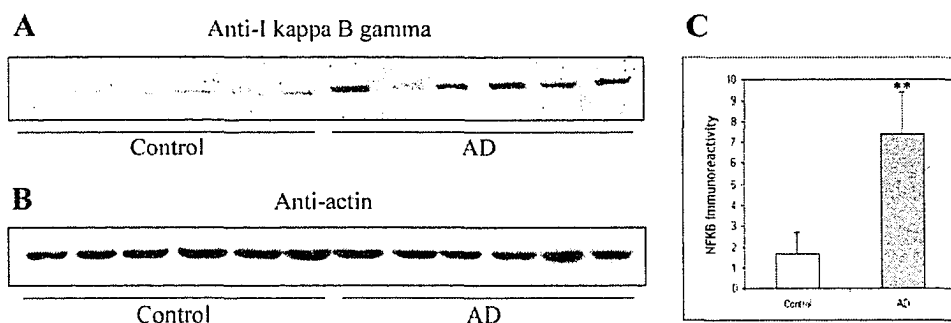


**Fig. 40. Western blots of homogenates from gray matter of control and AD brains.** A, Western blot was probed by anti-I $\kappa$ B $\gamma$  that recognizes both I $\kappa$ B $\gamma$  and p105. An immunopositive 105 kDa protein band was dramatically increased in AD group. B, The blot was re-probed by anti-actin to confirm the equal loading. C, Quantitation analysis of blot shown in panel A. \*\*,  $p < 0.01$  as compared with control.

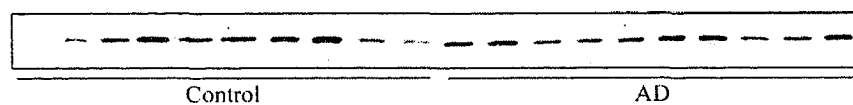


**Fig. 41. Western blots homogenates from white matter of control and AD brains.** Western blot was probed by anti-I $\kappa$ B $\gamma$ . The 105 kDa protein band showed no difference between control and AD groups.

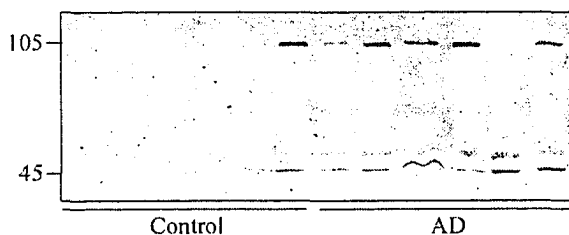


**Fig. 42. Western blots of Pellet 1 (nuclear fraction) of subcellular fractionation from control and AD brain homogenates.** Subcellular fractionation showed that the 45 kDa I $\kappa$ B $\gamma$  was enriched in nuclear fraction. Western blot of nuclear fraction from six pairs of control and AD brains was probed by I $\kappa$ B $\gamma$  antibody.

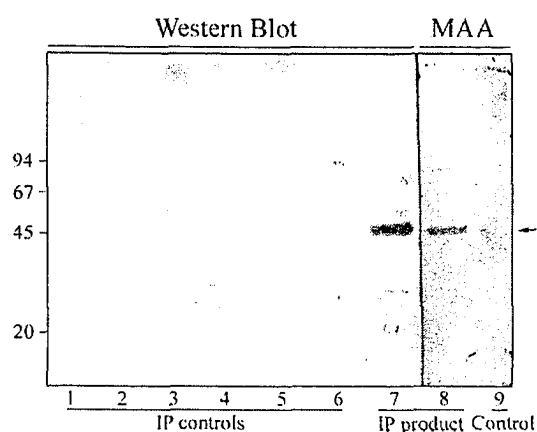


**Fig. 43. Immunoprecipitation of  $\text{IkB}\gamma$  from nuclear fraction of AD brain.** Lane 1 is the FL of protein G beads and anti- $\text{IkB}\gamma$  mixture; lane 2 is the first wash; lane 3 is Pellet 1 homogenized in IP buffer; lane 4 is Pellet 1 extract by sonication and centrifugation; lane 5 is the FL of Pellet 1 extract, anti- $\text{IkB}\gamma$  and protein G beads mixture; lane 6 is the sixth wash; lane 7 and 8 are duplicates of IP product; lane 9 is anti- $\text{IkB}\gamma$  antibody served as control. Lane 1 ~ 7 were probed by anti- $\text{IkB}\gamma$  antibody, while lane 8 and 9 were stained by MAA. Note that IP product is both anti- $\text{IkB}\gamma$  and MAA positive.

Since the 45 kDa MAA-positive protein was enriched in nuclear fraction (Fig. 37B), we prepared nuclear fractions from gray matter of control and AD brains and examined them by Western blots with anti- $\text{IkB}\gamma$ . In addition to p105 as we observed in homogenate samples, we also observed the 45 kDa band that was increased in nuclear fractions of AD as compared to controls (Fig. 42).

To confirm that the MAA-positive 45 kDa band was indeed  $\text{IkB}\gamma$  rather than other co-migrated glycoproteins, we immunoprecipitated  $\text{IkB}\gamma$  from nuclear fraction of an AD brain. Western blot analysis demonstrated that the  $\text{IkB}\gamma$  was successfully immunoprecipitated and the  $\text{IkB}\gamma$  was indeed stained by lectin MAA (Fig. 43). The positive MAA staining of the immunoprecipitate was not due to IgG (anti- $\text{IkB}\gamma$ ) that

itself is glycoprotein, because no significant staining was seen in lane 9 that contained the same amount of IgG as lane 8.

I $\kappa$ B $\gamma$  has not been reported to be glycosylated. To investigate whether the staining of I $\kappa$ B $\gamma$  with lectin MAA was due to an unusual glycosylation of this protein or was due to a cross reaction between MAA and I $\kappa$ B $\gamma$ , we treated blot with 0.1 N HCl at 80°C for 1 hour before probing with MAA. This treatment is commonly used to remove sialic acid from glycoproteins (Ref.). We found that the acid treatment did not reduce or abolish the I $\kappa$ B $\gamma$  staining with MAA (Fig. 44). This result suggested that I $\kappa$ B $\gamma$  was not glycosylated with sialic acid. The MAA staining of I $\kappa$ B $\gamma$  was likely due to a cross-reaction.

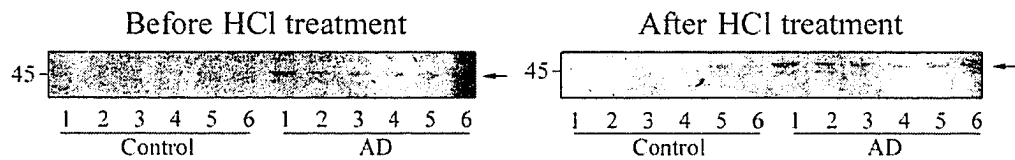


**Fig. 44. Removal of sialic acid by HCl treatment.** Control and AD brain homogenates were resolved by 10% SDS-PAGE (10  $\mu$ g / lane) in duplicates. After transfer, one blot was stained by MAA immediately and another one was treated with 0.1 M HCl at 80 °C for 1 hour and then stained by MAA. Arrow indicates the 45 kDa band.

Since the 45 kDa protein band that was used for protein identification by N-terminal sequencing was not highly purified, it is possible that this band was contaminated with a MAA-positive glycoprotein that is altered in AD. Hence, we further purified the eluted fractions that contained the 45 kDa protein from HPLC by ammonium sulfate precipitation and preparative SDS-gel electrophoresis. The collected fractions of preparative electrophoresis were analyzed by a analytic SDS-PAGE and lectin blot (Fig.

45). The MAA-positive 45 kDa band was then cut out and identified by mass spectrometry. We found that this protein was glial fibrillary acidic protein (GFAP). GFAP has been reported to be up regulated in AD brain (Delacourte, 1990; Vijayan, et al., 1991; Porchet, et al., 2003), but not as a glycoprotein.

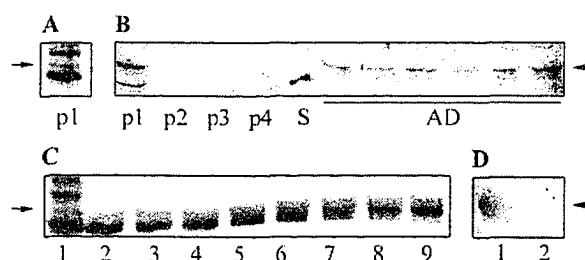


**Fig. 45. Further purification of 45 kDa band by ammonium sulfate precipitation and preparative SDS-gel electrophoresis.** A and B show the ammonium sulfate precipitation. A, Silver staining of 2  $\mu$ g of 25% ammonium sulfate precipitated pellet (p1). B, MAA blot (10  $\mu$ g/lane) of ammonium sulfate precipitated pellet at 25% (p1), 40% (p2), 50% (p3), and 60% (p4), 60% ammonium sulfate supernatant (S), and six cases of AD homogenates. Arrow indicates that the 45 kDa protein was enriched in p1. C, Silver staining of fractions from preparative SDS-PAGE of p1. Lane 1 is 2  $\mu$ g p1; lane 9 is the fraction which contains the purified 45 kDa protein. D, MAA blot of purified 45 kDa protein (lane 1) and p1 (lane 2, 10  $\mu$ g). Note that the purified 45 kDa protein is MAA positive and matched perfectly with MAA positive band in p1.

## 5. DISCUSSION

A cell contains besides nucleic acids three classes of macromolecules: proteins, lipids, and carbohydrates. They serve as major structural components of an organism. Lipids and carbohydrates can also work as intermediates in generating energy or as signaling molecules. The structural roles of carbohydrates become particularly important in complex multicellular organs and organisms, which require interactions among cells and with the surrounding matrix. All cells and many macromolecules in nature, including both proteins and lipids, also carry a dense and complex array of covalently attached sugar chains (called oligosaccharides or glycans). In some instances, these glycans can also be free-standing entities. Since most glycans are on the membrane or secreted macromolecules, they are in a position to modulate or mediate a wide variety of events in cell-cell and cell-matrix interactions crucial to the development and function of a complex multicellular organism. In addition, simple, highly dynamic protein-bound glycans, such as O-GlcNAc, are abundant in the nucleus and cytoplasm, where they appear to serve as regulatory switches (Varki et al., 1999)

During development, carbohydrate structures in central nervous system (CNS) change dramatically. In mature CNS, cell-cell interaction, signal transduction and information delivery also need carbohydrates (Fukuda and Hindsgaul, 2000). Several key proteins involved in the possible pathogenesis of AD are glycoproteins. Our previous findings that tau is abnormally glycosylated in AD brain and the tau glycosylation appears to play a role in the abnormal hyperphosphorylation of tau and consequent neurofibrillary degeneration suggest that protein glycosylation system might be altered in AD brain

(Wang, et al., 1996; Liu, et al., 2002a; 2002b; 2002c). However, a systematic study on glycoproteins in human brain have never been done. In the present study, we therefore isolated and identified the major glycoproteins in post-mortem human brain. For this purpose, we enriched glycoproteins from membrane fractions of human cerebral cortex by ConA affinity chromatography. The ConA-binding glycoproteins were further isolated by sequential DEAE-ion exchange chromatography and lectin chromatographies. This procedure allowed isolation of major brain glycoproteins that could be identified by mass spectrometry after separation in SDS-PAGE. Out of 13 protein bands dissected out of SDS-gel, 12 protein bands were identified from AD brain by mass spectrometry (Table 9). Nine of the 12 identified proteins were previously identified proteins, i.e., neuronal cell adhesion molecule,  $\beta$ -globin, IgM heavy chain VH1 region precursor, contactin precursor, dipeptidylpeptidase VI, CD81 partner 3, prenylcysteine lyase, adipocyte plasma membrane-associated protein and acid ceramidase (AC). All these nine proteins are known glycoproteins (Wing, et al., 1992; Berglund, et al., 1994; Castagnola, et al., 1989; Fan, et al., 1997; Tschantz, et al., 1999; Tartakoff and Vassalli, 1979; Morita, et al., 2000; Ferlinz, et al., 2001; and Stipp, et al., 2001). The other 3 were found in a protein database, but the proteins have not been purified and reported. According to the predicted primary sequences of these proteins, they all contain several consensus sequence Asn-X-Ser/Thr for N-glycosylation, which is consistent with our conclusion that they are major glycoproteins in human brain. The purification, characterization, and biophysical functions of these proteins deserve further investigation.

When we compare the lectin staining of ConA-binding glycoproteins between control and AD brains, we found an alteration of lectin-staining of three glycoproteins with

apparent molecular weight of 43 kDa, 35 kDa and 180 kDa, respectively. We identified the 43 kDa glycoprotein as  $\beta$ -subunit of AC that is one of the major glycoproteins in human brain (Table 9). Further studies suggested the level rather than the glycosylation (sugar content) of AC was elevated in AD brain. The 35 kDa and 180 kDa glycoproteins had very low abundance in human brain, so that the nature of these two altered glycoprotein could not be identified in this study. Whether the altered lectin staining of these two proteins represent altered glycosylation levels or merely protein levels in AD brain is unknown. Nevertheless, our observation indicates that in addition to the aberrant glycosylation of tau other glycoproteins are altered in AD brain.

Acid ceramidase was first described in rat brain by Gatt (1963, 1966). It belongs to a family of enzymes called ceramidases. Historically, ceramidases have been classified as acid, neutral, or alkaline, based on the pH optimum of their activities. Even though these enzymes share the same activity to catalyse the hydrolysis of ceramide into sphingosine (SPH) and free fatty acid, they have different locations in the cell and different expression levels in different tissues (Tani et al., 2000a; Mitsutake et al., 2001; Mao et al., 2001). Acid ceramidase is located in lysosome and has the highest expression level in brain and kidney (El Bawab, et al., 2002). Neutral and Alkaline ceramidases are enriched in mitochondria and ER and have higher expression in liver and kidney (Tani et al., 2000b). Acid ceramidase has been purified from various tissues including brain (Yavin and Gatt, 1969), placenta (Chen et al., 1981), and from urine (Bernardo et al., 1995). The acid ceramidase gene has been cloned and was found to be located on the short arm of chromosome 8 (Li et al., 1998; 1999). The estimated molecular mass of the purified heterodimeric human AC is ~50 kDa (Bernardo et al., 1995). It is reduced into two

subunits of ~13 kDa ( $\alpha$ ) and 40 kDa ( $\beta$ ) in SDS-PAGE. The 40 kDa  $\beta$ -subunit is glycosylated (Ferlinz, et al., 2001), which is consistent with our observation that its signal on Western blot was a smear and that PNGase F treatment reduced its apparent molecular weight to 30 kDa. Processing studies performed in human skin fibroblasts revealed that AC was first synthesized as a ~55 kDa precursor that was proteolytically processed into the two subunits within late endosomes or lysosomes (Koch et al., 1996). Most of the enzyme was found within cells, presumably in acidic compartments, but small amounts of the precursor and a partially processed 47 kDa form were also found extracellularly (Bernardo et al., 1995).

The known physiological function of human AC is to catalyze the hydrolysis of ceramide into sphingosine (SPH) and free fatty acid (Merrill and Wang, 1992). Ceramide serves as the precursor for most sphingolipids, and is a signalling molecule that induces apoptosis in a number of different cell types (Perry and Hannun, 1998; Kolesnick, 2002). Sphingosine is converted into sphingosine-1-phosphate (S1P) through the action of sphingosine kinase, another important cell signalling lipid that is “anti-apoptotic” and can counteract the effects of ceramide (Spiegel et al., 1998; Pyne, 2002). The only source of sphingosine in vertebrate cells is through ceramide hydrolysis, while ceramide can be generated by synthetic pathways or through the degradation of sphingomyelin or glycosphingolipids (Merrill and Wang, 1992; Mandon et al., 1992; Michel et al., 1997). Importantly, many of the enzymes of ceramide metabolism appear to be physiologically regulated. Thus, regulation of ceramide metabolizing enzymes may result in altered regulation of ceramide levels, which in turn, will modulate ceramide-mediated biology. Therefore, many of these enzymes emerge as important candidates in the regulation of

ceramide-mediated responses and for pharmacological development of novel chemotherapeutic agents (El Bawab et al., 2002).

Many extracellular agents or inducers of cell injury or stress such as tumor necrosis factor alpha (TNF $\alpha$ ), fas ligands,  $\gamma$ -interferon, interleukin-1 (IL-1), nerve growth factor (NGF), radiation, and several chemotherapeutic agents (Hannun, 1996; Mathias et al., 1998) cause the accumulation of endogenous ceramide through activation of sphingomyelinases and/or the de novo pathway of sphingolipid synthesis (Perry et al., 2000; Kroesen et al., 2001). The change in endogenous levels of ceramide in response to these agents occurs prior to the onset of the first biochemical signs of apoptosis such as activation of caspases (Hannun, 1996; Dbaiibo et al., 1997). More recent studies are beginning to show that ceramide is necessary for several cell responses. First, increase of intracellular levels of ceramide through inhibition of ceramidases induces cell death (Bielawska et al., 1996). Second, the suppression of ceramide formation prevents, at least in part, the cellular response in many cell types (Hannun and Luberto, 2000). Third, ionizing radiation has been shown to cause ceramide formation through activation of an acid sphingomyelinase, and animals deficient in this sphingomyelinase become resistant to high doses of irradiation, again demonstrating an important role for ceramide in apoptosis (Lavie et al., 1997; Liu et al., 1999). In particular, in many malignant cell lines (such as leukemia and breast carcinoma cells), ceramide rapidly and specifically induces apoptosis (Obeid et al., 1993). Ceramide has been shown to activate proteases of the ICE family (caspases), especially caspase-3 (Smyth et al., 1996; Mizushima et al., 1996). Importantly, activation of caspase-3 by ceramide and induction of apoptosis are inhibited by overexpression of bcl-2 (Smyth et al., 1996), and bcl-2 does not reduce the levels of

ceramide produced in response to extracellular agents (Zhang et al., 1996). Taken together, the generation of ceramide occurs upstream of the activation of proteases and upstream of the point at which bcl-2 interferes with this activation. Also, activation of PKC attenuates the ability of ceramide to induce apoptosis. It has been shown recently that activation of p53 is necessary for ceramide formation in response to DNA-damaging agents, suggesting a role for ceramide down stream of p53 (Dbaibo et al., 1998)

Although it was known long ago that a deficiency of AC activity causes Farber lipogranulomatosis, a lipid storage disorder (Sugita, et al., 1972; Koch, et al., 1996; Bar, et al., 2001), this enzyme has never been reported to be involved in AD. We report here for the first time that AC is one of the major brain glycoproteins and its level is significantly increased in AD. Since ceramide, the substrate of AC, and sphingosine-1-phosphate, which is derived from sphingosine (product of AC) are both important cell signalling molecules (Spiegel, et al., 1998; Pyne, 2002; Ruvolo, 2003), our finding raises an intriguing possibility that AC-mediated signalling pathways might be involved in AD.

It is not known how AC is elevated and what role the elevated AC plays in AD. Several factors including inflammation factors such as  $\gamma$ -interferon and interleukin-1 can induce accumulation of endogenous ceramide through de novo synthesis pathway (Perry, et al., 2000; Kroesen, et al., 2001). Inflammation and increased ceramide level have been seen in AD brain (Han, et al., 2002). Hence, one possibility of the elevated AC level might be a response of brain to inflammation-induced ceramide accumulation in AD. Several studies have demonstrated that ceramide rapidly induces apoptosis whereas sphingosine-1-phosphate counteracts ceramide's apoptosis-inducing activity (Obeid, et al., 1993; Spiegel, et al., 1998; Pyne, 2002). An incomplete apoptosis has been observed

in AD brain (for review, see Roth, 2001). It is therefore possible that the elevated AC might play a significant role in inhibition of brain apoptosis by converting ceramide, an apoptosis inducer, into sphingosine-1-phosphate, an anti-apoptosis agent.

Although AC was discovered nearly four decades ago, surprisingly the immunohistochemical study of this enzyme in mammalian central nervous system has not yet been done. We have found in this study that it is mainly expressed in neurons and some astrocytes in human brain. There was no noticeable difference in the distributions of AC between AD and control brains. Double immunostaining of NFTs were labelled with anti-AC and the latter co-localized with NFTs. A few of NFTs were not labelled for AC, which appeared morphologically like end stage ghost tangles where the neurons had been destroyed and almost all the subcellular structures and components had been lost. These immunohistochemical observations are consistent with the possibility that the elevated AC might be involved in the neurofibrillary degeneration of AD.

We also found that I $\kappa$ B $\gamma$ -2 with apparent molecular weight 45 kDa, an isoform of inhibitor of nuclear factor  $\kappa$ B (NF- $\kappa$ B) is up regulated in AD. NF- $\kappa$ B is a transcription factor that binds to 10 bp sequence in the enhancer region of the gene encoding  $\kappa$  light chain of antibody in B cells (that's why it's called NF- $\kappa$ B). NF- $\kappa$ B exists in a latent dimer form (p50/p65) in the cytoplasm of unstimulated cells because it is formed as a complex with an inhibitor protein I $\kappa$ B. There are five isoforms of NF- $\kappa$ B [NF- $\kappa$ B1 (p50), NF- $\kappa$ B2 (p52), RelA (p65), RelB, and c-Rel] and I $\kappa$ B (I $\kappa$ B $\alpha$ , I $\kappa$ B $\beta$ , I $\kappa$ B $\epsilon$ , I $\kappa$ B $\gamma$ , and Bcl-3). The most common forms of the latent NF- $\kappa$ B complex are p50/p65/I $\kappa$ B $\alpha$  and p50/p65/I $\kappa$ B $\beta$ . Cytoplasmic NF- $\kappa$ B complex is mobilized by a wide range of extracellular and intracellular signals which are thought to lead to phosphorylation and subsequent dissociation of I $\kappa$ B from

NF- $\kappa$ B, thereby allowing NF- $\kappa$ B to be translocated to nucleus and regulate gene transcription (Grumont and Gerondakis, 1994). The C-terminal half of NF- $\kappa$ B contains seven repeat structures, 35-40 amino acids each, that are related to the motifs found in erythrocyte ankyrin and involved in differentiation and cell cycle control (Nolan and Baltimore, 1992, Blank, et al., 1992). All I $\kappa$ B family members also contain six or seven ankyrin-like repeats, which are shown to be essential for preventing NF- $\kappa$ B nuclear translocation and inhibiting its DNA binding (Inoue, et al., 1992, Bours, et al., 1993). NF- $\kappa$ B p50/p65, I $\kappa$ B $\alpha$  and I $\kappa$ B $\beta$  are ubiquitously present in various tissues (Bakalkin, et al., 1993), whereas the tissue expression of I $\kappa$ B $\gamma$  has not yet well studied. Whether I $\kappa$ B $\gamma$  is present in mammalian brain was not previously known. Interestingly, the gene encoding the p105 precursor of the p50 subunit of NF- $\kappa$ B also encodes a p70 I $\kappa$ B protein, I $\kappa$ B $\gamma$ , which is identical to the C-terminal 607 amino acids of p105 (Inoue, et al., 1992, Gerondakis, et al., 1993). In addition to p70 I $\kappa$ B $\gamma$ , the other two isoforms of I $\kappa$ B $\gamma$ , I $\kappa$ B $\gamma$ -1 (~ 60 kDa) and 2 (~ 50 kDa) are generated from alternative RNA splicing (Raelene, et al., 1994). In contrast to cytoplasmic p70 I $\kappa$ B $\gamma$ , I $\kappa$ B $\gamma$ -1 is found in both the cytoplasm and nucleus, whereas I $\kappa$ B $\gamma$ -2 is predominantly nuclear, which is consistent with our finding that the 45 kDa protein is located in the nuclear fraction of brain homogenate.

NF- $\kappa$ B pathway has been shown to be activated in AD brain. Studies of post-mortem brain tissue from patients with AD have revealed that the p65 immunoactivity increased in neurons and astrocytes in the immediate vicinity of amyloid plaques (Kaltschmidt, et al., 1997) and in cholinergic neurons (Biossiere, et al., 1997). Gel shift assay indicated activation of NF- $\kappa$ B p50/p65 in nuclear extracts from temporal cortex of AD brain and the p50 immunoactivity increased in NFT-bearing neurons (Yan, et al., 1995). Interestingly, A $\beta$

strongly activates NF- $\kappa$ B in neuroblastoma (Behl, et al., 1994) and in primary neurons (Kaltschmidt, et al., 1997). Glycated tau also activates NF- $\kappa$ B through reactive oxygen intermediates (Yan, et al., 1995). NF- $\kappa$ B is also activated by TNF and soluble APP, and its activation results in neuroprotection such as enhanced survival of neurons treated with A $\beta$  (Barger, et al., 1995). However, I $\kappa$ B $\gamma$  family has never been studied in AD brain. In our study, we found that I $\kappa$ B $\gamma$ -2 level is increased in the post-mortem brain tissue from patients with AD, implying that I $\kappa$ B $\gamma$ -2 might be elevated as a response to and compensate for the increase of NF- $\kappa$ B activity in AD. Increased NF- $\kappa$ B activity might be neuroprotective in AD, and there are many signalling pathways that regulate NF- $\kappa$ B activity in neurons, communicating and cross-talking at the same time. Interestingly, ceramide can also induce the up-regulation of NF- $\kappa$ B activity in neurons (Mattson and Camandola, 2001). The exact cause of elevated I $\kappa$ B $\gamma$ -2 and its role in AD need further investigation.

In addition, we found that GFAP is increased in AD brains. This finding was already reported by other groups (Delacourte, 1990; Vijayan, et al., 1991). GFAP is a highly specific marker of astroglia cells in brain (Terenghi, et al., 1984). It has been reported that glia cells are stimulated in AD brain because of brain damage and inflammation. Accordingly, as a marker of them, GFAP formation is increased as well (Duffy, et al., 1980). A pathological glia activation, stimulated by inflammatory proteins, A $\beta$ , or brain ischemia, is thought to be a common pathogenic factor for progressive nerve cell damage in AD (Schubert, et al., 2000).

## 6. CONCLUSIONS

Our previous finding that microtubule-associated protein tau is abnormally glycosylated in addition to its abnormal hyperphosphorylation in AD brain suggested a possibility that the protein glycosylation might be affected in AD. In this study, we systematically investigated glycoproteins in AD brains as compared to controls and made the following findings:

1. We identified 12 major glycoproteins in AD brain. Nine of the identified proteins are previously known glycoproteins. The other three are unknown proteins that have never been identified before, but the sequences were deduced from human genome database. All of these unknown proteins contain the consensus N-glycosylation sites and predicted transmembrane domains.
2. We found altered lectin staining of three glycoproteins (35 kDa, 43 kDa and 180 kDa) in AD brain, suggesting that these glycoproteins may be dysregulated in AD.
3. We identified that one of these three glycoproteins, the 43 kDa protein, is the  $\beta$ -subunit of human acid ceramidase (AC). We found that AC is elevated in AD brain, mainly expressed in neurons, and co-localized with NFTs. These findings suggested a possible role of AC in the pathogenesis of AD.
4. We found that I $\kappa$ B $\gamma$ -2 and GFAP, both of which are inflammation-activated proteins, are up regulated in AD brain, providing a molecular mechanism of inflammation activation in AD brain.

## 7. REFERENCES

Adamec, E., Mohan, P.S., Cataldo, A.M., Vonsattel, J.P., and Nixon, R.A., 2000, Up-regulation of the lysosomal system in experimental models of neuronal injury: implications for Alzheimer's disease. *Neuroscience*. **100**: 663-675.

Alonso, A del C., Grundke-Iqbal, I., and Iqbal, K., 1996, Alzheimer's disease hyperphosphorylated tau sequesters normal tau into tangles of filaments and disassembles microtubules. *Nature Med.* **2**: 783-787.

Alonso, A del C., Grundke-Iqbal, I., Barra, H.S., and Iqbal, K., 1997, Abnormal phosphorylation of tau and the mechanism of Alzheimer neurofibrillary degeneration: Sequestration of MAP1 and MAP2 and the disassembly of microtubules by abnormal tau. *Proc. Natl. Acad. Sci. USA* **94**: 298-303.

Alonso, A del C., Zaidi, T., Grundke-Iqbal, I., and Iqbal, K., 1994, Role of abnormally phosphorylated tau in the breakdown of microtubules in Alzheimer's disease. *Proc. Natl. Acad. Sci. USA* **91**: 5562-5566.

Alonso, A., Zaidi, T., Novak, M., Barra, H.S., Grundke-Iqbal, I., and Iqbal, K., 2001b, Interaction of tau isoforms with Alzheimer's disease abnormally hyperphosphorylated tau and in vitro phosphorylation into the disease-like protein. *J. Biol. Chem.* **276**: 37967-37973.

Alonso, A., Zaidi, T., Novak, M., Grundke-Iqbal, I., and Iqbal, K., 2001a, Hyperphosphorylation induces self-assembly of tau into tangles of paired helical filaments/straight filaments. *Proc. Natl. Acad. Sci. USA* **98**: 6923-6928.

Arnold, C.S., Johnson, G.V.W., Cole, R.N., Dong, D.L.-Y., Lee, M., and Hart, G.W., 1996, The microtubule-associated protein tau is extensively modified with O-linked N-acetylglucosamine. *J. Biol. Chem.* **271**: 28741-28744.

Baeuerle, P.A., Baltimore, D., 1988, I kappa B: a specific inhibitor of the NF-kappa B transcription factor. *Science* **242**: 540-546.

Bar, J., Linke, T., Ferlinz, K., Neumann, U., Schuchman, E.H., and Sandhoff, K., 2001, Molecular analysis of acid ceramidase deficiency in patients with Farber disease. *Hum. Mut.* **17**: 199-209.

Barger, S.W., Horster, D., Furukawa, K., Goodman, Y., Kriegstein, J., and Mattson, M.P., 1995, Tumor necrosis factors alpha and beta protect neurons against amyloid beta-peptide toxicity: evidence for involvement of a kappa B-binding factor and attenuation of peroxide and Ca<sup>2+</sup> accumulation. *Proc Natl Acad Sci USA*. **92**: 9328-9332.

Bartus, R.T., 2000, On neurodegenerative diseases, models, and treatment strategies: lessons learned and lessons forgotten a generation following the cholinergic hypothesis. *Exp. Neurol*. **163**: 495-529.

Behl, C., 1999, Alzheimer's disease and oxidative stress: implications for novel therapeutic approaches. *Prog Neurobiol*. **57**: 301-323.

Behl, C., Davis, J.B., and Lesley, R., 1994, Schubert D. Hydrogen peroxide mediates amyloid beta protein toxicity. *Cell*. **77**: 817-827.

Berglund, E.O., Ranscht, B., 1994, Molecular cloning and in situ localization of the human contactin gene (CNTN1) on chromosome 12q11-q12. *Genomics*. **21**: 571-82.

Bernardo, K., Hurwitz, R., Zenk, T., Desnick, R.J., Ferlinz, K., Schuchman, E.H., and Sandhoff, K., 1995, Purification, characterization, and biosynthesis of human acid ceramidase. *J. Biol. Chem*. **270**: 11098-11102.

Bick, K.L., and Katzman, R., 2000, Alzheimer Disease: The road to 2000. *Neuroscience News* **3**: 8-13.

Bielawska, A., Greenberg, M.S., Perry, D., Jayadev, S., Shayman, J.A., McKay, C., and Hannun, Y.A., 1996, (1S,2R)-D-erythro-2-(N-myristoylamino)-1-phenyl-1-propanol as an inhibitor of ceramidase. *J. Biol. Chem*. **271**: 12646-12654.

Blank, V., Kourilsky, P., and Israel, A., 1992, NF-kappa B and related proteins: Rel/dorsal homologies meet ankyrin-like repeats. *Trends Biochem Sci*. **17**: 135-140.

Boissiere, F., Hunot, S., Faucheux, B., Duyckaerts, C., Hauw, J.J., Agid, Y., and Hirsch, E.C., 1997, Nuclear translocation of NF-kappaB in cholinergic neurons of patients with Alzheimer's disease. *Neuroreport*. **8**: 2849-2852.

Bours, V., Franzoso, G., Azarenko, V., Park, S., Kanno, T., Brown, K., and Siebenlist, U., 1993, The oncoprotein Bcl-3 directly transactivates through kappa B motifs via association with DNA-binding p50B homodimers. *Cell*. **72**: 729-739.

Bradford, M.M., 1976, A rapid and sensitive method for the quantitation of microgram quantities of protein utilizing the principle of protein-dye binding. *Anal. Biochem.* **72**: 248-254.

Bramblett, G.T., Goedert, M., Jakes, R., Merrick, S.E., Trojanowski, J.Q., and Lee, V.M., 1993, Abnormal tau phosphorylation at Ser396 in Alzheimer's disease recapitulates development and contributes to reduced microtubule binding. *Neuron* **10**: 1089-1099.

Bramblett, G.T., Trojanowski, J.Q., and Lee, V.M., 1992, Regions with abundant neurofibrillary pathology in human brain exhibit a selective reduction in levels of binding-competent tau and accumulation of abnormal tau-isoforms (A68 proteins). *Lab. Invest.* **66**: 212-222.

Breen, K.C., Coughlan, C.M., and Hayes, F.D., 1998, The role of glycoproteins in neural development, function, and disease. *Mole. Neurobiol.* **16**: 163-220.

Buee, L., Bussiere, T., Buee-Scherrer, V., Delacourte, A., and Hof, P.R., 2000, Tau protein isoforms, phosphorylation and role in neurodegenerative disorders. *Brain Res. Rev.* **33**: 95-130.

Castagnola, M., Cassiano, L., De Cristofaro, R., Luciani, S., Rossetti, D.V., and Landolfi, R., 1989, Purification of the isolated beta-chain of adult human haemoglobin from its post-translational modification. *J Chromatogr.* **494**: 310-317.

Chen M., 1998a, The Alzheimer's plaques, tangles and memory deficits may have a common origin. Part I: a calcium deficit hypothesis. *Front Biosci.* **3**: A27-31.

Chen M., 1998b, The Alzheimer's plaques, tangles and memory deficits may have a common origin. Part II: therapeutic rationale. *Front Biosci.* **3**: A32-37.

Chen M., 1998c, The Alzheimer's plaques, tangles and memory deficits may have a common origin. Part III: animal model. *Front Biosci.* **3**: A47-51.

Chen M., Fernandez H.L., 1999, The Alzheimer's plaques, tangles and memory deficits may have a common origin. Part V: why is  $\text{Ca}^{2+}$  signal lower in the disease? *Front Biosci.* **4**: A9-15.

Chen, W.W., Moser, A.B., and Moser, H.W., 1981, Role of lysosomal acid ceramidase in the metabolism of ceramide in human skin fibroblasts. *Arch. Biochem. Biophys.* **208**: 444-455.

Chou, C.F., Smith, A.J., and Omary, M.B., 1992, Characterization and dynamics of O-linked glycosylation of human cytokeratin 8 and 18. *J. Biol. Chem.* **267**: 3901-3906.

Coon, A.L., Wallace, D.R., Iactutus, C.F., and Booze R.I., 1999, L-type calcium channels in the hippocampus and cerebellum of Alzheimer's disease brain tissue. *Neurobiol. Aging* **20**: 597-603.

Culmsee, C., Zhu, X., Yu, Q.S., Chan, S.L., Camandola, S., Guo, Z., Greig, N.H., and Mattson, M.P., 2001, A synthetic inhibitor of p53 protects neurons against death induced by ischemic and excitotoxic insults, and amyloid beta-peptide. *J. Neurochem.* **77**: 220-228.

Cummings, J.L., Vinters, H.V., Cole, G.M., and Khachaturian, Z.S., 1998, Alzheimer's disease: etiologies, pathophysiology, cognitive reserve, and treatment opportunities. *Neurology.* **51**: S2-17; S65-67.

Cummings, R.D., 1994, Use of lectins in analysis of glycoconjugates. In: *Methods of Enzymology, Academic Press, Inc.* **230**: 66-86.

Dbaiibo, G.S., Perry, D.K., Gamard, D.J., and Hannun, Y.A., 1997, Cytokine response modifier A (CrmA) inhibits ceramide formation in response to tumor necrosis factor (TNF)- $\alpha$ : CrmA and Bcl-2 target distinct components in the apoptotic pathway. *J. Exp. Med.* **185**: 481-490.

Dbaiibo, G.S., Pushkareva, M.Y., Rachid, R.A., Alter, N., Smyth, M.J., Obeid, L.M., and Hannun, Y.A., 1998, p53-dependent ceramide response to genotoxic stress. *J. Clin. Invest.* **102**: 329-339.

De Felice, F.G., and Ferreira, S.T., 2002, Beta-amyloid production, aggregation, and clearance as targets for therapy in Alzheimer's disease. *Cell Mol. Neurobiol.* **22**: 545-563.

DeKosky, S.T., Ikonomic, M.D., Styren, S., Beckett, L., Wisniewski, S., Bennett, D.A., Cochran, E.J., Kordower, J.H., and Mufson, E.J., 2002, Upregulation of choline acetyltransferase activity in hippocampus and frontal cortex of elderly subjects with mild cognitive impairment. *Ann. Neurol.* **51**: 145-155.

Delacourte, A., 1990, General and dramatic glial reaction in Alzheimer brains. *Neurology*. **40**: 33-37.

Ding, M., and Vandre, D.D., 1996, High molecular weight microtubule-associated proteins contain O-linked N-acetylglucosamine. *J. Biol. Chem.* **271**: 12555-12561.

Dobrowsky, R.T., and Hannun, Y.A., 1992, Ceramide stimulates a cytosolic protein phosphatase. *J. Biol. Chem.* **267**: 5048-5051.

Dobrowsky, R.T., Kmibayashi, C., Mumby, M.C., and Hannun, Y.a., 1993, Ceramide activates heterotrimeric protein phosphatase 2A. *J. Biol. Chem.* **268**: 15523-15530.

Dong, L.Y., and Hart, G.W., 1994, Purification and characterization of an O-GlcNAc selective N-acetyl- $\beta$ -D-glucosaminidase from rat spleen cytosol. *J. Biol. Chem.* **269**: 19321-19330.

Dong, L.Y., Zu, Z.S., Chevrier, M.R., and Cotter, R.J., 1993, Glycosylation of mammalian neurofilaments. Localization of multiple O-linked N-acetylglucosamine moieties on neurofilament polypeptides L and M. *J. Biol. Chem.* **268**: 16679-16687.

Duffy, P.E., Rapport, M., and Graf, L., 1980, Glial fibrillary acidic protein and Alzheimer-type senile dementia. *Neurology*. **30**: 778-782.

El Bawab, S, Mao, C., Obeid, L.M., and Hannun, Y.A., 2002, Ceramidases in the regulation of ceramide levels and function. *Subcell. Biochem.* **36**: 187-205.

Emiliani, C., Urbanelli, L., Racanicchi, L., Orlacchio, A., Pelicci, G., Sorbi, S., Bernardi, G., and Oracchio, A., 2003, Up-regulation of glycohydrolases in Alzheimer's disease fibroblasts correlates with Ras activation. *J. Biol. Chem.* **278**: 38453-38460.

Fan, H., Meng, W., Kilian, C., Grams, S., and Reutter, W., 1997, Domain-specific N-glycosylation of the membrane glycoprotein dipeptidylpeptidase IV (CD26) influences its subcellular trafficking, biological stability, enzyme activity and protein folding. *Eur J Biochem.* **246**: 243-251.

Ferlinz, K., Kopal, G., Bernardo, K., Linke, T., Bar, J., Breiden, B., Neumann, U., Lang, F., Schuchman, E.H., and Sandhoff, K., 2001, Human acid ceramidase: processing, glycosylation, and lysosomal targeting. *J Biol Chem.* **276**: 35352-35360.

- Ferrer, I., and Blanco, R., 2000, N-myc and c-myc expression in Alzheimer's disease, Huntington disease and Parkinson disease. *Brain Res. Mol. Brain Res.* **77**: 270-276.
- Flamigni, F., Faenza, I., Marmioli, S., Stanic, I., Giaccari, A., Muscari, C., Stefanelli, C., and Rossoni, C., 1997, Inhibition of the expression of ornithine decarboxylase and c-myc by cell-permeant ceramide in difluoromethylornithine-resistant leukaemia cells. *Biochem. J.* **324**: 783-789.
- Floyd, R.A., and Hensley, K., 2002, Oxidative stress in brain aging. Implication for therapeutics of neurodegenerative diseases. *Neurobiol. Aging.* **23**: 795-807.
- Foster, N.L., Wilhelmsen, K., Sima, A.A., Jones, M.Z., and D'Amato, C.J., 1997, Frontotemporal dementia and parkinsonism linked to chromosome 17: a consensus conference. *Ann. Neurol.* **41**: 262-266.
- Fukuda, M., and Hindsgaul, O., Molecular and Cellular Glycobiology, 1<sup>st</sup> edition, *Oxford University Press*, 2000.
- Gabbita, S.P., Lovell, M.A., and Markesbery, W.R., 1998, Increased nuclear DNA oxidation in the brain in Alzheimer's disease. *J Neurochem.* **71**: 2034-2040.
- Galdari, S., Kishikawa, K., Kamibayashi, C., Mumby, M.C., and Hannun, Y.A., et al., 1998, Purification characterization of ceramide-activated protein phosphatases. *Biochemistry* **37**: 11232-11238.
- Gatt, S., 1963, Enzymatic hydrolysis of sphingolipids. 1. Hydrolysis and synthesis of ceramides by an enzyme from rat brain. *J. Biol. Chem.* **238**: 3131-3133.
- Gatt, S., 1966, Enzymatic hydrolysis of sphingolipids. *J. Biol. Chem.* **241**: 3724-3730.
- Georgopoulou, N., McLaughlin, M., McFarlane, I., and Breen, K.C., 2001, The role of post-translational modification in beta-amyloid precursor protein processing. *Biochem. Soc. Symp.* **67**: 23-36.
- Gerondakis, S., Morrice, N., Richardson, I.B., Wettenhall, R., Fecondo, J., and Grumont, R.J., 1993, The activity of a 70 kilodalton I kappa B molecule identical to the carboxyl terminus of the p105 NF-kappa B precursor is modulated by protein kinase A. *Cell Growth Differ.* **4**: 617-627.

Geula, C., and Mesulam, M-M., 1994, Cholinergic systems and related neuropathological predilection patterns in Alzheimer's disease. *In: Terry, R.D., Katzman, R., Bick, K.L., eds. Alzheimer's disease. New York: Raven, 263-291.*

Goate, A., Chartier-Harlin, M-C., Mullan, M., Brown, J., Crawford, F., Fidani, L., Giuffra, L., Haynes, A., Irving, N., James, L., Mant, R., Newton, P., Rooke, K., Roques, P., Talbot, C., Pericak-Vance, M., Roses, A., Williamson, R., Rossor, M., Owen, M., and Hardy, J., 1991, Segregation of a missense mutation in the amyloid precursor protein gene with familial Alzheimer's disease. *Nature* **349**: 704-706.

Goedert, M., Spillantini, M.G., Cairns, N.J., and Crowther, R.A., 1992, The proteins of Alzheimer paired helical filaments: Abnormal phosphorylation of all six brain isoforms. *Neuron* **8**: 159-168.

Goedert, M., Spillantini, M.G., Jakes, R., Rutherford, D., and Crowther, R.A., 1989, Multiple isoforms of human microtubule-associated protein tau: sequences and localization in neurofibrillary tangles of Alzheimer's disease. *Neuron* **3**: 519-526

Gong, C.X., Shaikh, S., Wang, J.Z., Zaidi, T., Grundke-Iqbal, I., and Iqbal, K., 1995, Phosphatase activity toward abnormally phosphorylated tau: decrease in Alzheimer disease brain. *J Neurochem.* **65**: 732-738.

Gong, C.X., Singh, T.J., Grundke-Iqbal, I., and Iqbal, K., 1993, Phosphoprotein phosphatase activities in Alzheimer disease. *J. Neurochem.* **61**: 921-927.

Gong, C.X., Wang, J.Z., Iqbal, K., and Grundke-Iqbal, I., 2003, Inhibition of protein phosphatase 2A induces phosphorylation and accumulation of neurofilaments in metabolically active rat brain slices. *Neurosci. Lett.* **340**: 107-110.

Gooch, M.D., and Stennett, D.J., 1996, Molecular basis of Alzheimer's disease. *Am. J. Health. Syst. Pharm.* **53**: 1545-1557.

Goux, W.J., Rodriguez.S., and Sparkman, D.R., 1995, Analysis of the core components of Alzheimer paired helical filaments: A gas chromatography/mass spectrometry characterization of fatty acids, carbohydrates and long-chain bases. *FEBS Lett.* **366**: 81-85.

Gray, E.G., Paula-Barbosa, M., and Roher, A., 1987, Alzheimer's disease: Paired helical filaments and cytomembranes. *Neuropathol. Appl. Neurobiol.* **13**: 91-110.

Greenberg, S.G., and Davies, P., 1990, A preparation of Alzheimer paired helical filaments that displays distinct tau proteins by polyacrylamide gel electrophoresis. *Proc. Natl. Acad. Sci. USA*. **87**: 5827-5831.

Griffith, L.S. and Schmitz, B., 1995, O-linked N-acetylglucosamine is upregulated in Alzheimer brains. *Biochem. Biophys. Res. Comm.* **213**: 424-431.

Grumont, R.J., Gerondakis, S., 1994, Alternative splicing of RNA transcripts encoded by the murine p105 NF-kappa B gene generates I kappa B gamma isoforms with different inhibitory activities. *Proc Natl Acad Sci USA*. **91**: 4367-4371.

Grundke-Iqbal, I., Iqbal, K., Quinlan, M., Tung, Y.C., Wisniewski, H.M., and Binder, L.I., 1986b, Abnormal phosphorylation of the microtubule associated protein tau in Alzheimer cytoskeletal pathology. *Proc. Natl. Acad. Sci. USA* **83**: 4913-4917.

Grundke-Iqbal, I., Iqbal, K., Quinlan, M., Tung, Y.C., Zaidi, M.S., and Wisniewski, H.M., 1986a, Microtubule-associated protein tau: A component of Alzheimer paired helical filaments. *J. Biol. Chem.* **261**: 6084-6089.

Gupta, R., Jung, E., and Brunak, S., 2002, Prediction of n-glycosylation sites in human proteins. *In preparation*.

Haltiwanger, R.S., Holt, G.D., and Hart, G.W., 1990, Enzymatic addition of O-GlcNAc to nuclear and cytoplasmic proteins. Identification of a uridine diphospho-N-acetylglucosamine: polypeptide  $\beta$ -N-acetylglucosaminyltransferase. *J. Biol. Chem.* **265**: 2563-2568.

Han, X., M Holtzman, D., McKeel, D.W. Jr., Kelley, J., Morris, J.C., 2002, Substantial sulfatide deficiency and ceramide elevation in very early Alzheimer's disease: potential role in disease pathogenesis. *J Neurochem.* **82**: 809-818.

Hannun, Y.A., 1996, Function of ceramide in coordinating cellular responses to stress. *Science* **274**: 1855-1859.

Hannun, Y.A., and Luberto, C., 2000, Ceramide in the eukaryotic stress response. *Trends Cell. Boil.* **10**: 73-80.

Hardy, J., 1996, New insights into the genetics of Alzheimer's disease. *Ann. Med.* **28**: 255-258.

- Hardy, J., and Selkoe, D.J., 2002, The amyloid hypothesis of Alzheimer's disease: Progress and problems on the road to therapeutics. *Science* **297**: 353-356.
- Hardy, J., Hutton, M., Farrer, M., and Crook, R., 2000, The genetic causes of the tau and synucleinopathies. *Neuroscience News* **3**: 21-27.
- Hart, G.W., 1997, Dynamic O-linked glycosylation of nuclear and cytoskeletal proteins. *Ann. Rev. Biochem.* **66**: 315-335.
- Hart, G.W., Kreppel, L.K., Comer, F.I., Arnold, C.S., Snow, D.M., Ye, Z., Cheng, X., DellaManna, D., Caine, D.S., Earles, B.J., Akimoto, Y., Cole, R.N., and Hayes, B.K., 1996, O-GlcNAcylation of key nuclear and cytoskeletal proteins: reciprocity with O-phosphorylation and putative roles in protein multimerization. *Glycobiology* **6**: 711-716.
- Ho, L.W., Carmichael, J., Swartz, J., Wytenbach, A., Rankin, J., and Rubinsztein, D.C., 2001, The molecular biology of Huntington's disease. *Psychol Med.* **31**: 3-14.
- Hoyer, S., 2000, Brain glucose and energy metabolism abnormalities in sporadic Alzheimer's disease. Causes and consequences: an update. *Exp. Gerontol.* **35**: 1363-1372.
- Hutton, M., Lendon, C.L., Rizzu, P., Baker, M., and Froelich, S., 1998, Association of missense and 5'-splice-site mutations in tau with the inherited dementia FTDP-17. *Nature* **393**: 702-705.
- Inoue, J., Kerr, L.D., Kakizuka, A., Verma, I.M., 1992, I $\kappa$ B $\gamma$ , a 70 kD protein identical to the C-terminal half of p110 NF- $\kappa$ B: a new member of the I $\kappa$ B family. *Cell* **68**: 1109-1120.
- Iqbal, K., Alonso, A.D., Gondal, J.A., Gong, C.X., Haque, N., Khatoon, S., Sengupta, A., Wang, J.Z., Grundke-Iqbal, I., 2000, Mechanism of neurofibrillary degeneration and pharmacologic therapeutic approach. *J. Neural. Transm. Suppl.* **59**: 213-222.
- Iqbal, K., Grundke-Iqbal, I., Smith, A.J., George, L., Tung, Y.C., and Zaidi, T., 1989, Identification and localization of a tau peptide to paired helical filaments of Alzheimer's disease. *Proc. Natl. Acad. Sci. USA* **86**: 5646-5650.

Iqbal, K., Zaidi, T., Bancher, C., and Grundke-Iqbal, I., 1994, Alzheimer paired helical filaments. Restoration of the biological activity by dephosphorylation. *FEBS Lett.* **349**: 104-108.

Kaltschmidt, B., Uherek, M., Volk, B., Baeuerle, P.A., and Kaltschmidt, C., 1997, Transcription factor NF-kappaB is activated in primary neurons by amyloid beta peptides and in neurons surrounding early plaques from patients with Alzheimer disease. *Proc Natl Acad Sci USA.* **94**: 2642-2647.

Kanfer, J.N., Hattori, H., and Orihel, D., 1986, Reduced phospholipase D activity in brain tissue samples from Alzheimer's disease patients. *Ann. Neurol.* **20**: 265-267.

Khatoon, S., Grundke-Iqbal, I., Iqbal, K., 1992, Brain levels of microtubule-associated protein tau are elevated in Alzheimer's disease: a radioimmuno-slot-blot assay of nanograms of the protein. *J. Neurochem.* **59**: 750-753.

Khatoon, S., Grundke-Iqbal, I., Iqbal, K., 1994, Levels of normal and abnormally phosphorylated tau in different cellular and regional compartments of Alzheimer's disease and control brains. *FEBS Lett.* **351**: 80-84.

Khatoon, S., Grundke-Iqbal, I., Iqbal, K., 1995, Guanosine triphosphate binding to beta-subunit of tubulin in Alzheimer's disease brain: role of microtubule-associated protein tau. *J. Neurochem.* **64**: 777-787.

Kirtikara, K., Lauderkind, S.J., Raghov, R., Kanekura, T., and Ballou, L.R., 1998, An accessory role for ceramide in interleukin-1 beta induced prostaglandin synthesis. *Mol. Cell Biochem.* **181**: 41-48.

Koch, J., Gartner, S., Li, C.M., Quintern, L.E., Bernardo, K., Levran, O., Schnabel, D., Desnick, R.J., Schuchman, E.H., and Sandhoff, K., 1996, Molecular cloning and characterization of a full-length complementary DNA encoding human acid ceramidase. Identification Of the first molecular lesion causing Farber disease. *J Biol Chem.* **271**: 33110-33115.

Kolesnick, R., 2002, The therapeutic potential of modulating the ceramide/sphingomyelin pathway. *J. Clin. Invest.* **10**: 3-8

Kopke, E., Tung, Y.C., Shaikh, S., Alonso, A. del C., Iqbal, K., and Grundke-Iqbal, I., 1993, Microtubule associated protein tau: Abnormal phosphorylation of a non-paired helical filament pool in Alzheimer disease. *J. Biol. Chem.* **268**: 24374-24384.

Koscielak, J., 1995, Diseases of aberrant glycosylation. *Acta Biochem. Pol.* **42**: 1-10.

Koutsilieris, E., Scheller, C., Grunblatt, E., Nara, K., Li, J., and Riederer, P., 2002, Free radicals in Parkinson's disease. *J Neurol.* **249**: II1-5.

Kroesen, B., Pettus, B., Luberto, C., Busman, M., Sietsma, H., De Leij, L., and Hannun, Y.A., 2001, Induction of apoptosis through B-cell receptor crosslinking occurs via de novo generated C16 ceramide and involves mitochondria. *J. Biol. Chem.* **276**: 13606-13614

Ksiezak-Reding, H., Binder, L.I., and Yen, S.H., 1990, Alzheimer's disease proteins (A68) share epitopes with tau but show distinct biochemical properties. *J. Neurosci. Res.* **25**: 420-430.

Laemmli, U.K., 1970, Cleavage of structural proteins during the assembly of the head of bacteriophage T4. *Nature* **227**: 680-685.

Lavie, Y., Cao, H.T., Volner, A., Lucci, A., Han, T.Y., Geffen, V., Giuliano, A.E., and Cabot, M.C., 1997, Agents that reverse multidrug resistance, tamoxifen, verapamil, and cyclosporin A, block glycosphingolipid metabolism by inhibiting ceramide glycosylation in human cancer cells. *J. Biol. Chem.* **272**: 1682-1687.

Lee, V.M., Balin, B.J., Otvos, L., and Trojanowski, J.Q., 1991, A68: A major subunit of paired helical filaments and derivatized forms of normal tau. *Science* **251**: 675-678.

Lee, V.M., Goedert, M., Trojanowski, J.Q., 2001, Neurodegenerative tauopathies. *Annu Rev Neurosci.* **24**: 1121-1159.

Leon, J., Cheng C.K., and Neumann, P.J., 1998, Alzheimer's disease care: costs and potential savings. *Health Aff. (Millwood)* **17**: 206-216.

Li, C.M., Hong, S.B., Kopal, G., He, X., Linke, T., Hou, W.S., Koch, J., Gatt, S., Sandhoff, K., and Schuchman E.H., 1998, Cloning and characterization of the full-length cDNA and genomic sequences encoding murine acid ceramidase. *Genomics* **50**: 267-274.

Li, C.M., Park, J.H., He, X., Levy, B., Chen, F., Arai, K., Adler, D.A., Disteché, C.M., Koch, J., Sandhoff, K., and Schuchman, E.H., 1999, The human acid ceramidase gene (ASAH): structure, chromosomal location, mutation analysis, and expression. *Genomics* **62**: 223-231.

Liu, F., Huang, Y., Iqbal, K., Grundke-Iqbal, I., and Gong, C.X., 2002c, Involvement of aberrant glycosylation in phosphorylation of tau by cdk5 and GSK-3 $\beta$ . *FEBS Lett.* **530**: 209-214.

Liu, F., Zaidi, T., Grundke-Iqbal, I., Iqbal, K., and Gong, C.X., 2002a, Role of glycosylation in hyperphosphorylation of tau in Alzheimer's disease. *FEBS Lett.* **512**: 101-106.

Liu, F., Zaidi, T., Grundke-Iqbal, I., Iqbal, K., and Gong, C.X., 2002b, Aberrant glycosylation modulates phosphorylation of tau by protein kinase A and dephosphorylation of tau by protein phosphatase 2A and 5. *Neurosci.* **115**: 829-837.

Liu, Y.Y., Han, T.Y., Giuliano, A.E., and Cabot, M.C., 1999, Expression of glucosylceramide synthase, converting ceramide to glucosylceramide, confers adriamycin resistance in human breast cancer cells. *J. Biol. Chem.* **274**: 1140-1146.

Lovell, M.A., and Markesbery, W.R., 2001, Ratio of 8-hydroxyguanine in intact DNA to free 8-hydroxyguanine is increased in Alzheimer disease ventricular cerebrospinal fluid. *Arch Neurol.* **58**: 392-396.

Lovestone, S., and Reynald, C.H., 1997, The hyperphosphorylation of tau: a critical stage in neurodevelopment and neurodegenerative processes. *Neurosci.* **78**: 309-324.

Luthi, T., Haltiwanger, R.S., Greengard, P., and Bahler, M., 1991, Synapsins contain O-linked N-acetylglucosamine. *J. Neurochem.* **56**: 1493-1498.

Maguire, T.M., and Breen, K.C., 1995, A decrease in neural sialyltransferase activity in Alzheimer's disease. *Dementia* **6**: 185-190.

Maley, F., Trimble R.B., Tarentino A.L., Plummer T.H.Jr., 1989, Characterization of glycoproteins and their associated oligosaccharides through the use of endoglycosidases. *Anal. Biochem.* **2**: 195-204.

Mandon, E.C., Ehses, I., Rother, J., Van Echten, G., and Sandhoff, K., 1992, Subcellular localization and membrane topology of serine palmitoyltransferase, 3-dehydrosphinganine reductase, and sphinganine N-acyltransferase in mouse liver. *J. Biol. Chem.* **267**: 11144-11148.

Mantyh, P.W., Weldon, D.T., and Maggio, J.E., 1997, New insights into the neuropathology and cell biology of Alzheimer's disease. *Geriatrics Vol. 52 Suppl. 2*: S13-S16.

Mao, C., Xu, R., Szulc, Z.M., Bielawska, A., Galadari, S.H., and Obeid, L.M., 2001, Cloning and characterization of a novel human alkaline ceramidase. A mammalian enzyme that hydrolyzes phytoceramide. *J. Biol. Chem.* **276**: 26577-26588.

Markesbery, W.R., and Carney, J.M., 1999, Oxidative alterations in Alzheimer's disease. *Brain Pathol.* **9**: 133-146.

Markesbery, W.R., and Lovell, M.A., 1998, Four-hydroxynonenal, a product of lipid peroxidation, is increased in the brain in Alzheimer's disease. *Neurobiol Aging.* **19**: 33-36.

Mathias, S., Pena, L.A., and Kolesnick, R.N., 1998, Signal transduction of stress via ceramide. *Biochem. J.* **335**: 465-480.

Mattson, M.P., 2002, Oxidative stress, perturbed calcium homeostasis, and immune dysfunction in Alzheimer's disease. *J Neurovirol.* **8**: 539-550.

Mattson, M.P., and Camandola, S., 2001, NF-kappaB in neuronal plasticity and neurodegenerative disorders. *J Clin Invest.* **107**: 247-254.

Mattson, M.P., Pedersen, W.A., Duan, W., Culmsee, C., and Camandola, S., 1999, Cellular and molecular mechanisms underlying perturbed energy metabolism and neuronal degeneration in Alzheimer's and Parkinson's diseases. *Ann N Y Acad Sci.* **893**: 154-175.

Merrill, A.H.Jr., and Wang, E., 1992, Enzymes of ceramide biosynthesis. *Methods Enzymol.* **209**:427-437.

Michel, C., Van Echten-Deckert, G., Rother, J., Sandhoff, K., Wang E., and Merrill, A.H.Jr., 1997, Characterization of ceramide synthesis. A Dihydroceramide desaturase introduces the 4,5-trans-double bond of sphingosine at the level of dihydroceramide. *J. Biol. Chem.* **272**: 22432-22437.

Mitsutake, S., Tani, M., Okino, N., Mori, K., Ichinose, S., Omori, A., Iida, H., Nakamura, T., and Ito, M., 2001, Purification, characterization, molecular cloning, and subcellular distribution of neutral ceramidase of rat kidney. *J. Biol. Chem.* **276**: 26249-26259.

Mizushima, N., Koike, R., Kohsaka, H., Kushi, Y., Handa, S., Yagita, H., Miyasaka, N., 1996, Ceramide induces apoptosis via CPP32 activation. *FEBS Lett.* **395**: 267-271.

Morita, M., Hara, Y., Tamai, Y., Arakawa, H., Nishimura, S., 2000, Genomic construct and mapping of the gene for CMAP (leukocystatin/cystatin F, CST7) and identification of a proximal novel gene, BSCv (C20orf3). *Genomics.* **67**: 87-91.

Moser et al., *The Metabolic & Molecular Bases of Inherited Diseases*, 8<sup>th</sup> edition, McGraw-Hill, New York, 2001.

National Institute on Aging and National Institutes of Health, *Progress report on Alzheimer's disease*. 1999; 2000.

Nolan, G.P., and Baltimore, D., 1992, The inhibitory ankyrin and activator Rel proteins. *Curr Opin Genet Dev.* **2**: 211-220.

Obeid, L.M., Linardic, C.M., Karolak, L.A., and Hannun, Y.A., 1993, Programmed cell death induced by ceramide. *Science* **259**: 1769-1771.

Otvos, L. Jr., Feiner, L., Lang, E., Szendrei, G.I., Goedert, M., Lee, V.M., 1994, Monoclonal antibody PHF-1 recognizes tau protein phosphorylated at serine residues 396 and 404. *J Neurosci Res.* **39**: 669-673.

Pasternak, S.H., Bagshaw, R.D., Guiral, M., Zhang, S., Ackerley, C.A., Pak, B.J., Callahan, J.W., and Mahuran, D.J., 2003, Presenilin-1, nicastrin, amyloid precursor protein, and  $\gamma$ -secretase activity are co-localized in the lysosomal membrane. *J. Biol. Chem.* **278**: 26687-26694.

Perry, D.K., and Hannun, Y.A., 1998, The role of ceramide in cell signaling. *Biochem. Biophys. Acta.* **1436**: 233-243.

Perry, D.K., Carton, J., Shah, A.K., Meredith, F., Uhlinger, D.J., and Hannun, Y.A., 2000, Serine palmitoyltransferase regulates de novo ceramide generation during etoposide-induced apoptosis. *J. Biol. Chem.* **275**: 9078-9084.

Persson, B., and Argos, P., 1994, Prediction of transmembrane segments in proteins utilizing multiple sequence alignments. *J. Mol. Biol.* **237**: 182-192.

Persson, B., and Argos, P., 1996, Topology prediction of membrane proteins. *Protein Sci.* **5**: 363-371.

Plummer T.H.Jr., and Tarentino A.L., 1991, Purification of the oligosaccharide-cleaving enzymes of flavobacterium meningosepticum. *Glycobiology* **3**: 257-263.

Poorkaj, P., Bird, T.D., Wijsman, E., Nemens, E., and Garruto, R.M., 1998, Tau is a candidate gene for chromosome 17 frontotemporal dementia. *Ann. Neurol.* **43**: 815-825.

Porchet, R., Probst, A., Bouras, C., Draberova, E., Draber, P., and Riederer, B.M., 2003, Analysis of gial acidic fibrillary protein in the human entorhinal cortex during aging and in Alzheimer's disease. *Proteomics* **3**:1476-1485.

Puglielli, L., Konopka, G., Pack-Chung, E., Ingano, L.A., Berezovska, O., Hyman, B.T., Chang, T.Y., Tanzi, R.E., and Kovacs, D.M., 2001, Acyl-coenzyme A: cholesterol acyltransferase modulates the generation of the amyloid beta-peptide. *Nat Cell Biol.* **3**: 905-912.

Puglielli, L., Tanzi, R.E., and Kovacs, D.M., 2003, Alzheimer's disease: the cholesterol connection. *Nat Neurosci.* **6**:345-351.

Pyne, S., 2002, Cellular signaling by sphingosine and sphingosine-1-phosphate. Their opposing roles in apoptosis. *Subell. Biochem.* **36**: 245-268.

Raina, A.K., Hochman, A., Ickes, H., Zhu, X., Ogawa, O., Cash, A.D., Shimohama, S., Perry, G., and Smith, M.A., 2003, Apoptotic promoters and inhibitors in Alzheimer's disease: Who wins out? *Prog. Neuropsychopharmacol. Biol. Psychiatry.* **27**: 251-254.

Refolo, L.M., Malester, B., LaFrancois, J., Bryant-Thomas, T., Wang, R., Tint, G.S., Sambamurti, K., Duff, K., and Pappolla, M.A., 2000, Hypercholesterolemia accelerates the Alzheimer's amyloid pathology in a transgenic mouse model. *Neurobiol Dis.* **7**: 321-331.

Refolo, L.M., Pappolla, M.A., LaFrancois, J., Malester, B., Schmidt, S.D., Thomas-Bryant, T., Tint, G.S., Wang, R., Mercken, M., Petanceska, S.S., and Duff, K.E., 2001, A

cholesterol-lowering drug reduces beta-amyloid pathology in a transgenic mouse model of Alzheimer's disease. *Neurobiol Dis.* **8**: 890-899.

Retz, W., Gsell, W., Munch, G., Rosler, M., and Riederer, P., 1998, Free radicals in Alzheimer's disease. *J Neural Transm Suppl.* **54**: 221-236.

Reyes, J.G., Robayna, I.G., Delgado, P.S., Gonzalez, I.H., Aguiar, J.Q., Rosas, F.E., Fanjul, L.F., and Galarreta, C.M., 1996, c-Jun is a downstream target for ceramide-activated protein phosphatase in A431 cells *J. Biol. Chem.* **271**: 21375-21380.

Roberts, S.B., 2002, Gamma-secretase inhibitors and Alzheimer's disease. *Adv. Drug. Deliv. Rev.* **54**: 1579-1588.

Roses, A.D., and Saunders, A.M., 1994, APOE is a major susceptibility gene for Alzheimer's disease. *Curr Opin Biotechnol.* **5**:663-667.

Roth, K.A., 2001, Caspases, apoptosis, and Alzheimer's disease: causation, correlation, and confusion. *J. Neuropathol. Exp. Neurol.* **60**: 829-838.

Ruvolo, P.P., 2003, Intracellular signal transduction pathways activated by ceramide and its metabolites. *Pharmacol. Res.* **47**: 383-392.

Schubert, P., Morino, T., Miyazaki, H., Ogata, T., Nakamura, Y., Marchini, C., Ferroni, S., 2000, Cascading glia reactions: a common pathomechanism and its differentiated control by cyclic nucleotide signaling. *Ann N Y Acad Sci.* **903**: 24-33.

Sherrington, R., Rogaev, E.I., Liang, Y., Rogaev, E.A., Levesque, G., Ikeda, M., Chi, H., Lin, C., Li, G., Holman, K., Tsuda, T., Mar, L., Foncin, J.F., Bruni, A.C., Montesi, M.P., Sorbi, S., Rainero, I., Pinessi, L., Nee, L., Chumakov, I., Pollen, D., Brookes, A., Sanseau, P., Polinsky, R.J., Wasco, W., Da Silva, H.A.R., Haines, J.L., Pericak-Vance, M.A., Tanzi, R.E., Roses, A.D., Fraser, P.E., Rommens, J.M., and St. George-Hyslop, P.H., 1995, Cloning of a gene bearing missense mutations in early onset familial Alzheimer's disease. *Nature* **375**: 754-760.

Smyth, M.J., Perry, D.K., Zhang, J., Poirier, G.G., Hannun, Y.A., and Obeid, L.M., 1996, pRICE: a downstream target for ceramide-induced apoptosis and for the inhibitory action of bcl-2. *Biochem. J.* **316**: 25-28.

Snow, D.M., and Hart, G.W., 1998, Nuclear and cytoplasmic glycosylation. *Int. Rev. Cyto.* **181**: 43-75.

Spiegel, S., Cuvillier, O., Edsall, L., Kohama, T., Menzeleev, R., Olivera, A., Thomas, D., Tu, Z., Van Borcklyn, J., and Wang, F., 1998, Roles of sphingosine-1-phosphate in cell growth, differentiation, and death. *Biochemistry* **63**: 69-73.

Spillantini, M.G., Murrell, J.R., Goedert, M., Farlow, M.R., Klug, A., and Ghetti, B., 1998c, Mutation in the tau gene in familial multiple system tauopathy with presenile dementia. *Proc. Natl. Acad. Sci. USA.* **95**: 7737-7741.

Stipp, C.S., Kolesnikova, T.V., Hemler, M.E., 2001, EWI-2 is a major CD9 and CD81 partner and member of a novel Ig protein subfamily. *J Biol Chem.* **276**: 40545-54.

Strelow, A., Bernardo, K., Adam-Klages, S., Linke, T., Sandhoff, K., Kronke, M., and Adam, D., 2000, Overexpression of acid ceramidase protects from tumor necrosis factor-induced cell death. *J. Exp. Med.* **192**: 601-612.

Strittmatter, W.J., and Roses, A.D., 1995, Apolipoprotein E and Alzheimer disease. *Proc Natl Acad Sci U S A.* **92**: 4725-4727.

Sugita, M., Dulaney, J.T., Moser, H.W., 1972, Ceramidase deficiency in Farber's disease (lipogranulomatosis). *Science* **178**: 1100-1102.

Swaab, D.F., Dubelaar, E.J., Hofman, M.A., Scherder, E.J., Van Someren E.J., and Verwer, R.W., 2002, Brain aging and Alzheimer's disease: use it or lose it. *Prog. Brain Res.* **138**: 343-373.

Tandon, A., and Fraser, P., 2002, The presenilins. *Genome. Biol.* **3**: reviews3014.

Tani, M., Okino, N., Mitsutake, S., Tanigawa, T., Izu, H., and Ito, M., 2000a, Purification and characterization of a neutral ceramidase from mouse liver. A single protein catalyzes the reversible reaction in which ceramide is both hydrolyzed and synthesized. *J. Biol. Chem.* **275**: 3462-3468.

Tani, M., Okino, N., Mori, K., Tanigawa, T., Izu, H., and Ito, M., 2000b, Molecular cloning of the full-length cDNA encoding mouse neutral ceramidase. A novel but highly conserved gene family of neutral/alkaline ceramidase. *J. Biol. Chem.* **275**: 11229-11234.

- Tartakoff, A., and Vassalli, P., 1979, Plasma cell immunoglobulin M molecules. Their biosynthesis, assembly, and intracellular transport. *J Cell Biol.* **83**: 284-299.
- Terenghi, G., Polak, J.M., Ballesta, J., Cocchia, D., Michetti, F., Dahl, D., Marangos, P.J., and Garner. A., 1984, Immunocytochemistry of neuronal and glial markers in retinoblastoma. *Virchows Arch A Pathol Anat Histopathol.* **404**: 61-73.
- Torres, C.R., and Hart, G.W., 1984, Topography and polypeptide distribution of terminal N-acetyl-glucosamine residues on the surfaces of intact lymphocytes. *J. Biol. Chem.* **259**: 3308-3317.
- Tschantz, W.R., Zhang, L., and Casey, P.J., 1999, Cloning, expression, and cellular localization of a human prenylcysteine lyase. *J Biol Chem.* **274**: 35802-35808.
- Van Gassen, G., and Annaert, W., 2003, Amyloid, presenilins, and Alzheimer's disease. *Neuroscientist* **9**: 117-126.
- Varki, A., Cummings, R., Esko, J., Freeze, H., Hart, G., and Marth, J., Essentials of Glycobiology, 1<sup>st</sup> edition, *Cold Spring Harbor Laboratory Press*, 1999.
- Venable, M.E., Bielawska, A., and Obeid, L.M., 1996, Ceramide inhibits phospholipase D in a cell-free system. *J. Biol. Chem.* **271**: 24800-24805.
- Verbert, A. and Cacan, R., 1999, "Glyco-deglyco" processes during the biosynthesis of glycoproteins. *J Soc. Biol.* **193**: 101-110.
- Verma, M., and Davidson, E.A., 1994, Mucin genes: structure, expression and regulation. *Glycoconj. J.* **11**: 172-179.
- Vijayan, S., El-Akkad, E., Grundke-Iqbal, I., and Iqbal, K., 2001, A pool of beta-tubulin is hyperphosphorylated at serine residues in Alzheimer's disease brain. *FEBS Lett.* **509**: 375-381.
- Vijayan, V.K., Geddes, J.W., Anderson, K.J., Chang-Chui, H., Ellis, W.G., and Cotman, C.W., 1991, Astrocyte hypertrophy in the Alzheimer's disease hippocampal formation. *Exp Neurol.* **112**: 72-78.

Wang, J.Z., Gong, C.X., Zaidi, T., Grundke-Iqbal, I., and Iqbal, K., 1995, Dephosphorylation of Alzheimer paired helical filaments by protein phosphatase-2A and -2B. *J. Biol. Chem.* **270**: 4854-4760.

Wang, J.Z., Grundke-Iqbal, I., and Iqbal, K., 1996, Glycosylation of microtubule-associated protein tau: An abnormal post-translational modification in Alzheimer's disease. *Nat. Med.* **2** (8): 871-875.

Wang, Y.P., Wei, Z.L., Wang, X.C., Wang, Q., Wang, J.Z., 2001, Comparative study of the expression and phosphorylation of neurofilament proteins of brain gray matter in Alzheimer's disease. *Zhongguo Yi Xue Ke Xue Yuan Xue Bao (Chinese)* **23**: 445-449.

Weiner, H.L., and Selkoe, D.J., 2002, Inflammation and therapeutic vaccination in CNS diseases. *Nature* **420**: 879-884.

Weingarten, M.D., Lockwood, A.H., Hwo, S.Y., and Kirschner, M.W., 1975, A protein factor essential for microtubule assembly. *Proc. Natl. Acad. Sci. USA* **72**: 1858-1862.

White, K.G., and Ruske, A.C., 2002, Memory deficits in Alzheimer's disease: the encoding hypothesis and cholinergic function. *Psychon. Bull. Rev.* **9**: 426-437.

Whittaker, V.P., Michaelson, I.A., and Kirkland, R.J.A., 1964, The separation of synaptic vesicles from nerve-ending particles (synaptosomes). *Biochem. J.* **90**: 293-303.

Wing, D.R., Rademacher, T.W., Schmitz, B., Schachner, M., and Dwek, R.A., 1992, Comparative glycosylation in neural adhesion molecules. *Biochem Soc Trans.* **20**: 386-390.

Wolff, R.A., Dobrowsky, R.T., Bielawska, A., Obeid, L.M., and Hannun, Y.A., 1994, Role of ceramide-activated protein phosphatase in ceramide-mediated signal transduction. *J. Biol. Chem.* **269**: 19605-19609.

Wong, P.T., McGeer, P.L., and McGeer, E.G., 1992, Decreased prostaglandin synthesis in post-mortem cerebral cortex from patients with Alzheimer's disease. *Neurochem. Int.* **21**: 197-202.

Yan, S.D., Yan, S.F., Chen, X., Fu, J., Chen, M., Kuppusamy, P., Smith, M.A., Perry, G., Godman, G.C., and Nawroth, P., 1995, Non-enzymatically glycosylated tau in Alzheimer's

disease induces neuronal oxidant stress resulting in cytokine gene expression and release of amyloid beta-peptide. *Nat Med.* **1**: 693-699.

Yanagisawa, K., and Matsuzaki, K., 2002, Cholesterol-dependent aggregation of amyloid beta-protein. *Ann N Y Acad Sci.* **977**: 384-386.

Yao, P.J. and Coleman, P.D., 1998, Reduced O-glycosylated clathrin assembly protein AP180: implication for synaptic vesicle recycling dysfunction in Alzheimer' disease. *NeuroSci. Lett.* **252**: 33-36.

Yavin, E., and Gatt, S., 1969, Enzymatic hydrolysis of sphingolipids. 8. Further purification and properties of rat brain ceramidase. *Biochemistry* **8**: 1692-1698.

Yazaki, M., Tagawa, K., Maruyama, K., Sorimachi, H., Tsuchiya, T., Ishiura, S., and Suzuki, K., 1996, Mutation of potential N-linked glycosylation sites in the Alzheimer's disease amyloid precursor protein (APP). *Neurosci. Lett.* **221**: 57-60.

Zachara, N.E., and Hart, G.W., 2002, The emerging significance of O-GlcNAc in cellular regulation. *Chem. Rev.* **102**: 431-438.

Zhang, J., Alter, N., Reed, J.C., Borner, C., Obeid, L.M., and Hannun, Y.A., 1996, Bcl-2 interrupts the ceramide-mediated pathway of cell death. *Proc. Natl. Acad. Sci. USA* **93**: 5325-5328.

Zhang, Y., Yao, B., Delikat, S., Bayoumy, S., Lin, X.H., Basu, S., McGinley, M., Chan-Hui, P.Y., Lichenstein, H., and Kolesnick, R., 1997, Kinase suppressor of Ras is ceramide-activated protein kinase. *Cell.* **89**:63-72.